Published in final edited form as:

*J Comp Neurol*. 2019 August 15; 527(12): 1940–1965. doi:10.1002/cne.24664.

# Differential Expression of Neurexin Genes in the Mouse Brain

**Motokazu Uchigashima**[1,2,*,†], **Amy Cheung**[*,1], **Julie Suh**[1], **Masahiko Watanabe**[2], and **Kensuke Futai**[1,†]

[1]Brudnick Neuropsychiatric Research Institute, Department of Neurobiology, University of Massachusetts Medical School, 364 Plantation Street, LRB-706 Worcester, MA 01605-2324, USA

[2]Department of Anatomy, Hokkaido University Graduate School of Medicine, Sapporo, Hokkaido 060-8638, Japan

## Abstract

Synapses, highly specialized membrane junctions between neurons, connect presynaptic neurotransmitter release sites and postsynaptic ligand-gated channels. Neurexins (Nrxns), a family of the presynaptic adhesion molecules, have been characterized as major regulators of synapse development and function. Via their extracellular domains, Nrxns bind to different postsynaptic proteins, generating highly diverse functional readouts through their postsynaptic binding partners. Not surprisingly given these versatile protein interactions, mutations and deletions of *Nrxn* genes have been identified in patients with autism spectrum disorders, intellectual disabilities and schizophrenia. Therefore, elucidating the expression profiles of the *Nrxns* in the brain is of high significance. Here, using chromogenic and fluorescence *in situ* hybridization, we characterize the expression patterns of *Nrxn* isoforms throughout the brain. We found that each *Nrxn* isoform displays a unique expression profile in a region-, cell type- and sensory system-specific manner. Interestingly, we also found that *αNrxn1* and *αNrxn2* mRNAs are expressed in non-neuronal cells, including astrocytes and oligodendrocytes. Lastly, we found diverse expression patterns of genes that encode Nrxn binding proteins, such as Neuroligins (*Nlgns*), Leucine-rich repeat transmembrane neuronal protein (*Lrrtms*) and Latrophilins (*Adgrls*), suggesting that Nrxn proteins can mediate numerous combinations of trans-synaptic interactions. Together, our anatomical profiling of *Nrxn* gene expression reflects the diverse roles of Nrxn molecules.

## Graphical Abstract

[†]Corresponding authors: u-moto@med.hokudai.ac.jp, Kensuke.Futai@umassmed.edu, Tel: 1-774-455-4318.

ROLE OF AUTHORS

M.U., A.C. and K.F. designed research; M.U., A.C., J.S. and K.F. carried out experiments; M.U., and A.C. analyzed data; M.U., A.C., W.M. and K.F. wrote the paper.

[*]Contributed equally to this work.

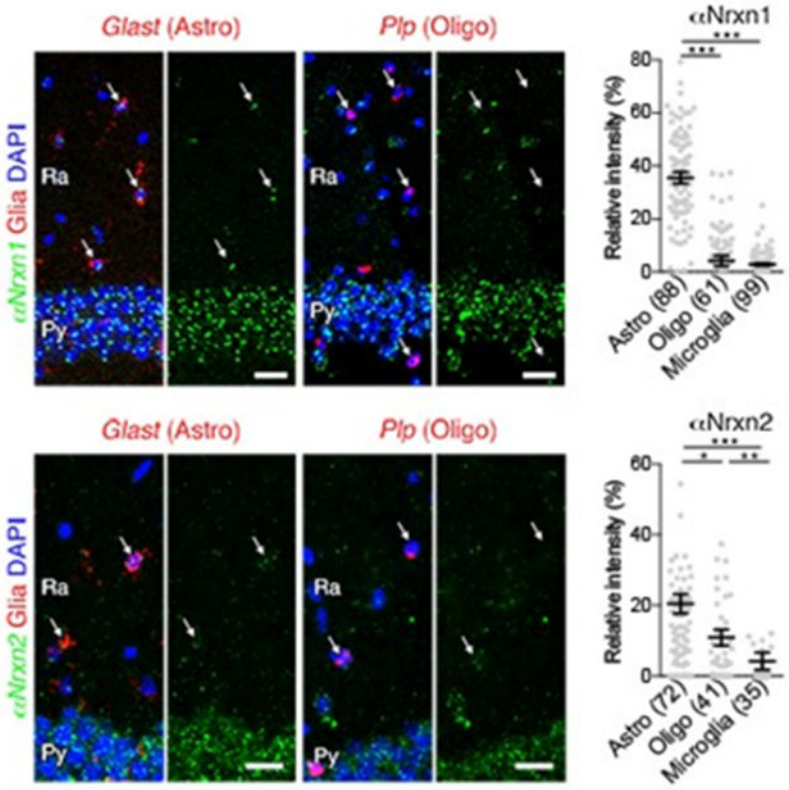


**Keywords**

brain; in situ hybridization; mice; Neurexin; synapse; trans-synaptic adhesion; RRIDs: RRID SCR_003070; RRID AB_840257; RRID AB_514500

## INTRODUCTION

Neurexin (Nrxn) is a presynaptic cell adhesion molecule that was originally identified as an α-latrotoxin receptor (Ushkaryov et al., 1992). In mammals, three Nrxn genes (*Nrxn1*, *Nrxn2*, and *Nrxn3*) are transcribed as longer alpha (*αNrxn1, αNrxn2*, *αNrxn3*), shorter beta (*βNrxn1, βNrxn2*, *βNrxn3*), and *Nrxn1*-specific gamma (*γNrxn1*) isoforms from two different promoters (Tabuchi and Sudhof, 2002; Sterky et al., 2017). The longer isoforms, αNrxns, have six extracellular laminin/neurexin/sex-hormone-binding globulin (LNS) domains, three interspersed epidermal growth factor-like repeats, an O-linked sugar modification sequence, a cysteine loop, a transmembrane region, and a short intracellular carboxyl terminal. Shorter isoforms, βNrxns, contain a unique β isoform-specific domain with the sixth LNS and intracellular domain of αNrxns (Sudhof, 2017). *Nrxn* isoforms also have six alternative splicing sites, resulting in thousands of potential Nrxn variants (Puschel and Betz, 1995; Ullrich et al., 1995; Gorecki et al., 1999; Schreiner et al., 2014; Treutlein et al., 2014).

The diversity of the Nrxn isoforms are thought to encode synapse specification (Sudhof, 2017). In fact, they can bind to various postsynaptic binding partners at different extracellular sites in the presence or absence of splicing sites (Boucard et al., 2005; Reissner et al., 2008; Koehnke et al., 2010). Neuroligins (Nlgns) (Ichtchenko et al., 1995; Ichtchenko et al., 1996), LRRTMs (leucine rich repeat transmembrane neuronal protein) (de Wit et al., 2009; Ko et al., 2009), $GABA_A$ receptors (Zhang et al., 2010), cerebellins (Uemura et al., 2010), SPARCL1 (secreted protein acidic and rich in cysteines 1, also referred to as Hevin) (Singh et al., 2016), and latrophilins (Boucard et al., 2012) can bind to the sixth LNS domain shared with both αNrxns and βNrxns. Emerging evidence reveals that interactions of Nrxns with Nlgns play a key role in synaptogenesis and excitatory and inhibitory synaptic transmission (Graf et al., 2004; Boucard et al., 2005; Nam and Chen, 2005; Chih et al., 2006; Futai et al., 2007; Kang et al., 2008; Futai et al., 2013). Interestingly, a variety of molecules critical for synaptogenesis have been reported to bind to specific Nrxn isoforms. For example, neurexophilins (Missler et al., 1998) and dystroglycan (Sugita et al., 2001) bind to the second LNS domain specific to αNrxns. lgSF21 can promote presynaptic differentiation of inhibitory synapses through the first LNS domain of αNrxn2 (Tanabe et al., 2017). C1ql2/3 can interact with the fifth splicing site of α/βNrxn3, and recruit kainate receptors to synaptic sites (Matsuda et al., 2016). These findings suggest isoform-specific roles of Nrxns in synapse specification.

Mutations and deletions of *Nrxn* loci have been associated with neuropsychiatric and neurodevelopmental disorders. Copy number alterations (Sebat et al., 2007; Szatmari et al., 2007) and deleterious (Yan et al., 2008; Zahir et al., 2008) mutations in *αNrxn1* are the most commonly reported Nrxn isoform-specific modifications predisposing people to autism spectrum disorder (ASD), attention deficit hyperactivity disorder (ADHD), intellectual disability, schizophrenia, and Tourette syndrome (Kim et al., 2008; Ching et al., 2010; Clarke et al., 2012). Increasing genetic evidence, including deletions in chromosome 2p16.3 where *Nrxn1* is located, reveals an overlap between ASD and schizophrenia comorbidity and symptomatology (Vinas-Jornet et al., 2014; Autism Spectrum Disorders Working Group of The Psychiatric Genomics, 2017). Mutations in *Nrxn3* have also been identified in rare ASD cases (Vaags et al., 2012; RK et al., 2017). Taken together, these findings suggest that Nrxn expression should prevail in brain regions that coordinate higher cognitive functions. However, brain region- and cell type-specific expression of Nrxns is poorly understood.

The three *Nrxn* genes are transcribed in the brain, but display differential expression patterns, with the abundance of *αNrxn*s exceeding that of *βNrxn*s (Ullrich et al., 1995). Some studies have revealed cell type-specific *Nrxn* expression and distinct expression of *Nrxn* mRNA splice variants in a given cell by single cell RT-PCR or RNA-Seq (Schreiner et al., 2014; Treutlein et al., 2014). Proteomic analysis highlights the specificity of Nrxn splice isoform expression in different brain regions (Schreiner et al., 2015). However, our knowledge of Nrxn expression in different brain regions and subregions is still limited. To fill this current knowledge gap, we conducted brain-wide mapping of α and β isoforms of *Nrxn1*, *Nrxn2*, and *Nrxn3* by *in situ* hybridization, and report region- and cell type-dependent expression of *Nrxn* isoforms in the mouse brain.

# MATERIALS AND METHODS

## Animals and section preparations

All animal protocols were approved by the Institutional Animal Care and Use Committee (IACUC) at the University of Massachusetts Medical School. C57BL6 male mice at postnatal day 28 were used, which represents the age when the expression levels of major synaptic proteins has stabilized (Gonzalez-Lozano et al., 2016). For chromogenic *in situ* hybridization, mice were transcardially perfused with 4% paraformaldehyde/0.1M phosphate buffer (PB, pH 7.2) under isoflurane anesthesia and postfixed for 3 days with the same fixatives. For double fluorescent *in situ* hybridization (FISH), brains were freshly obtained under isoflurane anesthesia and immediately frozen with powdered dry ice. Sections (20 μm) were prepared on a cryostat (CM3050S; Leica Microsystems). Fresh frozen sections were further mounted on silane-coated slides.

## Plasmids

Total RNA was extracted from hippocampal primary cultures (days *in vitro* 14) using RNAqueous Micro Kits (Ambion) and reverse-transcribed using Superscript III kits (Invitrogen). *Nrxn*, tyrosine hydroxylase (*Th*). P2Y purinoceptor 12 (*P2ry12*), *Nlgn, Lrrtm*, and *Adgrl* fragments listed in Table 1 were PCR amplified and sub-cloned into the pBluescript-SK(−) vector (Stratagene). We obtained the *Nlgn3* probe from Dr. Tanaka (Tanaka et al., 2010). All Nrxn probes were designed for the coding regions and/or 5'-untranslated regions (5'-UTRs) to detect all splice variants for each Nrxn isoform.

## Preparation of cRNA probes

Chromogenic and double fluorescent *in situ* hybridization were performed as previously described (Yamasaki et al., 2001; Yamasaki et al., 2010; Kudo et al., 2012). cRNA probes used in the present study are shown in Table 1. By using linearized pBluescript-SK(−) clones as templates, fluorescein- or digoxigenin (DIG)-labeled cRNA probes were transcribed with RNA labeling kit (Sigma) and T3 or T7 RNA polymerase (Promega). cRNA probes were suspended in 50% formamide.

## Chromogenic *in situ* hybridization

All experiments were carried out at room temperature, unless otherwise noted. Sections were pretreated as follows: acetylation with 0.25% acetic anhydride/0.1M triethanolamine-HCl (pH 8.0) for 10 min, wash with 2× SSC (1× SSC is composed of 150 mM NaCl and 15 mM sodium citrate) in 0.1% Tween 20 for 10 min, and prehybridization with hybridization buffer (50% formamide, 33 mM Tris-HCl [pH 8.0], 0.1% N-Laurosylsarcosine sodium salt, 1× Denhardt's solution, 0.6 M NaCl, 200 μg/ml of tRNA, 1 mM EDTA, 10% dextran sulfate) for 30 min. Hybridization was carried out at 63.5 or 75°C in a 1:1,000 or 1:10,000 dilution of DIG-labeled cRNA probe (see Table 1) supplemented with hybridization buffer. Successive post-hybridization washing was done at 61 or 75°C; 5× SSC, 0.0005% Tween 20 for 20 min, 4× SSC, 50% formamide, 0.001% Tween 20 for 40 min, 2× SSC, 50% formamide, 0.001% Tween 20 for 40 min, and 0.1× SSC, 0.0005% Tween 20 for 20 min. For Nrxn1β mRNA, sections were alternatively washed with 2× SSC, 0.1 % Tween 20 at 75°C

for 30 min twice, 20 μg/ml RNase, 0.5M NaCl, 10 mM Tris-HCl (pH 8.0), 1 mM EDTA at 37°C for 30 min, and 0.2× SSC, 0.1% Tween 20 at 37°C for 30 min. Sections were incubated with 20 μM iodoacetamide, 0.5 M NaCl, 0.01 M Tris-HCl [pH 8.0], 5 mM EDTA, 0.0005% Tween 20 for 30 min, DIG blocking solution (1% DIG blocking reagent [Sigma] in maleinic acid buffer [pH 7.5]) for 30 min, and alkaline phosphatase-conjugated anti-DIG antibody (1:500, Roche Diagnostics) in DIG blocking buffer for 2 hours. After washing with TNT buffer (0.1 M Tris-HCl [pH 7.5] and 0.15 M NaCl) three times, sections were incubated with NBT/BCIP solution (1:50; Roche Diagnostics) in 0.01 M Tris-HCl (pH 9.5), 0.01M $MgCl_2$ at 4°C for up to 3 days. Sections were mounted on gelatin-coated slides and dehydrated in 100% methanol for 10 min, 100% ethanol two times for 10 min each, 100% Xylene three times for 10 min each, and embedded with Entellan New (Millipore). The specificity of cRNA probes against each Nrxn isoform mRNA was validated by the identical signal pattern obtained by two different probes and lack of hybridization signals with their sense probes (Figure 1).

## Double-labeled fluorescent *in situ* hybridization

Fresh frozen sections were fixed with 4% paraformaldehyde, 0.1M PB for 30 min, acetylated with 0.25% acetic anhydride in 0.1M triethanolamine-HCl (pH 8.0) for 10 min, and prehybridized with hybridization buffer for 30 min. After dehydration, hybridization was then performed with a mixture of fluorescein- or DIG-labeled cRNA probes at a dilution of 1:1,000 or 1:10,000 (see Table 1) in hybridization buffer. Post-hybridization washing was performed as described for chromogenic *in situ* hybridization. To visualize signals, we adopted a two-step detection method. For the first detection, sections were blocked with DIG blocking solution for 30 min and 0.5% tryamide signal amplification (TSA) blocking reagent in TNT buffer for 30 min, and incubated with peroxidase-conjugated anti-fluorescein antibody (1:500, Roche Diagnostics) for 1 hour. After washing with TNT buffer three times, sections were incubated by using TSA Plus Fluorescein amplification kit (PerkinElmer) for 10 min. Residual peroxidase activity was inactivated with 3% $H_2O_2$ in TNT buffer for 30 min. For the second detection, sections were again blocked with DIG blocking solution and 0.5% TSA blocking reagent in TNT buffer for 30 min each, and incubated with peroxidase-conjugated anti-DIG antibody (1:500 Roche Diagnostics) for 1 hour. After washing with TNT buffer three times, signals were visualized with TSA Plus Cy3 amplification kit (PerkinElmer) for 10 min. Nuclear counterstaining was performed with DAPI (1:5000, Sigma-Aldrich) for 10 min. The specificity of cRNA probes for *Th* and *P2ry12*, which were newly generated in this study, were validated by unique signal patterns with labeled cells distributed selectively in catecholaminergic nuclei (Figures 14 **and** 15) and scattered in the neuropil region (Figures 16 **and** 17), respectively.

## Image acquisition, analysis and quantification

Chromogenic images were acquired with a dissecting microscope (SZX16, Olympus) equipped with a CCD digital camera (INFINITY3–1UC, Lumenera) or a fluorescence microscope (BZ-X710, Keyence) with a 20× objective lens (NA 0.75). Images were analyzed with ImageJ software (SCR 003070). Briefly, images were converted to grayscale with the dark background. The mean *Nrxn* signal intensity in a given region was measured and normalized to the mean intensity in the pyramidal cell layer of the piriform cortex,

which exhibited high signals for all isoforms (Figures 2g–l **and** 3a–f). The background noise was defined as the mean intensity outside the section and subtracted from each density before normalization. We scored >70% of the normalized intensity as strong (+++), 30–70% as moderate (++), 10–30% as weak (+), and <10% as very weak or not detected (−) (Table 2). FISH images were acquired with a fluorescence microscope (BZ-X710, Keyence) with a 20× objective lens (NA 0.75) or a confocal microscope (FV1200, Olympus) with a UPlanSapo 20× objective (NA 0.75). The images were captured with exposure times respective to each Nrxn isoform. On the confocal, the size of images was 800 × 800 or 1000 × 1000 pixels. For quantification, simultaneously stained sets of cells on the same slide were imaged using identical settings. Measurements were performed with one section from each brain by using ImageJ software. Briefly, background levels were determined with the signal intensity in DAPI-negative neuropil regions, and subtracted from each image. The same circular region of interest (ROI) was applied to cell bodies containing DAPI+ nuclei with or without labeling for cell type-specific markers, and the mean signal intensity was measured.

The expression of *Nrxns* in glutamatergic and GABAergic neurons were examined with double FISH sections for glutamic acid decarboxylase 1 (Gad1), a marker of GABAergic neurons, and *Nrxn* mRNAs. In the somatosensory cortex, most DAPI+ nuclei were divided into two types: large and pale nuclei containing a few heavily stained puncta for DAPI, reflecting decondensed chromatin (arrowheads in Figure 8a, b), and small and dark nuclei (arrows in Figure 8a, b). The former DAPI+ nuclei were classified as neuronal nuclei, and the latter as non-neuronal nuclei (Yu et al., 2015). Most glutamatergic and GABAergic neurons, identified by type 1 vesicular glutamate transporter (*Vglut1*) and *Gad1* mRNA expression, respectively, displayed large and pale DAPI signals (*Vglut1*: 99.2% /total 249 *Vglut1+* nuclei; *Gad1:* 98.8% /84). All cells with small and dark DAPI+ nuclei (n = 134 nuclei) did not express *Vglut1* or *Gad1.* Thus, Gad1(−) cells with large and pale DAPI+ nuclei were analyzed as glutamatergic neurons. Occasionally, cells with small and dark DAPI+ nuclei were found, but not used for quantitative analysis. In the hippocampus and cerebellar cortex, glutamatergic neurons were densely distributed in pyramidal or granule cell layers, and predominate over other types of cells. Thus, *Gad1(−)* cells in these cell layers were classified as glutamatergic neurons.

### Statistical analyses

The data were obtained from two mice and pooled. Results are reported as means ± SEM. For comparison between two neuronal types, Mann-Whitney non-parametric test was performed. For multiple comparisons, Kruskal-Wallis non-parametric ANOVA followed by Dunn's post hoc test were performed using Prism 5 (Graph Pad Software). Statistical significance was set at $p < 0.05$.

## RESULTS

### 1. Overall expression in the brain and validation of ISH probes

Two non-overlapping antisense probes for the unique amino terminus and/or 5′-UTR region of each *Nrxn* isoform (total, 12 probes) were used to determine overall expression in the brain (Figure 1). Chromogenic *in situ* hybridization with sagittal brain sections showed

distinct signal patterns for each isoform. Strong signals for *αNrxn1 αNrxn2*, and *βNrxn2* mRNAs were distributed in the olfactory bulb, neocortex, hippocampus, and cerebellum (Figure 1a–d, i, j). Expression of *βNrxn1* mRNA was high in the neocortex, hippocampus, and cerebellum (Figure 1g, h). High expression of *αNrxn3* mRNA was observed in the olfactory bulb, neocortex, hippocampus, and caudate-putamen (Figure 1e, f), while *βNrxn3* mRNA was enriched in the olfactory bulb and cerebellum (Figure 1k, I). In the thalamus and brainstem, all isoforms of *Nrxn* mRNAs were differentially expressed at low to moderate levels. Two cRNA probes for each isoform yielded somewhat different intensities, particularly for *αNrxn3* and *βNrxn1* labeling, but importantly, exhibited the same spatial patterns of labeling. Furthermore, no signals were found with the sense cRNA probes (Figure 1m–x). These results indicate the specificity of cRNA probes and hybridizing signals with use of them.

## 2. Region-specific expression of *Nrxn* isoforms

To map the expression of each *Nrxn* isoform in the brain, we used coronal sections of mouse brains at the age of one month. In the following analysis, two non-overlapping cRNA probes were used in mixture to increase the intensity of hybridizing signals. The expression levels of each *Nrxn* isoform were assessed based on signal intensity (Table 2).

### 2.1. Telencephalon

**2.1.1 Olfactory bulb:** All six *Nrxn* isoforms were detected in the olfactory bulb (Figure 2a–f), consistent with a previous study (Ullrich et al., 1995). *αNrxn1* and *αNrxn3* mRNAs were highly expressed in each neuronal layer, i.e., the glomerular, mitral cell, and granule cell layers, while *αNrxn2* mRNA was more enriched in the mitral and granule cell layers than in the glomerular layer. All three *βNrxn* mRNAs were, though generally low compared with *αNrxn*s, dominantly expressed in the mitral cell layer.

**2.1.2 Neocortex:** In the neocortex, distinct laminar patterns were observed (Figures 2g–l, 3, **and** 4), as previously described in rat brains (Ullrich et al., 1995). Among six isoforms, *αNrxn1* mRNA was expressed uniformly in cortical layers 2-6 (Figures 2g, 3a, **and** 4a), while others varied among cortical layers. *αNrxn2* mRNA peaked in layers 2/3 and 5 (Figures 2h **and** 3b), *αNrxn3* mRNA peaked in layers 5 and 6 (Figures 2i, 3c, **and** 4c), and *βNrxn1* and *βNrxn2* mRNAs were dominantly expressed in layers 2/3 and 4 (Figures 2j, k, 3d, e, **and** 4d, e). Layers with the highest level of *βNrxn3* mRNA varied in different neocortical areas: layers 2/3 in the primary motor (Figure 2I), layer 4 in the primary somatosensory (Figure 3f), and layers 2/3 and 4 in the primary auditory cortex (Figures 3f **and** 4f).

High expression of all six isoforms was found in the pyramidal cell layer of the piriform cortex (Figures 2g–l **and** 3a–f). Similarly, all six isoforms were highly expressed in the upper layers of the lateral entorhinal cortex at rostral levels (Figure 4a–f). At more caudal levels, *αNrxn3* and *βNrxn3* mRNA signal intensities were lower in the lateral and medial entorhinal cortex (Figure 5c, f), whereas expression levels were maintained there for other isoforms (Figure 5a, b, d, e). This suggests a rostrocaudal gradient of *αNrxn3* and *βNrxn3* expression within the entorhinal cortex.

**2.1.3 Hippocampus:** The hippocampal formation, including the Ammon's horn (CA1-CA3), subiculum, and dentate gyrus, was one of the regions with the highest signals for each isoform in the brain (Figures 3a–f **and** 4a–f). Consistent with previous studies (Ullrich et al., 1995; Nguyen et al., 2016), expression patterns in neuronal cell layers varied by *Nrxn* isoforms and hippocampal subregion. *αNrxn1* and *βNrxn2* mRNAs were uniformly expressed across different subregions (Figures 3a, e **and** 4a, e). In contrast, *αNrxn2* mRNA expression peaked in the CA2 (Figure 3b), *αNrxn3* mRNA in the CA1-CA3 (Figures 3c **and** 4c), and *αNrxn1* mRNA in the CA3 and dentate gyrus (Figures 3d **and** 4d). The expression pattern of *βNrxn3* mRNA was unique, in that it was hardly detected in the rostral portion of the dentate gyrus (Figure 3f), but expressed in more caudal portions of the dentate gyrus, particularly its ventral part (Figure 4f), suggesting a septotemporal gradient of *βNrxn3* expression within the dentate gyrus. In neuropil layers, some scattered cells were labeled for *αNrxn1-3* and *βNrxn3* mRNAs, suggesting their expression in interneurons (arrows in Figure 4a–c, f).

**2.1.4 Cerebral nuclei:** In the caudate-putamen and nucleus accumbens, *αNrxn3* mRNA was predominantly expressed (Figure 2i). The island of Calleja showed intense signals for *αNrxn2*, *αNrxn3*, *βNrxn1*, and *βNrxn3* mRNAs (Figure 2h–j, l). In the lateral septal nucleus and nucleus of the diagonal band, three *αNrxn* isoforms were discernible, but *βNrxn* isoforms were at low or undetectable levels (Figure 2g–l). In the amygdala, *αNrxn1*, *αNrxn2*, *αNrxn3*, and *βNrxn2* mRNAs were uniformly expressed in three subnuclei, the lateral, basal and central nuclei, while *βNrxn2* and *βNrxn3* mRNAs were more enriched in the lateral or central nucleus, respectively (Figure 3a–f).

**2.2. Diencephalon—**In the medial habenular nucleus, high to moderate expression was noted for *αNrxn1*, *αNrxn2*, and *βNrxn2* mRNAs, and *αNrxn3* mRNA expression was confined to its dorsomedial portion (Figure 3a–c, e). Expression levels were generally low in the lateral habenular nucleus, with relatively higher levels for *αNrxn1* mRNA (Figure 3a). In the thalamus, *αNrxn1*, *βNrxn1*, and *βNrxn3* mRNAs were expressed widely and highly, as exemplified by ventral posteromedial and posterolateral nuclei, mediodorsal nucleus, and medial geniculate nucleus (Figures 3a–f **and** 4a–f). In the subthalamic nucleus and reticular thalamic nucleus, *αNrxn1* or *αNrxn3* mRNA, respectively, was a predominant isoform (Figure 3a, c). In the hypothalamus, three *αNrxn* isoforms were predominantly expressed, with some different intensities among the lateral, dorsomedial, ventromedial, and arcuate nuclei (Figure 3a–f). A moderate expression level was also found for *βNrxn2* mRNA in the arcuate nucleus (Figure 3e).

**2.3. Midbrain—**Three *αNrxn* isoforms were widely and predominantly expressed in the midbrain, showing heterogeneous regional patterns (Figures 4a–c, 5a–c, and 6a–c). *αNrxn2* mRNA was predominant in the Edinger-Westphal nucleus (Figure 4b) and the dorsal raphe nucleus (Figure 5b). while *αNrxn3* mRNA was predominant in the substantia nigra pars compacta, ventral tegmental area, Nucleus of Darkschewitsch, and lateral part of the dorsal raphe nucleus (Figures 4c **and** 5c). Sparse cells within the inferior colliculus expressed *αNrxn3* mRNA at high levels (Figure 6c). Expression levels of three *βNrxn* isoforms were generally low or undetectable in the midbrain (Figures 4d–f, 5d–f, **and** 6d–f), but *βNrxn3*

mRNA was detected in some sparse cells in the inferior colliculus (Figure 6f) and other midbrain regions.

**2.4. Pons—**In the pons, *αNrxn3* mRNA was predominant in many nuclei (Figures 5c **and** 6c), with the strongest signals in the nucleus of the trapezoid body (Figure 5c) and the lowest signals in the facial nucleus (Figure 6c). *αNrxn1* and *αNrxn2* mRNAs were expressed at low to moderate levels in the pontine tegmentum, including the lateral and medial parabrachial nuclei, locus coeruleus (LC), and laterodorsal tegmental nucleus (Figure 6a, b). In addition, *αNrxn2* mRNA expression was moderately expressed in the facial nucleus (Figure 6b). Three *βNrxn* mRNAs were generally low in the pons, except for moderate expression of *βNrxn2* mRNA in the LC (Figure 6e) and *βNrxn3* mRNA in the dorsal part of the lateral parabrachial nucleus (Figure 6f). Cells expressing *βNrxn3* mRNA were scattered over the pons, such as in the ventral cochlear nucleus and principal sensory nucleus of trigeminal nerve (Figure 6f).

**2.5. Medulla—**Like in the pons, *αNrxn3* mRNA was most prevalent in the medulla (Figures 6c **and** 7c). However, *αNrxn3* mRNA was not detected in the inferior olivary complex, where *αNrxn1*, *αNrxn2*, *βNrxn1*, and *βNrxn2* mRNAs were weakly expressed (Figure 7a, b, d, e). The nucleus of the tractus solitarius (NTS) and dorsal motor nucleus of vagus nerve expressed high levels of all three *αNrxn* isoforms and low to moderate levels of all three *βNrxn* isoforms (Figure 7a–f).

**2.6. Cerebellum—**In the cerebellar cortex, all six *Nrxn* isoforms were highly expressed in the granule cell layer, where *αNrxn3* mRNA was restricted to a few scattered cells and the rest were expressed diffusely (Figures 6 **and** 7). In the molecular layer, *αNrxn3* mRNA was expressed predominantly in scattered cells (Figures 6c **and** 7c). Various isoforms were less expressed in the Purkinje cell layer, with the highest level for *αNrxn3* mRNA.

## 3. Cell type-specific expression of *Nrxn* isoforms

To address the type of cells expressing each *Nrxn* isoform, we employed double FISH for *Nrxns* and cellular markers, and measured the fluorescent intensity of each *Nrxn* isoform in given types of cells.

**3.1. Glutamatergic and GABAergic neurons—**Using *Gad1* mRNA as a neuronal marker of GABAergic neurons, we measured the signal intensity of *Gad1(+)* GABAergic and *Gad1*(−) glutamatergic neurons in the primary somatosensory cortex (Figures 8 **and** 9), hippocampus (Figures 10 **and** 11), and cerebellar cortex (Figures 12 **and** 13). Indeed, in the primary somatosensory cortex, cells that had large and DAPI-pale nuclei expressed either *Vglutt* which is selectively expressed in cortical glutamatergic neurons (arrowheads in Figure 8a), or *Gad1* (arrowheads in Figure 8b) mRNA, thus being assigned as glutamatergic and GABAergic neurons, respectively. Cells having small and DAPI-dark nuclei without *Vglut1* or *Gad1* mRNA are likely glial cells (arrows in Figure 8a, b; See Materials and Methods) (Yu et al., 2015). The mean intensity in each neuronal layer of the primary somatosensory cortex was calculated for glutamatergic and GABAergic neurons (Figures 8c–h **and** 9a–f). The mean fluorescent intensity in glutamatergic neurons (blue dots in

Figures 8d, f, h **and** 9b, d, f) was comparable to optical intensity by chromogenic *in situ* hybridization (Figure 3a–f). Compared to glutamatergic neurons, *Nrxn* expression in GABAergic neurons exhibited different laminar patterns (red dots in Figures 8d, f, h **and** 9b, d, f). Significantly higher levels in GABAergic neurons than in glutamatergic neurons in the same layer were noted for *αNrxn2* mRNA in layers 4 and 6 (Figure 8e, f), *αNrxn3* mRNA in layers 4–6 (Figure 8g, h), *βNrxn1* mRNA in layer 6 (Figure 9a, b). *βNrxn2* mRNA in layers 4 and 6 (Figure 9c, d). and *βNrxn3* mRNA in layers 2/3, 5, and 6 (Figure 9e, f). Conversely, significantly lower levels were noted for *Nrxn1* mRNA in layers 4 and 5 (Figure 8c,d) and *βNrxn1* mRNA in layers 2-4 (Figure 9a,b).

In the dorsal hippocampus, the pattern of mean *Nrxn* fluorescent intensity in *Gad1*(−) glutamatergic neurons among different subregions (Figures 10 **and** 11) was generally comparable to that of chromogenic signals (Figure 3a–f). In the CA1-CA3 subregions, GABAergic neurons tended to be significantly lower in *Nrxn* mRNA expression than glutamatergic neurons. In the dentate gyrus, by contrast, GABAergic neurons expressed significantly higher levels for all three *αNrxn* and *βNrxn3* mRNAs (Figure 11a, b).

In the cerebellar cortex, distinct neuron type-dependent expression, as suggested from distinct layer labeling and sparse vs. diffuse labeling (Figures 6 **and** 7), was substantiated by double FISH (Figures 12 **and** 13). GABAergic interneurons in the molecular layer mainly expressed *αNrxn3* mRNA, with additional very low signals for *αNrxn1*, *αNrxn2*, *βNrxn1*, and *βNrxn2* mRNAs. GABAergic Purkinje cells expressed *αNrxn3* mRNA at the highest level, and more or less expressed the other isoforms. On the other hand, all six *Nrxn* isoforms were highly expressed in GABAergic Golgi cells. Granule cells highly expressed all six *Nrxn* isoforms except for *αNrxn3* mRNA.

### 3.2. Catecholaminergic neurons—

We also examined the expression patterns of *Nrxn* mRNAs in catecholaminergic neurons including dopaminergic (DA) neurons in the midbrain and noradrenergic (NA) neurons in the LC and NTS (Figures 14 **and** 15). Catecholaminergic neurons were identified as cells positive for tyrosine hydroxylase (*Th*) mRNA, the rate-limiting enzyme for catecholamine biosynthesis. *αNrxn1* mRNA was expressed at higher levels in midbrain DA neurons and NTS NA neurons than in LC NA neurons (Figure 14a, b). In contrast, *αNrxn2* mRNA was expressed at higher levels in both NA neurons than in midbrain DA neurons (Figure 14c, d). *αNrxn3* mRNA expression is the highest in midbrain DA neurons (Figure 14e, f). *βNrxn1* mRNA was hardly detected in the three catecholaminergic neurons analyzed (Figure 15a, b). *βNrxn2* and *βNrxn3* mRNAs were expressed at the highest level in locus coeruleus NA neurons and midbrain DA neurons, respectively (Figure 15c–f). Taken together, our double FISH data demonstrate that *Nrxn* expression in given neural regions is highly variable depending on neuron types and subregions, but that there is no specific or preferential assignment of given *Nrxn* isoforms to neurochemical types of neurons.

## 4. Non-neuronal expression of *αNrxn1* and *αNrxn2* mRNA

In our double FISH data, we encountered signals for *αNrxn1* and *αNrxn2* mRNA in *Gad1*(−) putative glial cells in the hippocampus and cortex. Therefore, we first addressed the

expression of six *Nrxn* mRNAs in non-neuronal cells in the hippocampal CA1 region (Figure 16a–f) and somatosensory cortex layers 2/3 (Figure 17a–f). Non-neuronal *Nrxn* signal intensities were normalized to the neuronal expression. Neuronal and non-neuronal cells were identified as pyramidal neurons and *Gad1(−)* neuropil cells in the hippocampus, and the cells with large and pale DAPI+ nuclei and small and dark DAPI+ nuclei in the somatosensory cortex, respectively. Prominent expression of *αNrxn1* and *αNrxn2* was found in nonneuronal cells in both brain areas (Figures 16g **and** 17g). Next, we performed double FISH for *αNrxn1* and *αNrxn2,* and glial markers: glutamate/aspartate transporter *(Glast)* for astrocytes, proteolipid protein *(Plp)* for oligodendrocytes, and purinergic receptor P2Y *(P2ry12)* for microglia to identify the cell type expressing *αNrxn1* and *αNrxn2* (Figures 16h–o **and** 17h–o). Signals for *αNrxn1* mRNA frequently overlapped with those for *Glast* mRNA, but not Plp or *P2ny12* mRNA, in the hippocampal CA1 (Figure 16h–k), somatosensory cortex (Figure 17h–k), and other brain regions examined (data not shown), thus demonstrating *αNrxn1* expression in astrocytes. In contrast, signals for *αNrxn2* mRNA overlapped with those for *Glast* or *Plp*, but not *P2ny12* mRNA, in the hippocampal CA1 (Figure 16l–o), somatosensory cortex (Figure 17l–o) and other brain regions examined (data not shown), thus revealing *αNrxn2* expression in astrocytes and oligodendrocytes.

## 5. Gene expression of trans-synaptic Nrxn binding proteins in the brain

Both diverse expression patterns of *Nrxn* in the brain and the variety of postsynaptic Nrxn binding partners should generate massive combinations of trans-synaptic protein interactions (Sudhof, 2017). Importantly, the expression of Nrxns and their trans-synaptic binding partners have not been well compared. Therefore, we studied the expression of the genes encoding the major trans-synaptic Nrxn binding partners, *Nlgn1-3* (Ichtchenko et al., 1995: Ichtchenko et al., 1996), *Lnntm1-4* (de Wit et al., 2009: Ko et al., 2009) and *Adanl1-3* (Latrophilin1-3) (Boucard et al., 2012), in the brain using chromogenic *in situ* hybridization (Figure 18a–j). For this analysis, cRNA probes were designed for unigue coding and/or 5'-UTR region of each *Nlgn, Lnntm and Adgnl* isoform (total, 11 probes). No signals were found using the corresponding sense probes (Figure 18a–j, **insets**), indicating the specificity of hybridization signals.

### 5.1 Nlgns—

*Nlgn1* mRNA expression was weak throughout the brain with the highest signals in the hippocampus (Figure 18a). In contrast, we observed much stronger signals for *Nlgn2* and *Nlgn3* mRNAs. Striking expression of *Nlgn2* mRNA was noted in not only the hippocampus, but also olfactory mitral cell layer and cerebellar Purkinje cell layer (Figure 18b). *Nlgn3* mRNA was ubiquitously expressed throughout the brain with peak signal levels visualized in the hippocampus (Figure 18c).

### 5.2. Lrrtms—

*Lrrtm1* mRNA displayed prominent expression in the hippocampus, neocortex, thalamus, and olfactory bulb (Figure 18d). Similarly, *Lrrtm2* mRNA expression was discernible in the hippocampus, neocortex, and thalamus (Figure 18e). The hippocampus exhibited similar expression patterns of *Lrrtm1* and *Lrrtm2* mRNAs with higher intensity in the CA1 and dentate gyrus than in the CA3. In contrast, *Lrrtm3* and *Lrrtm4* mRNAs were predominant in the cerebellum (Figure 18f) and dentate gyrus (Figure 18g), respectively.

**5.3. *Adgrls* (Latrophilins)—***Adgrl1* mRNA was widely and richly expressed throughout the brain (Figure 18h). *Adgrl2* and *Adgrl3* mRNAs were also expressed ubiquitously (Figure 18i, j). However, the signal intensities for *Adgrl2* and *Adgrl3* mRNAs were much weaker than that for *Adgrl1* mRNA. *Adgrl2* mRNA showed peak intensity in the hippocampal CA1 region (Figure 18i), while *Adgrl3* mRNA was highly expressed in the hippocampal CA1 and dentate gyrus regions (Figure 18j).

## DISCUSSION

In this study, *Nrxn* mRNA expression was systematically mapped by *in situ* hybridization in the adult mouse brain. Consistent with previous reports (Puschel and Betz, 1995; Ullrich et al., 1995; Gorecki et al., 1999; Schreiner et al., 2014; Treutlein et al., 2014), we confirmed highly diverse expression profiles of *Nrxns* throughout the brain. Although the translational regulation of Nrxn proteins should be considered, our brain-wide and detailed expression analysis revealed distinct regional and cellular expression patterns of the six principal isoforms of *Nrxns* at the mRNA level.

First, we found cortical layer- or subregion-dependent differences in *Nrxn* mRNA expression in glutamatergic and GABAergic neurons. In the somatosensory cortex, the mean signal intensities for *αNrxn2*, *αNrxn3*, and *βNrxn3* mRNAs were significantly higher in GABAergic neurons than in glutamatergic neurons (Figures 8f, h **and** 9f). In the hippocampus, the mean signal intensities for all six isoforms were significantly lower in GABAergic neurons than in glutamatergic neurons (Figures 10b, d, f **and** 11b, d, f). This difference may underlie to some extent brain region-specific phenotypes on synaptic transmission in Nlgn3 KO or Nlgn3 R451C mice, which lack or decrease postsynaptic expression of Nlgn3, one of the binding partners of Nrxn proteins (Tabuchi et al., 2007; Etherton et al., 2011). In addition, the variance of the signal intensities of *Nrxn* mRNAs appeared high in cortical GABAergic neurons (Figures 8–11). This is supported by the notion that distinct subsets of inhibitory neurons in cortical structures differ in their expression patterns of *Nrxn* mRNAs (Fuccillo et al., 2015; Chen et al., 2017). In particular, we found some inhibitory neurons with high signals for *αNrxn2* mRNA in the deep cortical layer (Figure 8e, f). *αNrxn2* can selectively induce inhibitory presynaptic differentiation via its interaction with postsynaptic lgSF21, which is expressed in the deep layer neurons (Tanabe et al., 2017). This molecular interaction could contribute to synapse specification at a subset of inhibitory synapses.

Next, we found unique expression of *Nrxn* mRNAs in the hippocampus. Consistent with previous studies (Ullrich et al., 1995; Nguyen et al., 2016), the CA1 pyramidal cell layer highly expressed mRNAs for all the isoforms except *βNrxn1* (Figures 3 **and** 4). The CA2 and CA3 pyramidal layers expressed all *Nrxn* mRNAs, however, *αNrxn2* was preferentially expressed in the CA2 region (Figures 1c, d, k **and** 3b) and *βNrxn3* had septotemporal gradient expression in the CA3 region (Figures 1k, I, 3f, **and** 4f). Furthermore, the dentate gyrus had a septotemporal gradient of *βNrxn3* (Figures 3f **and** 4f) mRNA expression, and its upstream entorhinal cortex also had a rostrocaudal gradient of *αNrxn3* (Figures 4c **and** 5c) and *βNrxn3* (Figures 4f **and** 5f) mRNA expressions. Different parts of the entorhinal cortex project to different septotemporal levels of the dentate gyrus (Amaral and Pierre, 2006). The

rostromedial entorhinal cortex, which expresses both *αNrxn3* and *βNrxn3* mRNAs at high levels, projects to the temporal half of the dentate gyrus, which highly expresses *βNrxn3* mRNA. In contrast, the caudolateral entorhinal cortex, which expresses *αNrxn3* and *αNrxn3* mRNAs at low levels, projects to the septal half, where *βNrxn3* mRNA expression is low. This coincidence of the topographic projections and *Nrxn3* expression between the entorhinal cortex and dentate gyrus could underlie a unique function of *Nrxn3* in memory formation. Furthermore, a specific splicing variant of Nrxn3 protein can recruit postsynaptic kainate receptors via C1ql2/3 at dentate gyrus-CA3 synapses (Matsuda et al., 2016). Although we did not map splicing variants of *Nrxn3* gene in this study, our data raise a possibility of topographical differences in the postsynaptic recruitment of kainate receptors.

We also investigated the region- and cell type- dependent expression of *Nrxn* mRNAs in catecholaminergic neurons including midbrain DA neurons and LC and NTS NA neurons (Figures 14 **and** 15). Similar to glutamatergic and GABAergic neurons, midbrain DA neurons expressed multiple *Nrxn* isoforms, consistent with Nrxn protein expression at striatal DA synapses formed by midbrain DA neurons (Uchigashima et al., 2016). In addition, we found *Nrxn* mRNA expressions with different combinations in LC and NTS NA neurons. Different expression patterns of *Nrxn* mRNAs among catecholaminergic neurons may provide distinct molecular bases to control the release of each catecholamine. Indeed, pan-*Nrxn* deletion causes different phenotypes in synaptic transmissions from distinct neurons with their own repertories of *Nrxn* mRNAs (Chen et al., 2017). Therefore, region- and cell type-dependent expression patterns of *Nrxn* mRNAs would provide the molecular-anatomical basis for the diversity of synapse specification at various types of synapses.

We found a unique expression of the *Nrxn3* gene in the auditory system. Several auditory relay stations, including the ventral cochlear nucleus, nucleus of trapezoid body, and inferior colliculus, displayed high expressions of *αNrxn3*, *βNrxn3*, or both mRNAs (Figures 5c **and** 6c, f). The medial geniculate nucleus, which is the thalamic nucleus relaying auditory information to the neocortex, highly expressed both *αNrxn3* and *βNrxn3* mRNAs as well as other *Nrxn* isoforms (Figure 4a–f). Furthermore, the primary auditory cortex had a unique expression pattern of *βNrxn3* mRNA. *βNrxn3* mRNA was expressed with a peak density in layers 2/3 as well as layer **4** region (Figures 3f **and** 4f), while the primary somatosensory cortex exhibited peak expression in layer **4** only (Figure 3f). Above all, the predominant expression of *αNrxn3* and *βNrxn3* mRNAs may suggest the importance of Nrxn3 in auditory function. Indeed, a patient with a rare mutation of the *Nrxn3* gene exhibited difficulty in auditory processing (Vaags et al., 2012).

In the olfactory system, all isoforms of *Nrxn* mRNAs were highly expressed in mitral cell layer neurons (Figure 2a–f), the second order neurons receiving input from olfactory cells, and in pyramidal neurons in the piriform cortex (Figures 2g–l **and** 3), which are the third order neurons receiving input from mitral cell layer neurons. We also noted striking expression of *αNrxn* mRNA in the granule cells of the olfactory bulb (Figure 2a–c), and of *αNrxn2*, *αNrxn3*, *βNrxn1*, and *βNrxn3* mRNAs in the island of Calleja (Figure 2h, i, l), which is anatomically associated with the piriform cortex (Fallon et al., 1978). Interestingly, some ASP patients exhibit olfactory deficits (Galle et al., 2013). *αNrxn3* KO mice have

impaired GABAergic synaptic transmission in the olfactory bulb, leading to deficits in olfactory function (Aoto et al., 2015). Interestingly, both *αNrxn1* and *αNrxn2* KO mice, which show autism-related behaviors, have been reported to have intact olfaction, highlighting the importance of *Nrxn3* in olfaction (Grayton et al., 2013; Dachtler et al., 2014).

Some nuclei in the brainstem share similar *Nrxn* mRNA expression patterns. *αNrxn2* mRNA was remarkable in facial nucleus (Figure 6b) and hypoglossal nucleus (Figure 7b), consistent with the requirement of αNrxns in high fidelity synaptic transmission at mouse neuromuscular junctions and relay synapses (Sons et al., 2006). Our findings suggest that neurons associated with particular functions could partly share a similar expression profile with the six principal isoforms of *Nrxn* mRNAs.

It is important to note that we did not find any neuronal populations that express only a single *Nrxn* isoform. This provides support for the redundancy of Nrxn proteins, which could reduce deleterious conseguences of synaptic dysfunction if one of the co-expressed Nrxns has detrimental mutations. We identified brain regions that express all six *Nrxn* isoforms, including olfactory bulb mitral cell layer, hippocampal CA3 and piriform cortex pyramidal cell layers. The expression of all *Nrxns* were particularly high in piriform cortex. Piriform cortex is the first cortical area receiving olfactory information and contains strong associational circuits (Hagiwara et al., 2012). Expression of multiple *Nrxn* isoforms may be important to maintain the connectivity of this high-fidelity circuit.

We identified *αNrxn1* as the most ubiguitous *Nrxn* isoform in any brain region. Importantly, *αNrxn1* mRNA was expressed in neuronal cell types (glutamatergic, GABAergic, catecholaminergic neurons) and astrocytes. This may explain the strong association of *αNrxn1* mutations with neurodevelopmental disorders, including ASD, ADHD, intellectual disability, schizophrenia, and Tourette syndrome (Sebat et al., 2007; Szatmari et al., 2007; Kim et al., 2008; Yan et al., 2008; Zahir et al., 2008; Ching et al., 2010; Clarke et al., 2012; Vinas-Jornet et al., 2014; Autism Spectrum Disorders Working Group of The Psychiatric Genomics, 2017).

We found the non-neuronal expressions of *αNrxn1* and *αNrxn2*. It is important to identify the cell type(s) that interacts with *αNrxn1* and *αNrxn2* mRNA-expressing astrocytes. It has been reported that Nlgns expressed in astrocytes control synaptogenesis and astrocyte morphogenesis (Stogsdill et al., 2017). It is intriguing to address the role of Nlgn-Nrxn protein interaction between astrocytes. Addressing the involvement of Nrxns on gliotransmission or exocytotic release of neurotransmitters and factors from astrocytes to neurons should help to elucidate the role of Nrxns in astrocytes (Parpura and Zorec, 2010). We found *αNrxn2* as a major *Nrxn* mRNA in oligodenrtocytes (Figures 16 m, o **and** 17m, o). αNrxn2 protein expression was reported in oligodendrocyte-like cells in the early developing human cerebral cortex (Harkin et al., 2017). It has been suggested that Nlgn3 expressed in oligodendrocytes and axonal Nrxn protein interactions are important for oligodendrocyte differentiation (Proctor et al., 2015). Further studies addressing the role of *αNrxn2* in oligodendrocyte development and function are reguired.

Lastly, we examined the mRNA expression patterns of three gene families, *Nlgns, Lrrtms* and *Adgrls*, that encode major Nrxn binding proteins, and compared their brain region-specific expression patterns to that of *Nrxns.* All three gene families had diverse expression profiles throughout the brain (Figure 18). In particular, hippocampal CA1 pyramidal neurons, which receive excitatory inputs from CA3 pyramidal neurons, expressed most of these genes except *Lrrtm3* and *Lrrtm4*, likely contributing to numerous combinations of trans-synaptic interactions. In contrast, CA3 pyramidal neurons, which form associational circuits with each other, expressed only *Nlgns* and *Adgrl1* at high levels. Considering the expression of multiple *Nrxn* isoforms in CA3 pyramidal cells, the differential expression of Nrxn binding partners in postsynaptic neurons could underlie the distinct distributions of different Nrxn proteins at presynaptic terminals, thus providing unique region- and cell type-specific connections important for synaptic transmission (Sudhof, 2017).

## ACKNOWLEDGEMENT

We thank Dr. Paul D. Gardner for valuable discussions and Dr. Kenji Tanaka for a gift of a *Nlgn3* probe. This work was supported by grants from the Riccio Fund for Neuroscience (to K.F.), the Whitehall Foundation (to K.F.), National Institutes of Health Grant (R01NS085215 to K.F.), Grants-in-Aid for Scientific Research (15K06732 to M.U.), and The Naito Foundation (to M.U.). The authors thank Ms. Naoe Watanabe for her skillful technical assistance.

## ABBREVIATIONS

| | |
|---|---|
| **3v:** | Third ventricle |
| **A1:** | Primary auditory cortex |
| **aq:** | Cerebral aqueduct |
| **Arc:** | Arcuate nucleus |
| **BA:** | Basal nucleus of amygdala |
| **BS:** | Brainstem |
| **CA:** | Central nucleus of amygdala |
| **CA1:** | Field CA1 of hippocampus |
| **CA2:** | Field CA2 of hippocampus |
| **CA3:** | Field CA3 of hippocampus |
| **Cb:** | Cerebellum |
| **Cl:** | Claustrum |
| **CM:** | Centromedian thalamic nucleus |
| **CPu:** | Caudate-putamen |
| **Cx:** | Cortex |
| **DG:** | Dentate gyrus |

| | |
|---|---|
| **DLL:** | Dorsal nucleus of lateral lemniscus |
| **DMH:** | Dorsomedial hypothalamus |
| **DMX:** | Dorsal motor nucleus of vagus nerve |
| **DRD:** | Dorsal part of dorsal raphe nucleus |
| **DRL:** | Lateral part of dorsal raphe nucleus |
| **DRV:** | Ventral part of dorsal raphe nucleus |
| **Epl:** | External plexiform layer of olfactory bulb |
| **EW:** | Edinger-Westphal nucleus |
| **Gl:** | Glomerular layer of olfactory bulb |
| **GrC:** | Granule cell layer of cerebellum |
| **GrO:** | Granule cell layer of olfactory bulb |
| **GRN:** | Gigantocellular reticular nucleus |
| **Hi:** | Hippocampus |
| **IC:** | Inferior colliculus |
| **ICj:** | Islands of Calleja |
| **IL:** | Infralimbic cortex |
| **IO:** | Inferior olivary complex |
| **IPN:** | Interpeduncular nucleus |
| **L1:** | Cortical layer 1 |
| **L2/3:** | Cortical layers 2/3 |
| **L4:** | Cortical layer 4 |
| **L5:** | Cortical layer 5 |
| **L6:** | Cortical layer 6 |
| **LA:** | Lateral nucleus of amygdala |
| **LC:** | Locus coeruleus |
| **LD:** | Laterodorsal thalamic nucleus |
| **LDTg:** | Laterodorsal tegmental nucleus |
| **LEnt:** | Lateral entorhinal cortex |
| **LH:** | Lateral hypothalamus |

| | |
|---|---|
| **LHb:** | Lateral habenula |
| **LP:** | Lateral posterior thalamic nucleus |
| **LPB:** | Lateral parabrachial nucleus |
| **LRN:** | Lateral reticular nucleus |
| **LS:** | Lateral septal nucleus |
| **M1:** | Primary motor cortex |
| **MD:** | Mediodorsal thalamic nucleus |
| **MEnt:** | Medial entorhinal cortex |
| **MGN:** | Medial geniculate nucleus |
| **MHb:** | Medial habenula |
| **Mi:** | Mitral layer of olfactory bulb |
| **ML:** | Molecular layer of cerebellum |
| **MPB:** | Medial parabrachial nucleus |
| **MRN:** | Medullary reticular nucleus |
| **NAc:** | Nucleus accumbens |
| **ND:** | Nucleus of Darkschewitsch |
| **NDB:** | Nucleus of diagonal band |
| **NTB:** | Nucleus of trapezoid body |
| **NTS:** | nucleus of tractus solitaries |
| **Ob:** | Olfactory bulb |
| **OT:** | Olfactory tubercle |
| **PAG:** | Periaqueductal gray |
| **PBG:** | Parabigeminal nucleus |
| **PCL:** | Purkinje cell layer of cerebellum |
| **Pir:** | Piriform cortex |
| **PRN:** | Pontine reticular nucleus |
| **PrV:** | Principal sensory nucleus of trigeminal nerve |
| **PrL:** | Prelimbic cortex |
| **PVT:** | Paraventricular thalamic nucleus |

| | |
|---|---|
| **RSG:** | Retrosplenial granular cortex |
| **Rt:** | Reticular thalamic nucleus |
| **S1:** | Primary somatosensory cortex |
| **SC:** | Superior colliculus |
| **SNc:** | Substantia nigra pars compacta |
| **SNr:** | Substantia nigra pars reticulate |
| **SOP:** | Paraolivary region of superior olivary complex |
| **SpV:** | Spinal nucleus of trigeminal nerve |
| **STN:** | Subthalamic nucleus |
| **Su:** | Subiculum |
| **Th:** | Thalamus |
| **V1:** | Primary visual cortex |
| **VC:** | Ventral cochlear nucleus |
| **VII:** | Facial nucleus |
| **VMH:** | Ventromedial hypothalamus |
| **VPL:** | Ventral posterolateral thalamic nucleus |
| **VPM:** | Ventral posteromedial thalamic nucleus |
| **VTA:** | Ventral tegmental area |
| **XII:** | Hypoglossal nucleus |

## LITERATURE CITED

Amaral D, Pierre L. 2006 Hippocampal Neuroanatomy The Hippocampus Book.

Aoto J, Foldy C, Ilcus SM, Tabuchi K, Sudhof TC. 2015 Distinct circuit-dependent functions of presynaptic neurexin-3 at GABAergic and glutamatergic synapses. Nat Neurosci 18(7):997–1007. [PubMed: 26030848]

Autism Spectrum Disorders Working Group of The Psychiatric Genomics C. 2017 Meta-analysis of GWAS of over 16,000 individuals with autism spectrum disorder highlights a novel locus at 10q24.32 and a significant overlap with schizophrenia. Mol Autism 8:21. [PubMed: 28540026]

Boucard AA, Chubykin AA, Comoletti D, Taylor P, Sudhof TC. 2005 A splice code for trans-synaptic cell adhesion mediated by binding of neuroligin 1 to alpha- and beta-neurexins. Neuron 48(2):229–236. [PubMed: 16242404]

Boucard AA, Ko J, Sudhof TC. 2012 High affinity neurexin binding to cell adhesion G-protein-coupled receptor CIRL1/latrophilin-1 produces an intercellular adhesion complex. J Biol Chem 287(12):9399–9413. [PubMed: 22262843]

Chen LY, Jiang M, Zhang B, Gokce O, Sudhof TC. 2017 Conditional Deletion of All Neurexins Defines Diversity of Essential Synaptic Organizer Functions for Neurexins. Neuron 94(3):611–625 e614. [PubMed: 28472659]

Chih B, Gollan L, Scheiffele P. 2006 Alternative splicing controls selective trans-synaptic interactions of the neuroligin-neurexin complex. Neuron 51(2):171–178. [PubMed: 16846852]

Ching MS, Shen Y, Tan WH, Jeste SS, Morrow EM, Chen X, Mukaddes NM, Yoo SY, Hanson E, Hundley R, Austin C, Becker RE, Berry GT, Driscoll K, Engle EC, Friedman S, Gusella JF, Hisama FM, Irons MB, Lafiosca T, LeClair E, Miller DT, Neessen M, Picker JD, Rappaport L, Rooney CM, Sarco DP, Stoler JM, Walsh CA, Wolff RR, Zhang T, Nasir RH, Wu BL, Children's Hospital Boston Genotype Phenotype Study G. 2010 Deletions of NRXN1 (neurexin-1) predispose to a wide spectrum of developmental disorders. Am J Med Genet B Neuropsychiatr Genet 153B(4):937–947. [PubMed: 20468056]

Clarke RA, Lee S, Eapen V. 2012 Pathogenetic model for Tourette syndrome delineates overlap with related neurodevelopmental disorders including Autism. Translational psychiatry 2:e158. [PubMed: 22948383]

Dachtler J, Glasper J, Cohen RN, Ivorra JL, Swiffen DJ, Jackson AJ, Harte MK, Rodgers RJ, Clapcote SJ. 2014 Deletion of alpha-neurexin II results in autism-related behaviors in mice. Translational psychiatry 4:e484. [PubMed: 25423136]

de Wit J, Sylwestrak E, O'Sullivan ML, Otto S, Tiglio K, Savas JN, Yates JR 3rd, Comoletti D, Taylor P, Ghosh A 2009 LRRTM2 interacts with Neurexin1 and regulates excitatory synapse formation. Neuron 64(6):799–806. [PubMed: 20064388]

Etherton MR, Tabuchi K, Sharma M, Ko J, Sudhof TC. 2011 An autism-associated point mutation in the neuroligin cytoplasmic tail selectively impairs AMPA receptor-mediated synaptic transmission in hippocampus. EMBO J 30(14):2908–2919. [PubMed: 21642956]

Fallon JH, Riley JN, Sipe JC, Moore RY. 1978 The islands of Calleja: organization and connections. J Comp Neurol 181(2):375–395. [PubMed: 80412]

Fuccillo MV, Foldy C, Gokce O, Rothwell PE, Sun GL, Malenka RC, Sudhof TC. 2015 Single-Cell mRNA Profiling Reveals Cell-Type-Specific Expression of Neurexin Isoforms. Neuron 87(2):326–340. [PubMed: 26182417]

Futai K, Doty CD, Baek B, Ryu J, Sheng M. 2013 Specific trans-synaptic interaction with inhibitory interneuronal neurexin underlies differential ability of neuroligins to induce functional inhibitory synapses. J Neurosci 33(8):3612–3623. [PubMed: 23426688]

Futai K, Kim MJ, Hashikawa T, Scheiffele P, Sheng M, Hayashi Y. 2007 Retrograde modulation of presynaptic release probability through signaling mediated by PSD-95-neuroligin. Nat Neurosci 10(2):186–195. [PubMed: 17237775]

Galle SA, Courchesne V, Mottron L, Frasnelli J. 2013 Olfaction in the autism spectrum. Perception 42(3):341–355. [PubMed: 23837210]

Gonzalez-Lozano MA, Klemmer P, Gebuis T, Hassan C, van Nierop P, van Kesteren RE, Smit AB, Li KW. 2016 Dynamics of the mouse brain cortical synaptic proteome during postnatal brain development. Scientific reports 6:35456. [PubMed: 27748445]

Gorecki DC, Szklarczyk A, Lukasiuk K, Kaczmarek L, Simons JP. 1999 Differential seizure-induced and developmental changes of neurexin expression. Mol Cell Neurosci 13(3):218–227. [PubMed: 10408888]

Graf ER, Zhang X, Jin SX, Linhoff MW, Craig AM. 2004 Neurexins induce differentiation of GABA and glutamate postsynaptic specializations via neuroligins. Cell 119(7):1013–1026. [PubMed: 15620359]

Grayton HM, Missler M, Collier DA, Fernandes C. 2013 Altered social behaviours in neurexin 1alpha knockout mice resemble core symptoms in neurodevelopmental disorders. PLoS One 8(6):e67114. [PubMed: 23840597]

Hagiwara A, Pal SK, Sato TF, Wienisch M, Murthy VN. 2012 Optophysiological analysis of associational circuits in the olfactory cortex. Frontiers in neural circuits 6:18. [PubMed: 22529781]

Harkin LF, Lindsay SJ, Xu Y, Alzu'bi A, Ferrara A, Gullon EA, James OG, Clowry GJ. 2017 Neurexins 1-3 Each Have a Distinct Pattern of Expression in the Early Developing Human Cerebral Cortex. Cereb Cortex 27(1):216–232. [PubMed: 28013231]

Ichtchenko K, Hata Y, Nguyen T, Ullrich B, Missler M, Moomaw C, Sudhof TC. 1995 Neuroligin 1: a splice site-specific ligand for beta-neurexins. Cell 81(3):435–443. [PubMed: 7736595]

Ichtchenko K, Nguyen T, Sudhof TC. 1996 Structures, alternative splicing, and neurexin binding of multiple neuroligins. J Biol Chem 271(5):2676–2682. [PubMed: 8576240]

Kang Y, Zhang X, Dobie F, Wu H, Craig AM. 2008 Induction of GABAergic postsynaptic differentiation by alpha-neurexins. J Biol Chem 283(4):2323–2334. [PubMed: 18006501]

Kim HG, Kishikawa S, Higgins AW, Seong IS, Donovan DJ, Shen Y, Lally E, Weiss LA, Najm J, Kutsche K, Descartes M, Holt L, Braddock S, Troxell R, Kaplan L, Volkmar F, Klin A, Tsatsanis K, Harris DJ, Noens I, Pauls DL, Daly MJ, MacDonald ME, Morton CC, Quade BJ, Gusella JF. 2008 Disruption of neurexin 1 associated with autism spectrum disorder. Am J Hum Genet 82(1): 199–207. [PubMed: 18179900]

Ko J, Fuccillo MV, Malenka RC, Sudhof TC. 2009 LRRTM2 functions as a neurexin ligand in promoting excitatory synapse formation. Neuron 64(6):791–798. [PubMed: 20064387]

Koehnke J, Katsamba PS, Ahlsen G, Bahna F, Vendome J, Honig B, Shapiro L, Jin X. 2010 Splice form dependence of beta-neurexin/neuroligin binding interactions. Neuron 67(1):61–74. [PubMed: 20624592]

Kudo T, Uchigashima M, Miyazaki T, Konno K, Yamasaki M, Yanagawa Y, Minami M, Watanabe M. 2012 Three types of neurochemical projection from the bed nucleus of the stria terminalis to the ventral tegmental area in adult mice. J Neurosci 32(50):18035–18046. [PubMed: 23238719]

Matsuda K, Budisantoso T, Mitakidis N, Sugaya Y, Miura E, Kakegawa W, Yamasaki M, Konno K, Uchigashima M, Abe M, Watanabe I, Kano M, Watanabe M, Sakimura K, Aricescu AR, Yuzaki M. 2016 Transsynaptic Modulation of Kainate Receptor Functions by C1q-like Proteins. Neuron 90(4):752–767. [PubMed: 27133466]

Missler M, Hammer RE, Sudhof TC. 1998 Neurexophilin binding to alpha-neurexins. A single LNS domain functions as an independently folding ligand-binding unit. J Biol Chem 273(52):34716–34723. [PubMed: 9856994]

Nam CI, Chen L. 2005 Postsynaptic assembly induced by neurexin-neuroligin interaction and neurotransmitter. Proc Natl Acad Sci U S A 102(17):6137–6142. [PubMed: 15837930]

Nguyen TM, Schreiner D, Xiao L, Traunmuller L, Bornmann C, Scheiffele P. 2016 An alternative splicing switch shapes neurexin repertoires in principal neurons versus interneurons in the mouse hippocampus. eLife 5.

Parpura V, Zorec R. 2010 Gliotransmission: Exocytotic release from astrocytes. Brain research reviews 63(1-2):83–92. [PubMed: 19948188]

Proctor DT, Stotz SC, Scott LOM, de la Hoz CLR, Poon KWC, Stys PK, Colicos MA. 2015 Axo-glial communication through neurexin-neuroligin signaling regulates myelination and oligodendrocyte differentiation. Glia 63(11):2023–2039. [PubMed: 26119281]

Puschel AW, Betz H. 1995 Neurexins are differentially expressed in the embryonic nervous system of mice. J Neurosci 15(4):2849–2856. [PubMed: 7722633]

Reissner C, Klose M, Fairless R, Missler M. 2008 Mutational analysis of the neurexin/neuroligin complex reveals essential and regulatory components. Proc Natl Acad Sci U S A 105(39):15124–15129. [PubMed: 18812509]

RK CY, Merico D, Bookman M, J LH, Thiruvahindrapuram B, Patel RV, Whitney J, Deflaux N, Bingham J, Wang Z, Pellecchia G, Buchanan JA, Walker S, Marshall CR, Uddin M, Zarrei M, Deneault E, D'Abate L, Chan AJ, Koyanagi S, Paton T, Pereira SL, Hoang N, Engchuan W, Higginbotham EJ, Ho K, Lamoureux S, Li W, MacDonald JR, Nalpathamkalam T, Sung WW, Tsoi FJ, Wei J, Xu L, Tasse AM, Kirby E, Van Etten W, Twigger S, Roberts W, Drmic I, Jilderda S, Modi BM, Kellam B, Szego M, Cytrynbaum C, Weksberg R, Zwaigenbaum L, Woodbury-Smith M, Brian J, Senman L, Iaboni A, Doyle-Thomas K, Thompson A, Chrysler C, Leef J, Savion-Lemieux T, Smith IM, Liu X, Nicolson R, Seifer V, Fedele A, Cook EH, Dager S, Estes A, Gallagher L, Malow BA, Parr JR, Spence SJ, Vorstman J, Frey BJ, Robinson JT, Strug LJ, Fernandez BA, Elsabbagh M, Carter MT, Hallmayer J, Knoppers BM, Anagnostou E, Szatmari P, Ring RH, Glazer D, Pletcher MT, Scherer SW. 2017 Whole genome sequencing resource identifies 18 new candidate genes for autism spectrum disorder. Nat Neurosci 20(4):602–611. [PubMed: 28263302]

Schreiner D, Nguyen TM, Russo G, Heber S, Patrignani A, Ahrne E, Scheiffele P. 2014 Targeted combinatorial alternative splicing generates brain region-specific repertoires of neurexins. Neuron 84(2):386–398. [PubMed: 25284007]

Schreiner D, Simicevic J, Ahrne E, Schmidt A, Scheiffele P. 2015 Quantitative isoform-profiling of highly diversified recognition molecules. eLife 4:e07794. [PubMed: 25985086]

Sebat J, Lakshmi B, Malhotra D, Troge J, Lese-Martin C, Walsh T, Yamrom B, Yoon S, Krasnitz A, Kendall J, Leotta A, Pai D, Zhang R, Lee YH, Hicks J, Spence SJ, Lee AT, Puura K, Lehtimaki T, Ledbetter D, Gregersen PK, Bregman J, Sutcliffe JS, Jobanputra V, Chung W, Warburton D, King MC, Skuse D, Geschwind DH, Gilliam TC, Ye K, Wigler M. 2007 Strong association of de novo copy number mutations with autism. Science 316(5823):445–449. [PubMed: 17363630]

Singh SK, Stogsdill JA, Pulimood NS, Dingsdale H, Kim YH, Pilaz LJ, Kim IH, Manhaes AC, Rodrigues WS Jr., Pamukcu A, Enustun E, Ertuz Z, Scheiffele P, Soderling SH, Silver DL, Ji RR, Medina AE, Eroglu C 2016 Astrocytes Assemble Thalamocortical Synapses by Bridging NRX1alpha and NL1 via Hevin. Cell 164(1-2):183–196. [PubMed: 26771491]

Sons MS, Busche N, Strenzke N, Moser T, Ernsberger U, Mooren FC, Zhang W, Ahmad M, Steffens H, Schomburg ED, Plomp JJ, Missler M. 2006 alpha-Neurexins are required for efficient transmitter release and synaptic homeostasis at the mouse neuromuscular junction. Neuroscience 138(2):433–446. [PubMed: 16406382]

Sterky FH, Trotter JH, Lee SJ, Recktenwald CV, Du X, Zhou B, Zhou P, Schwenk J, Fakler B, Sudhof TC. 2017 Carbonic anhydrase-related protein CA10 is an evolutionarily conserved pan-neurexin ligand. Proc Natl Acad Sci U S A 114(7):E1253–E1262. [PubMed: 28154140]

Stogsdill JA, Ramirez J, Liu D, Kim YH, Baldwin KT, Enustun E, Ejikeme T, Ji RR, Eroglu C. 2017 Astrocytic neuroligins control astrocyte morphogenesis and synaptogenesis. Nature 551(7679): 192–197. [PubMed: 29120426]

Sudhof TC. 2017 Synaptic Neurexin Complexes: A Molecular Code for the Logic of Neural Circuits. Cell 171(4):745–769. [PubMed: 29100073]

Sugita S, Saito F, Tang J, Satz J, Campbell K, Sudhof TC. 2001 A stoichiometric complex of neurexins and dystroglycan in brain. J Cell Biol 154(2):435–445. [PubMed: 11470830]

Szatmari P, Paterson AD, Zwaigenbaum L, Roberts W, Brian J, Liu XQ, Vincent JB, Skaug JL, Thompson AP, Senman L, Feuk L, Qian C, Bryson SE, Jones MB, Marshall CR, Scherer SW, Vieland VJ, Bartlett C, Mangin LV, Goedken R, Segre A, Pericak-Vance MA, Cuccaro ML, Gilbert JR, Wright HH, Abramson RK, Betancur C, Bourgeron T, Gillberg C, Leboyer M, Buxbaum JD, Davis KL, Hollander E, Silverman JM, Hallmayer J, Lotspeich L, Sutcliffe JS, Haines JL, Folstein SE, Piven J, Wassink TH, Sheffield V, Geschwind DH, Bucan M, Brown WT, Cantor RM, Constantino JN, Gilliam TC, Herbert M, Lajonchere C, Ledbetter DH, Lese-Martin C, Miller J, Nelson S, Samango-Sprouse CA, Spence S, State M, Tanzi RE, Coon H, Dawson G, Devlin B, Estes A, Flodman P, Klei L, McMahon WM, Minshew N, Munson J, Korvatska E, Rodier PM, Schellenberg GD, Smith M, Spence MA, Stodgell C, Tepper PG, Wijsman EM, Yu CE, Roge B, Mantoulan C, Wittemeyer K, Poustka A, Felder B, Klauck SM, Schuster C, Poustka F, Bolte S, Feineis-Matthews S, Herbrecht E, Schmotzer G, Tsiantis J, Papanikolaou K, Maestrini E, Bacchelli E, Blasi F, Carone S, Toma C, Van Engeland H, de Jonge M, Kemner C, Koop F, Langemeijer M, Hijmans C, Staal WG, Baird G, Bolton PF, Rutter ML, Weisblatt E, Green J, Aldred C, Wilkinson JA, Pickles A, Le Couteur A, Berney T, McConachie H, Bailey AJ, Francis K, Honeyman G, Hutchinson A, Parr JR, Wallace S, Monaco AP, Barnby G, Kobayashi K, Lamb JA, Sousa I, Sykes N, Cook EH, Guter SJ, Leventhal BL, Salt J, Lord C, Corsello C, Hus V, Weeks DE, Volkmar F, Tauber M, Fombonne E, Shih A, Meyer KJ. 2007 Mapping autism risk loci using genetic linkage and chromosomal rearrangements. Nat Genet 39(3):319–328. [PubMed: 17322880]

Tabuchi K, Blundell J, Etherton MR, Hammer RE, Liu X, Powell CM, Sudhof TC. 2007 A neuroligin-3 mutation implicated in autism increases inhibitory synaptic transmission in mice. Science 318(5847):71–76. [PubMed: 17823315]

Tabuchi K, Sudhof TC. 2002 Structure and evolution of neurexin genes: insight into the mechanism of alternative splicing. Genomics 79(6):849–859. [PubMed: 12036300]

Tanabe Y, Naito Y, Vasuta C, Lee AK, Soumounou Y, Linhoff MW, Takahashi H. 2017 IgSF21 promotes differentiation of inhibitory synapses via binding to neurexin2alpha. Nature communications 8(1):408.

Tanaka KF, Ahmari SE, Leonardo ED, Richardson-Jones JW, Budreck EC, Scheiffele P, Sugio S, Inamura N, Ikenaka K, Hen R. 2010 Flexible Accelerated STOP Tetracycline Operator-knockin

(FAST): a versatile and efficient new gene modulating system. Biol Psychiatry 67(8):770–773. [PubMed: 20163789]

Treutlein B, Gokce O, Quake SR, Sudhof TC. 2014 Cartography of neurexin alternative splicing mapped by single-molecule long-read mRNA sequencing. Proc Natl Acad Sci U S A 111(13):E1291–1299. [PubMed: 24639501]

Uchigashima M, Ohtsuka T, Kobayashi K, Watanabe M. 2016 Dopamine synapse is a neuroligin-2-mediated contact between dopaminergic presynaptic and GABAergic postsynaptic structures. Proc Natl Acad Sci U S A 113(15):4206–4211. [PubMed: 27035941]

Uemura T, Lee SJ, Yasumura M, Takeuchi T, Yoshida T, Ra M, Taguchi R, Sakimura K, Mishina M. 2010 Trans-synaptic interaction of GluRdelta2 and Neurexin through Cbln1 mediates synapse formation in the cerebellum. Cell 141(6):1068–1079. [PubMed: 20537373]

Ullrich B, Ushkaryov YA, Sudhof TC. 1995 Cartography of neurexins: more than 1000 isoforms generated by alternative splicing and expressed in distinct subsets of neurons. Neuron 14(3):497–507. [PubMed: 7695896]

Ushkaryov YA, Petrenko AG, Geppert M, Sudhof TC. 1992 Neurexins: synaptic cell surface proteins related to the alpha-latrotoxin receptor and laminin. Science 257(5066):50–56. [PubMed: 1621094]

Vaags AK, Lionel AC, Sato D, Goodenberger M, Stein QP, Curran S, Ogilvie C, Ahn JW, Drmic I, Senman L, Chrysler C, Thompson A, Russell C, Prasad A, Walker S, Pinto D, Marshall CR, Stavropoulos DJ, Zwaigenbaum L, Fernandez BA, Fombonne E, Bolton PF, Collier DA, Hodge JC, Roberts W, Szatmari P, Scherer SW. 2012 Rare deletions at the neurexin 3 locus in autism spectrum disorder. Am J Hum Genet 90(1):133–141. [PubMed: 22209245]

Vinas-Jornet M, Esteba-Castillo S, Gabau E, Ribas-Vidal N, Baena N, San J, Ruiz A, Coll MD, Novell R, Guitart M. 2014 A common cognitive, psychiatric, and dysmorphic phenotype in carriers of NRXN1 deletion. Molecular genetics & genomic medicine 2(6):512–521. [PubMed: 25614873]

Yamasaki M, Matsui M, Watanabe M. 2010 Preferential localization of muscarinic M1 receptor on dendritic shaft and spine of cortical pyramidal cells and its anatomical evidence for volume transmission. J Neurosci 30(12):4408–4418. [PubMed: 20335477]

Yamasaki M, Yamada K, Furuya S, Mitoma J, Hirabayashi Y, Watanabe M. 2001 3-Phosphoglycerate dehydrogenase, a key enzyme for l-serine biosynthesis, is preferentially expressed in the radial glia/astrocyte lineage and olfactory ensheathing glia in the mouse brain. J Neurosci 21(19):7691–7704. [PubMed: 11567059]

Yan J, Noltner K, Feng J, Li W, Schroer R, Skinner C, Zeng W, Schwartz CE, Sommer SS. 2008 Neurexin 1alpha structural variants associated with autism. Neurosci Lett 438(3):368–370. [PubMed: 18490107]

Yu P, McKinney EC, Kandasamy MM, Albert AL, Meagher RB. 2015 Characterization of brain cell nuclei with decondensed chromatin. Developmental neurobiology 75(7):738–756. [PubMed: 25369517]

Zahir FR, Baross A, Delaney AD, Eydoux P, Fernandes ND, Pugh T, Marra MA, Friedman JM. 2008 A patient with vertebral, cognitive and behavioural abnormalities and a de novo deletion of NRXN1alpha. J Med Genet 45(4):239–243. [PubMed: 18057082]

Zhang C, At a soy D, Arac D, Yang X, Fucillo MV, Robison AJ, Ko J, Brunger AT, Sudhof TC. 2010 Neurexins physically and functionally interact with GABA(A) receptors. Neuron 66(3):403–416. [PubMed: 20471353]

Here we used chromogenic and fluorescence *in situ* hybridization to characterize the expression pattern of Neurexin (Nrxn) isoforms. While each Nrxn isoform displayed a unique expression profile in different regions and cell types, αNrxn1 and αNrxn2 mRNAs were interestingly expressed in non-neuronal cells, including astrocytes and oligodendrocytes. Nrxn postsynaptic binding partners, such as Neuroligins and Latrophilins, were also diversely expressed throughout the mouse brain, emphasizing the numerous combinations of trans-synaptic interactions that can occur between these molecules.

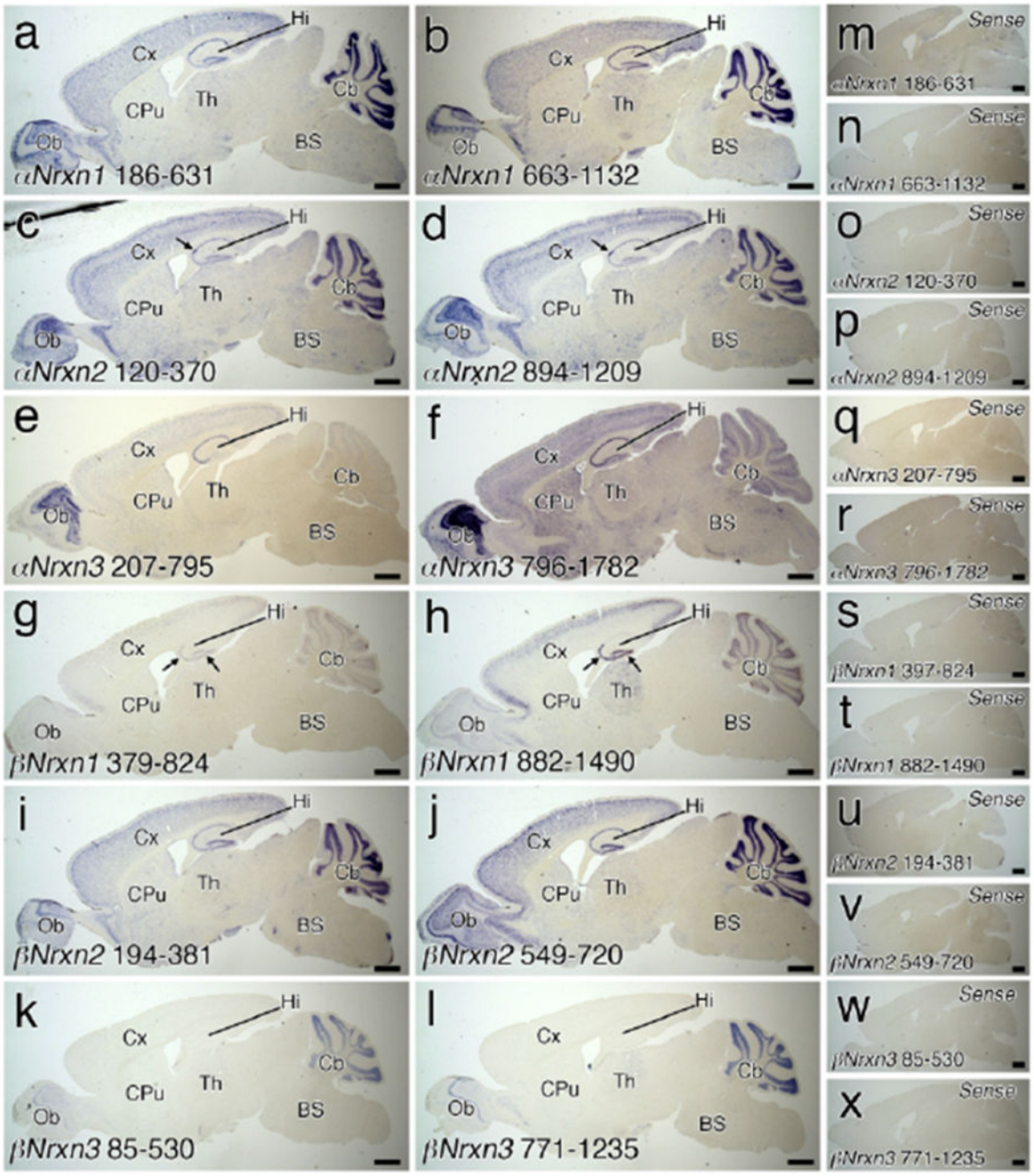


**Figure 1.**

Validation of Nrxn ISH probes in the brain. (a-l) Whole brain sagittal views of chromogenic hybridization signals with Nrxn-isoform-specific antisense cRNA probes. Two cRNA probes are prepared for αNrxn1 (a, b), αNrxn2 (c, d), αNrxn3 (e, f), βNrxn1 (g, h), βNrxn2 (i, j), and βNrxn3 (k, l) mRNAs. Arrows indicate dense staining patterns in the CA2 for αNrxn2 mRNA (c, d) and in the CA3 and dentate gyrus for βNrxn1 mRNA (g, h). (m-x) Whole brain sagittal views of chromogenic hybridization signals with two sense cRNA probes lacking

signal for αNrxn1 (m, n), αNrxn2 (o, p), αNrxn3 (q, r), βNrxn1 (s, t), βNrxn2 (u, v), and βNrxn3 (w, x) mRNAs. For abbreviations, see list. Scale bars, 1 mm.

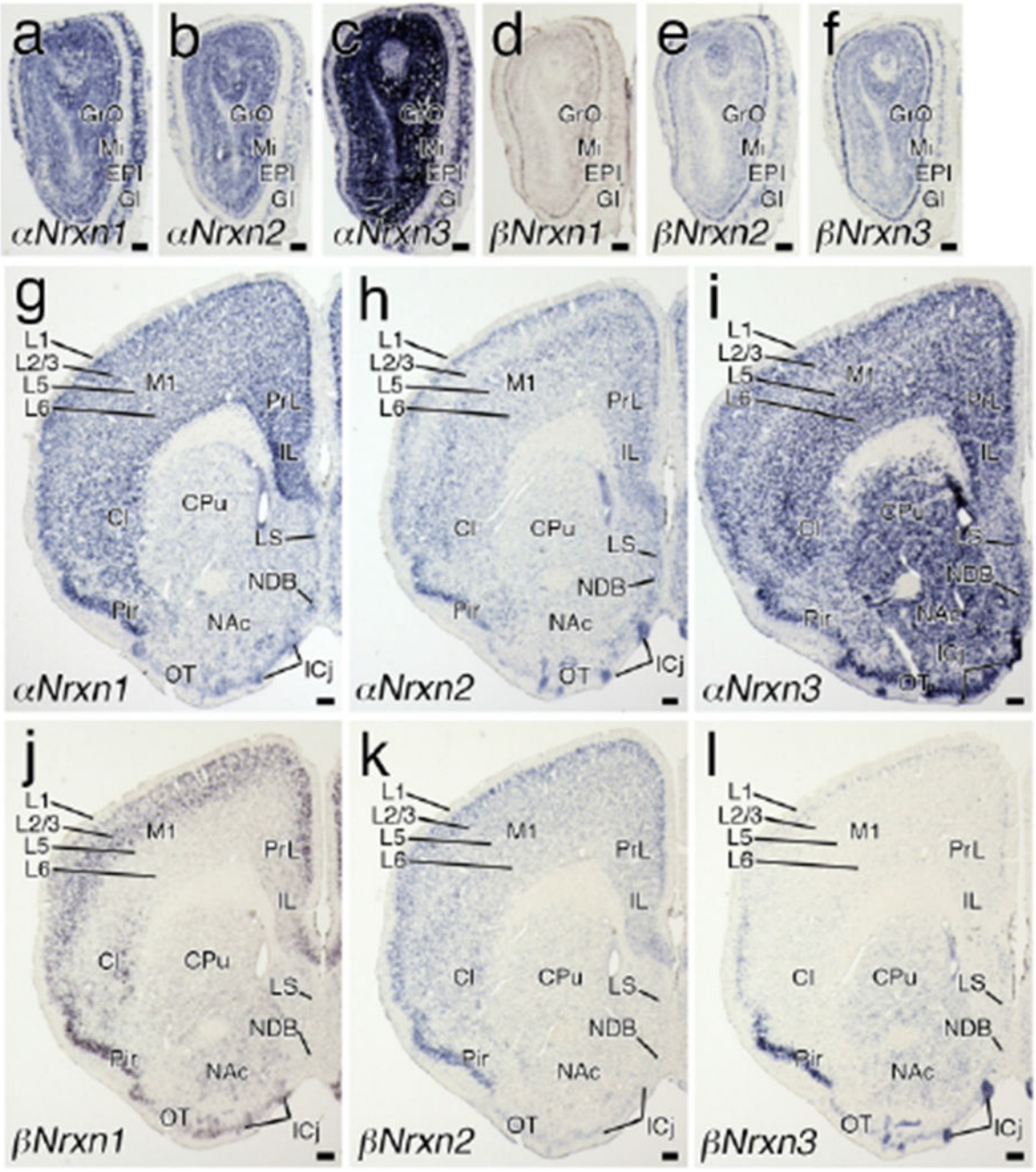


**Figure 2.**

Region-specific expression of Nrxn mRNAs in the telencephalon and diencephalon. Coronal views of chromogenic hybridization signals for αNrxn1 (a, g), αNrxn2 (b, h), αNrxn3 (c, i), βNrxn1 (d, j), βNrxn2 (e, k), and βNrxn3 (f, I) mRNAs in the mouse brain. For abbreviations, see list. Scale bars, 200 μm.

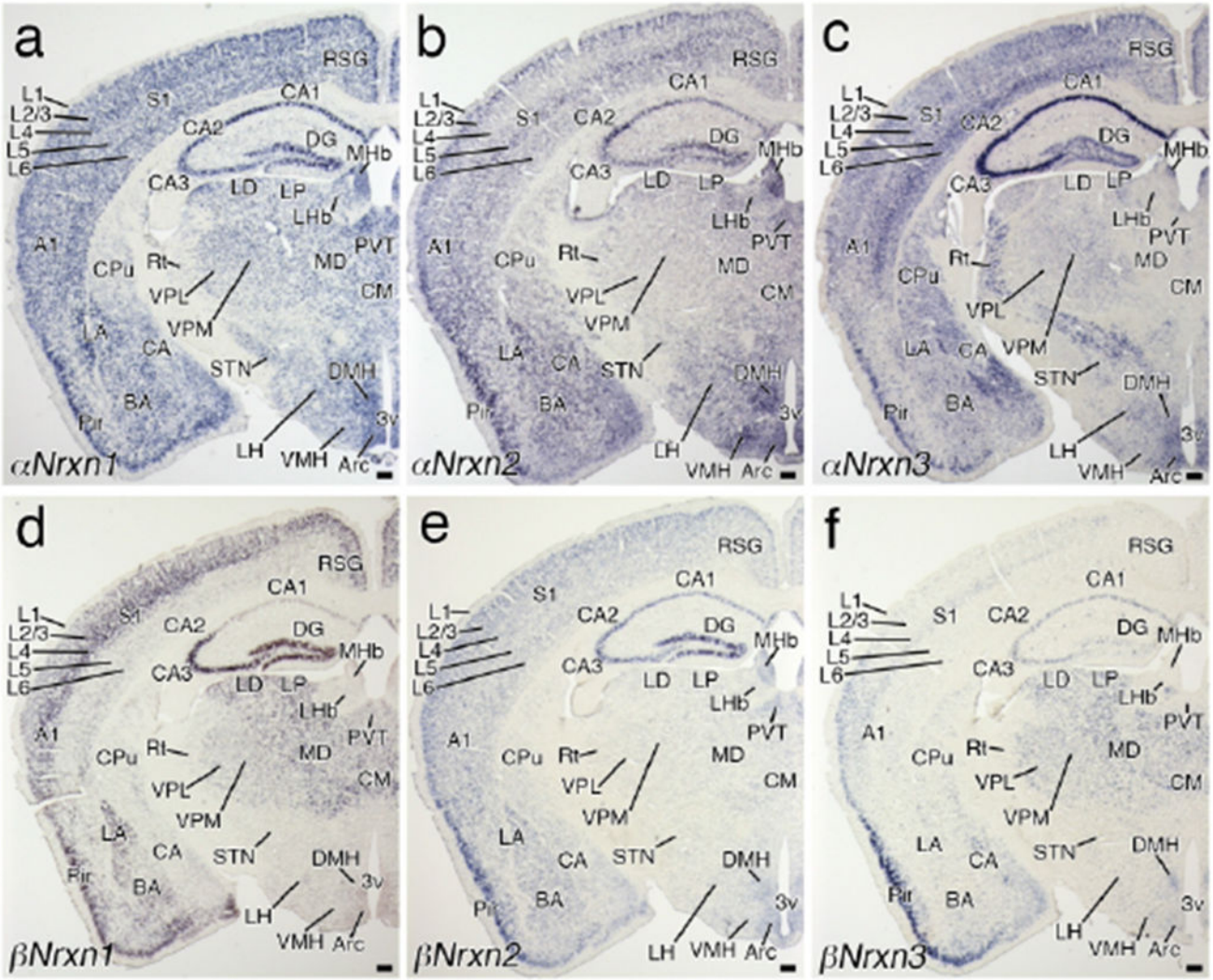


**Figure 3.**

Region-specific expression of Nrxn mRNAs in the telencephalon and diencephalon. Coronal views of chromogenic hybridization signals for αNrxn1 (a), αNrxn2 (b), αNrxn3 (c), βNrxn1 (d), βNrxn2 (e), and βNrxn3 (f) mRNAs in the mouse brain. For abbreviations, see list. Scale bars, 200 μm.

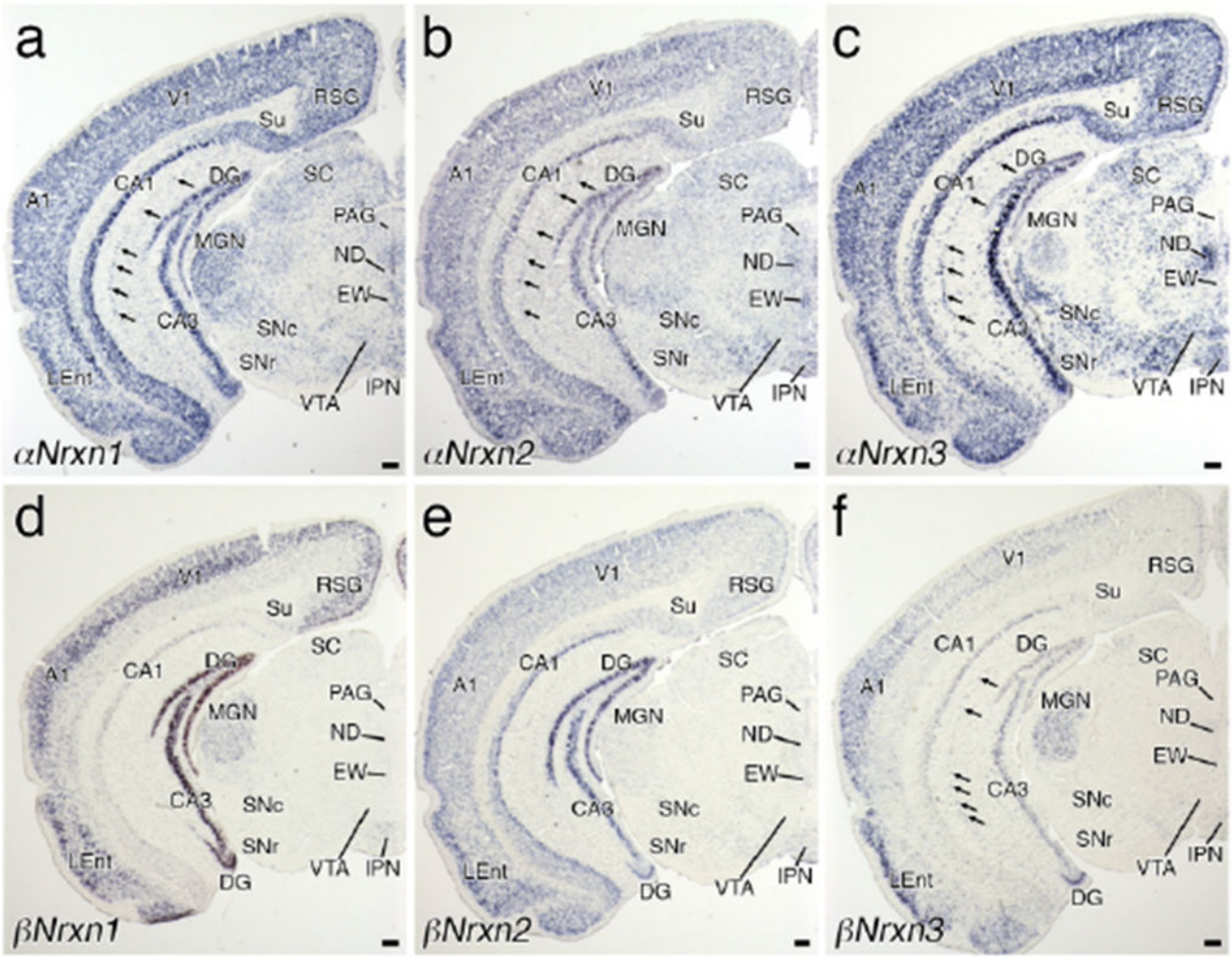


**Figure 4.**

Region-specific expression of Nrxn mRNAs in the midbrain. Coronal views of chromogenic hybridization signals for αNrxn1 (a), αNrxn2 (b), αNrxn3 (c), βNrxn1 (d), βNrxn2 (e), and βNrxn3 (f) mRNAs in the mouse brain. Arrows indicate cells expressing αNrxn1 (a), αNrxn2 (b), αNrxn3 (c), and αNrxn3 (f) mRNAs in the neuropil layer of the hippocampus. For abbreviations, see list. Scale bars, 200 μm.

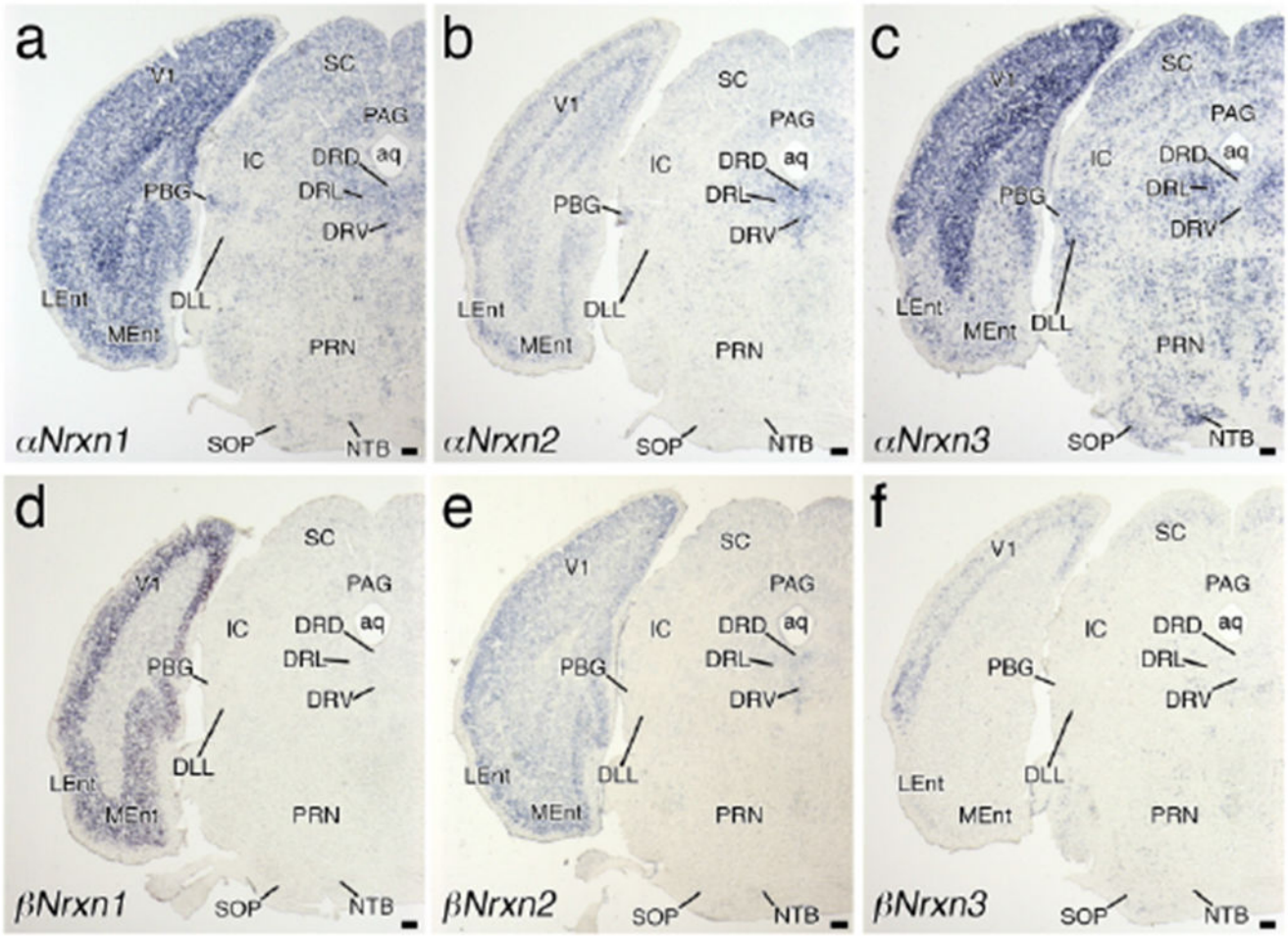


**Figure 5.**

Region-specific expression of Nrxn mRNAs in the pons. Coronal views of chromogenic hybridization signals for αNrxn1 (a), αNrxn2 (b), αNrxn3 (c), βNrxn1 (d), βNrxn2 (e), and βNrxn3 (f) mRNAs in the mouse brain. For abbreviations, see list. Scale bars, 200 μm.

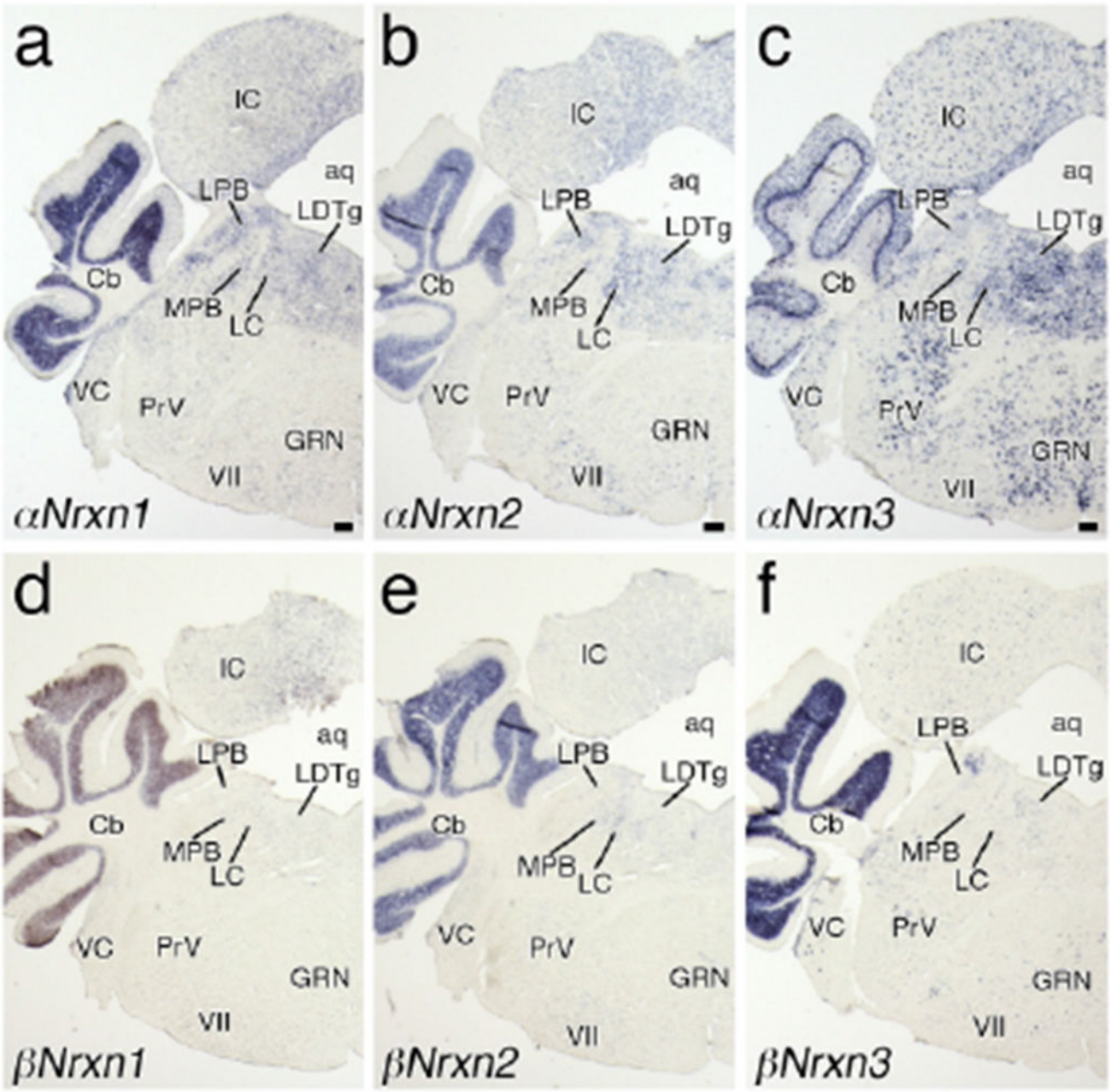


**Figure 6.**

Region-specific expression of Nrxn mRNAs in the anterior medulla. Coronal views of chromogenic hybridization signals for αNrxn1 (a), αNrxn2 (b), αNrxn3 (c), βNrxn1 (d), βNrxn2 (e), and βNrxn3 (f) mRNAs in the mouse brain. For abbreviations, see list. Scale bars, 200 μm.

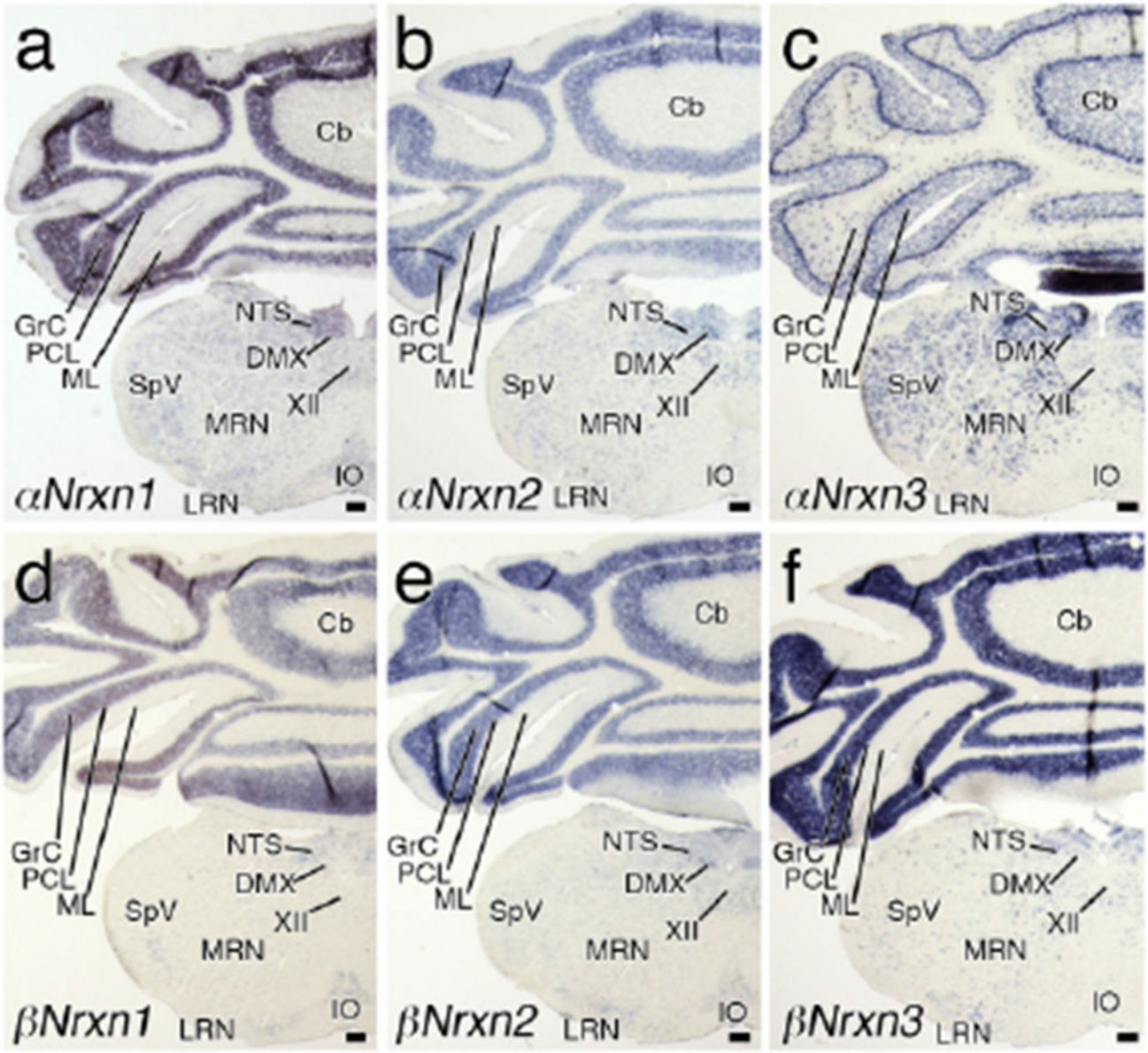


**Figure 7.**

Region-specific expression of Nrxn mRNAs in the posterior medulla. Coronal views of chromogenic hybridization signals for αNrxn1 (a), αNrxn2 (b), αNrxn3 (c), βNrxn1 (d), βNrxn2 (e), and βNrxn3 (f) mRNAs in the mouse brain. For abbreviations, see list. Scale bars, 200 μm.

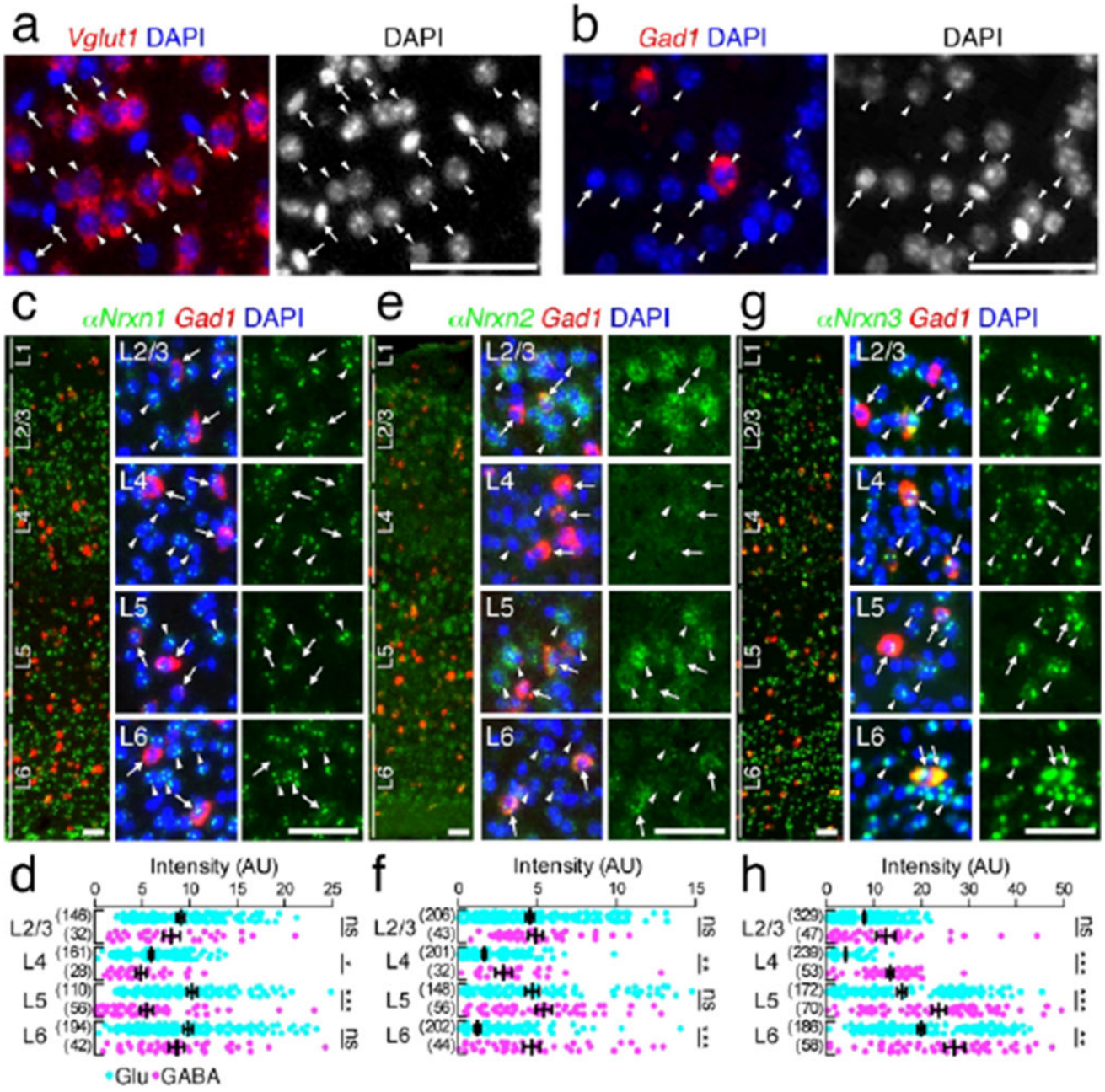


**Figure 8.**

Layer-specific expression of a αNrxn mRNAs in the primary somatosensory neocortex. (a, b) Single FISH for Vglut1 (red, a) and Gad1 (red, b) mRNAs with DAPI staining (blue and gray on the left and right, respectively). Note that Vglut1 (a) or Gad1 (b) mRNA-expressing neurons have large and pale DAPI+ nuclei (arrowheads), but not small and dark DAPI+ nuclei (arrows), (c, e, g) Double FISH for αNrxn1 (c), αNrxn2 (e), αNrxn3 (g) and Gad1 mRNAs showing distinct laminar-specific patterns of Nrxn mRNAs (green) between Gad1(+) GABAergic (red, arrows) and Gad1(−) glutamatergic (arrowheads) neurons. The left panel presents a low power-magnified image including the entire cortical layers, and the

middle and right panels present high power-magnified images of layers 2/3, 4, 5, and 6 (L2/3, L4, L5, and L6) in order from the top. Note that the signals for Nrxns in GABAergic neurons tend to be variable. Nuclei were stained with DAPI (blue). (d, f, h) Summary scatter plots for αNrxn1 (d), αNrxn2 (f), or αNrxn3 (h) mRNA in glutamatergic (aqua) and GABAergic (magenta) neurons. The numbers of cells analyzed are indicated in the parenthesis to the left of each column. Data are represented as means ± SEM. ns, not significant; * $P < 0.05$; ** $P < 0.01$; *** $P < 0.001$ (Mann-Whitney test). Scale bars, 50 μm.

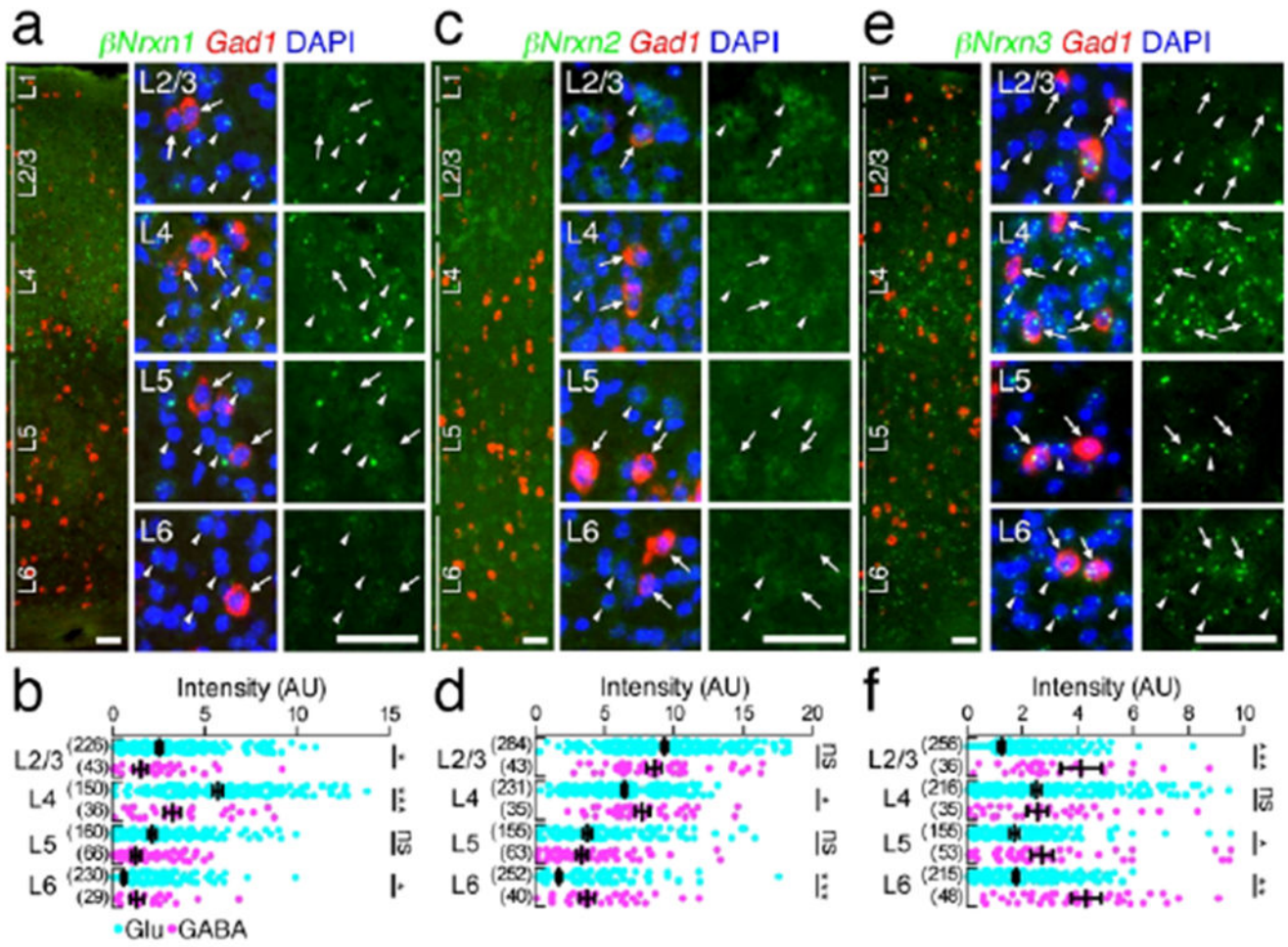


**Figure 9.**

Layer-specific expression of βNrxn mRNAs in the primary somatosensory neocortex. (a, c, e) Double FISH for βNrxn1 (a), βNrxn2 (c), or βNrxn3 (e) and Gad1 mRNAs showing distinct laminar-specific patterns of Nrxn mRNAs (green) between Gad1(+) GABAergic (red, arrows) and Gad1(−) glutamatergic (arrowheads) neurons. The left panel presents a low power-magnified image including the entire cortical layers, and the middle and right panels present high power-magnified images of layers 2/3, 4, 5, and 6 (L2/3, L4, L5, and L6) in order from the top. Note that the signals for Nrxns in GABAergic neurons tend to be variable. Nuclei were stained with DAPI (blue). (b, d, f) Summary scatter plots for βNrxn1 (b), βNrxn2 (d), or βNrxn3 (f) mRNA in glutamatergic (aqua) and GABAergic (magenta) neurons. The numbers of cells analyzed are indicated in the parenthesis to the left of each column. Data are represented as means ± SEM. ns, not significant; * $P < 0.05$; ** $P < 0,01$; *** $P < 0,001$ (Mann-Whitney test). Scale bars, 50 μm.

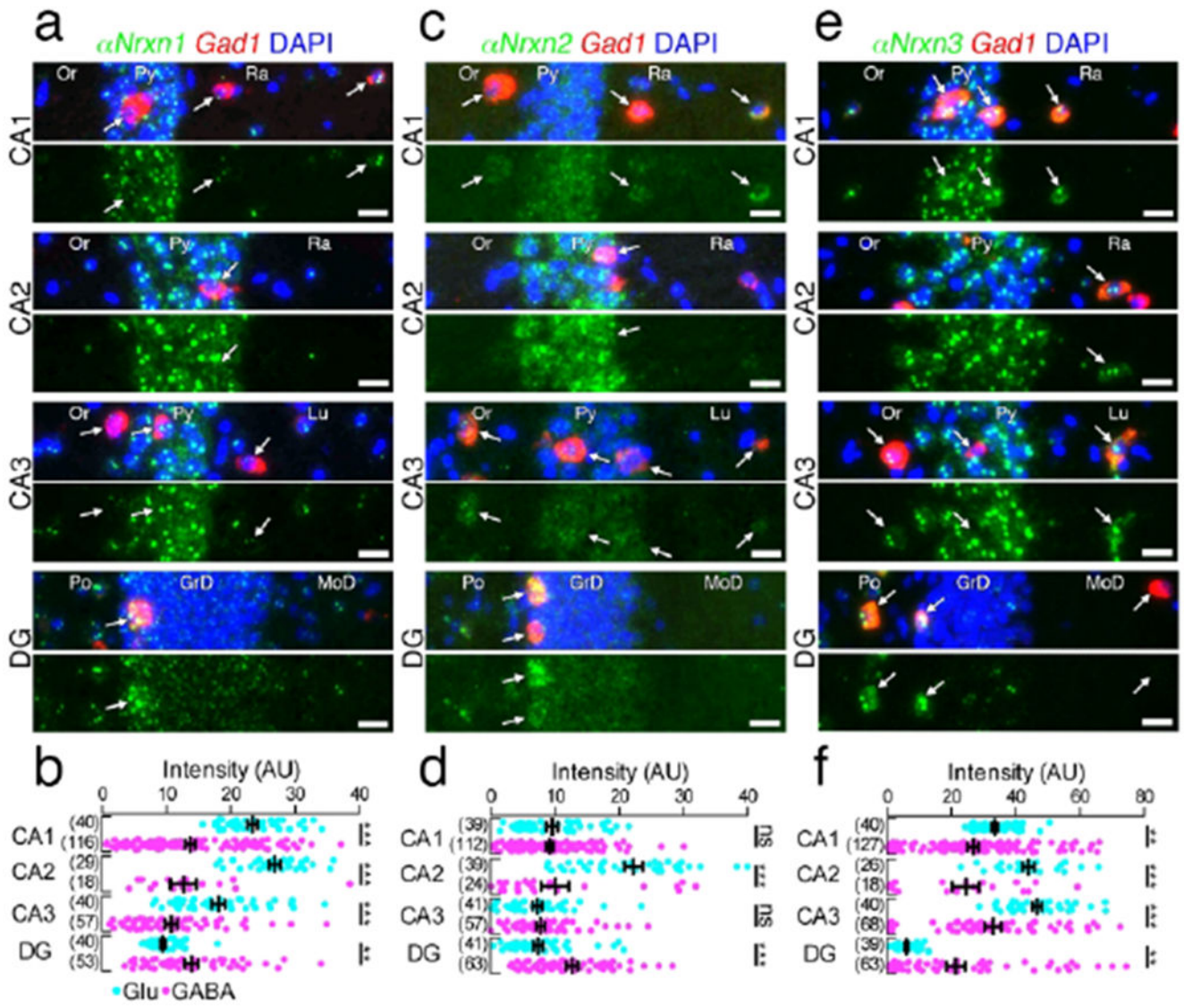


**Figure 10.**

Hippocampal subregion-specific expression of αNrxn mRNAs. (a, c, e) Double FISH for αNrxn1 (a), αNrxn2 (c), or αNrxn3 (e) and Gad1 mRNAs in the hippocampus showing different subregion-specific patterns of Nrxn mRNAs (green) between Gad1(+) GABAergic (red, arrows) and Gad1(−) glutamatergic neurons. The four pairs of panels show the CA1, CA2, CA3, and dentate gyrus (DG) in order from the top. Note that the signal intensity in individual GABAergic neurons is variable, compared with that in glutamatergic neurons. Nuclei were stained with DAPI (blue). Or, stratum oriens; Py, Pyramidal cell layer; Ra, stratum radiatum; Lu, stratum lucidum; Po, polymorphic layer; GrD, granule cell layer; MoD, molecular layer. (b, d, f) Summary scatter plots for αNrxn1 (b), αNrxn2 (d), or αNrxn3 (f) mRNA in glutamatergic (aqua) and GABAergic (magenta) neurons. The number in the parentheses next to each column indicates the number of cells analyzed. Data are represented as means ± SEM. ns, not significant; * $P < 0.05$; ** $P < 0.01$; *** $P < 0.001$ (Man-Whitney test). Scale bars, 20 μm.

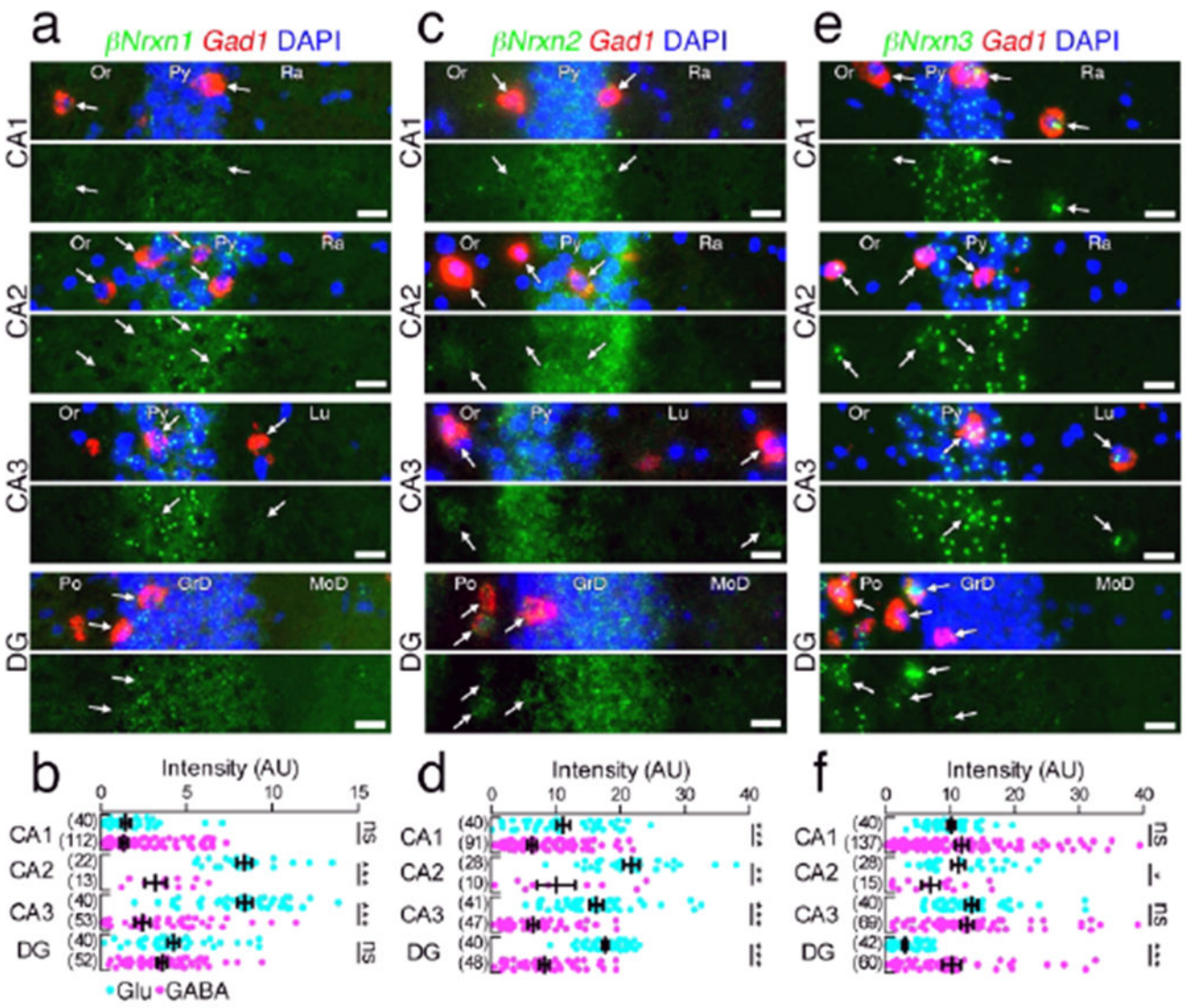


**Figure 11.**

Hippocampal subregion-specific expression of βNrxn mRNAs. (a, c, e) Double FISH for βNrxn1 (a), βNrxn2 (c), or βNrxn3 (e) and Gad1 mRNAs in the hippocampus showing different subregion-specific expression patterns of Nrxn mRNAs (green) between Gad1(+) GABAergic (red, arrows) and Gad1(−) glutamatergic neurons. The four pairs of panels show the CA1, CA2, CA3, and dentate gyrus (DG) in order from the top. Note that the signal intensity in individual GABAergic neurons is variable, compared with that in glutamatergic neurons. Nuclei were stained with DAPI (blue). Or, stratum oriens; Py, Pyramidal cell layer; Ra, stratum radiatum; Lu, stratum lucidum; Po, polymorphic layer; GrD, granule cell layer; MoD, molecular layer. (b, d, f) Summary scatter plots for βNrxn1 (b), βNrxn2 (d), or βNrxn3 (f) mRNA in glutamatergic (agua) and GABAergic (magenta) neurons. The number in the parentheses next to each column indicates the number of cells analyzed. Data are represented as means ± SEM. ns, not significant; * P < 0,05; ** P < 0,01; *** P < 0,001 (Man-Whitney test). Scale bars, 20 μm.

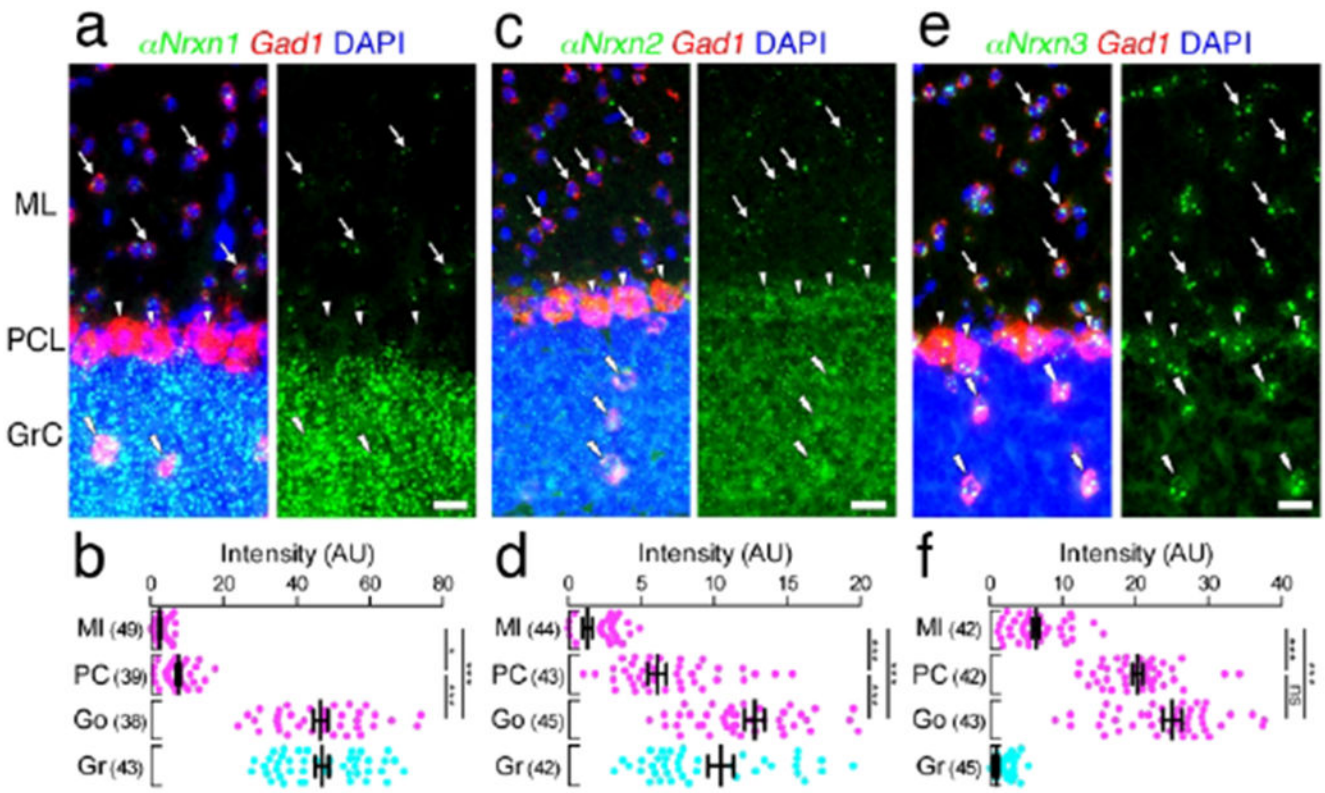


**Figure 12.**

Cell type-dependent expression of αNrxn mRNAs in the cerebellar cortex. (a, c, e, g, i, k) Double FISH for αNrxn1 (a), αNrxn2 (c), or αNrxn3 (e) and Gad1 mRNAs in the cerebellar cortex showing different expression patterns of Nrxn mRNAs (green) in Gad1 mRNA (red)-labeled molecular layer interneurons (arrows), Purkinje cells (arrowheads), and Golgi cells (double arrowheads) and Gad1 mRNA-unlabeled granule cells. Nuclei were stained with DAPI (blue). (b, d, f) Summary scatter plots for αNrxn1 (b), αNrxn2 (d), or αNrxn3 (f) mRNA in molecular layer interneurons (magenta, Ml), Purkinje cells (magenta, PC), Golgi cells (magenta, Go), and granule cells (agua, Gr). The number in the parentheses next to each column indicates the number of cells analyzed. Data are represented as means ± SEM. ns, not significant; * $P < 0.05$; ** $P < 0.01$; *** $P < 0.001$ (Kruskal-Wallis test with post hoc Dunn's test). Scale bars, 20 μm.

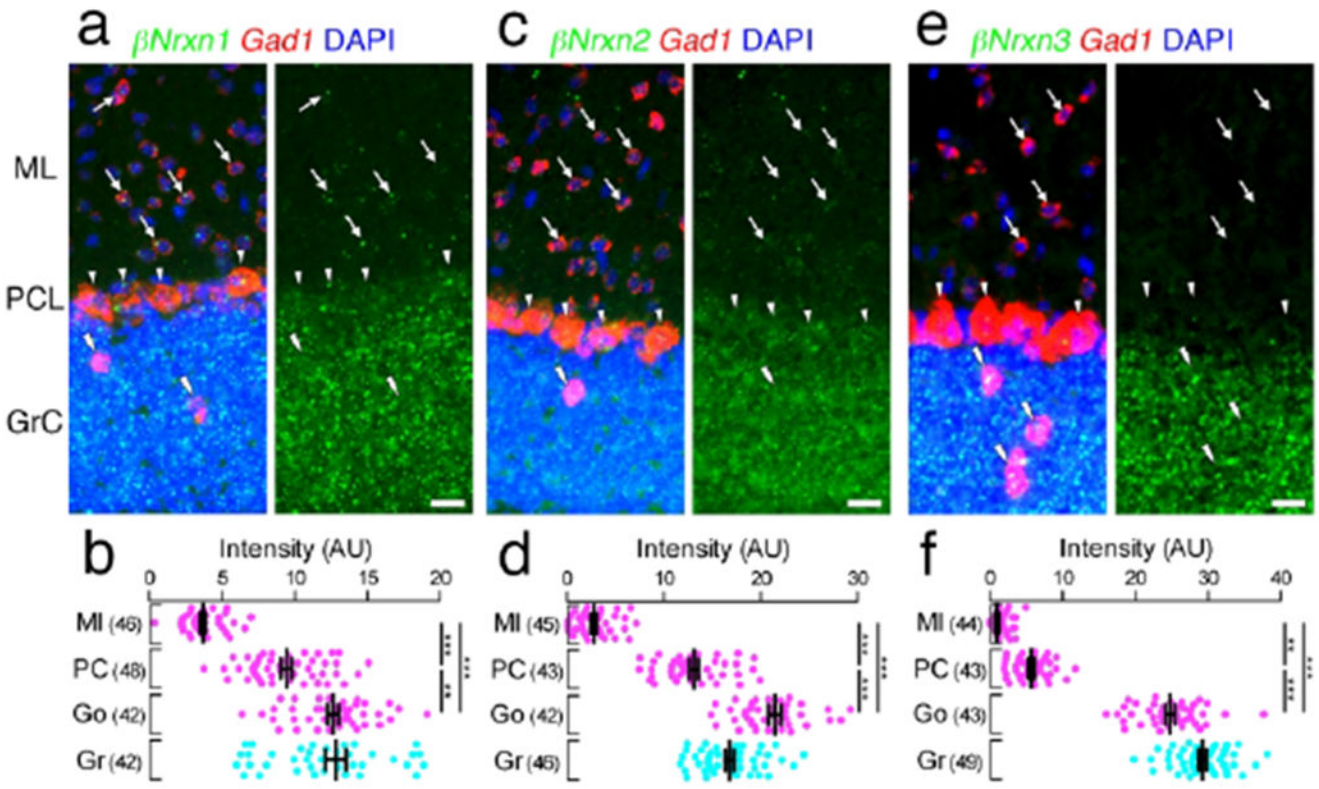


**Figure 13.**

Cell type-dependent expression of βNrxn mRNAs in the cerebellar cortex. (a, c, e) Double FISH for βNrxn1 (a), βNrxn2 (c), or βNrxn3 (e) and Gad1 mRNAs in the cerebellar cortex showing different expression patterns of Nrxn mRNAs (green) in Gad1 mRNA (red)-labeled molecular layer interneurons (arrows), Purkinje cells (arrowheads), and Golgi cells (double arrowheads) and Gad1 mRNA-unlabeled granule cells. Nuclei were stained with DAPI (blue). (b, d, f) Summary scatter plots for βNrxn1 (b), βNrxn2 (d), or βNrxn3 (f) mRNA in molecular layer interneurons (magenta, MI), Purkinje cells (magenta, PC), Golgi cells (magenta, Go), and granule cells (agua, Gr). The number in the parentheses next to each column indicates the number of cells analyzed. Data are represented as means ± SEM. ns, not significant; * $P < 0.05$; ** $P < 0,01$; *** $P < 0,001$ (Kruskal-Wallis test with post hoc Dunn's test). Scale bars, 20 μm.

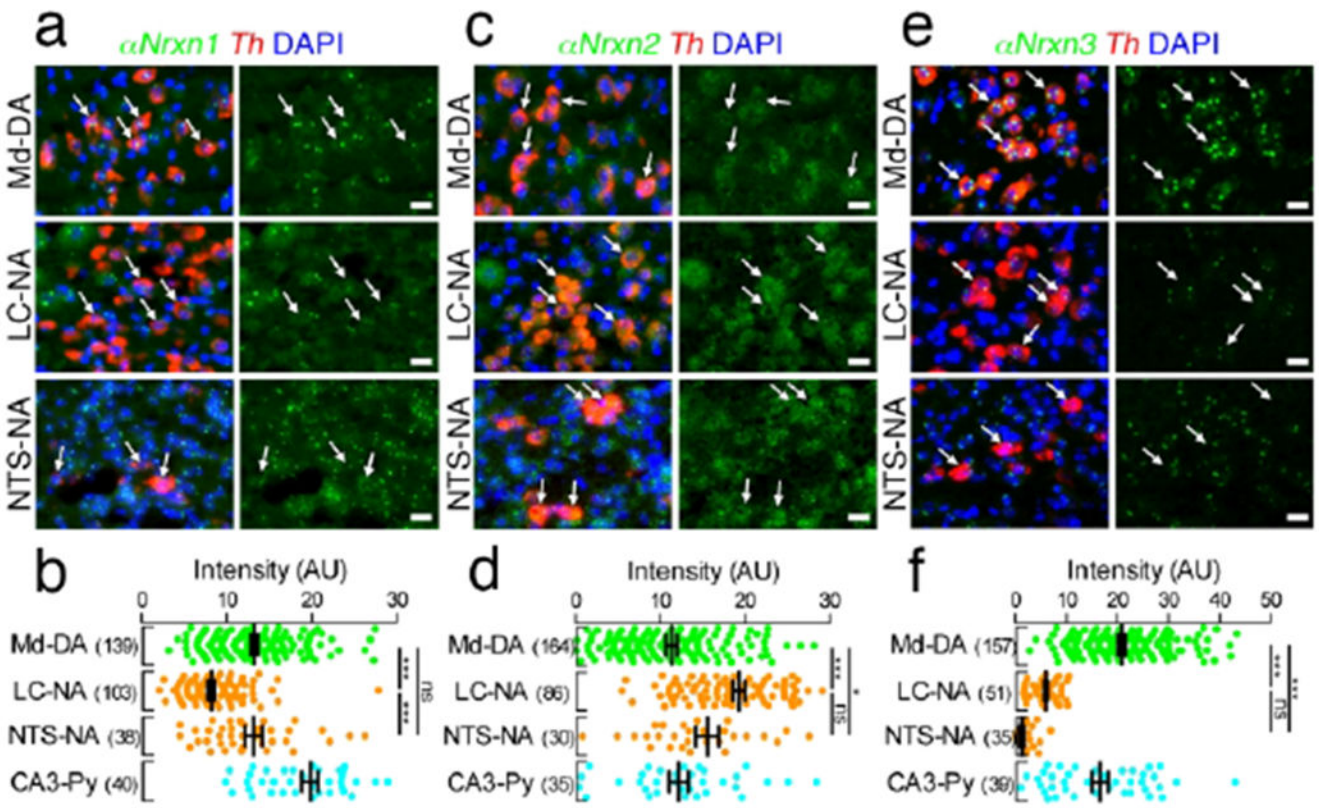


**Figure 14.**

Distinct expression of αNrxn mRNAs in catecholaminergic neurons. (a, c, e) Double FISH for αNrxn1 (a), αNrxn2 (c), or αNrxn3 (e) and Th mRNAs showing distinct expression patterns of Nrxn mRNAs (green) in Th mRNA (red)-labeled DA neurons in the midbrain (Md-DA, top) and NA neurons in the LC (LC-NA, middle) and NTS (NTS-NA, bottom). Arrows indicate catecholaminergic neurons. Nuclei were stained with DAPI (blue). (b, d, f) Summary scatter plots for αNrxn1 (b), αNrxn2 (d), or αNrxn3 (f) mRNA in Md-DA (green), LC-NA (orange), and NTS-NA (orange) neurons. Signals are compared to hippocampal CA3 pyramidal neurons (CA3-Py) obtained from the same section (aqua). The number in the parentheses next to each column indicates the number of cells analyzed. Data are represented as means ± SEM. ns, not significant; * $P < 0.05$; ** $P < 0.01$; *** $P < 0.001$ (Kruskal-Wallis test with post hoc Dunn's test). Scale bars, 20 μm.

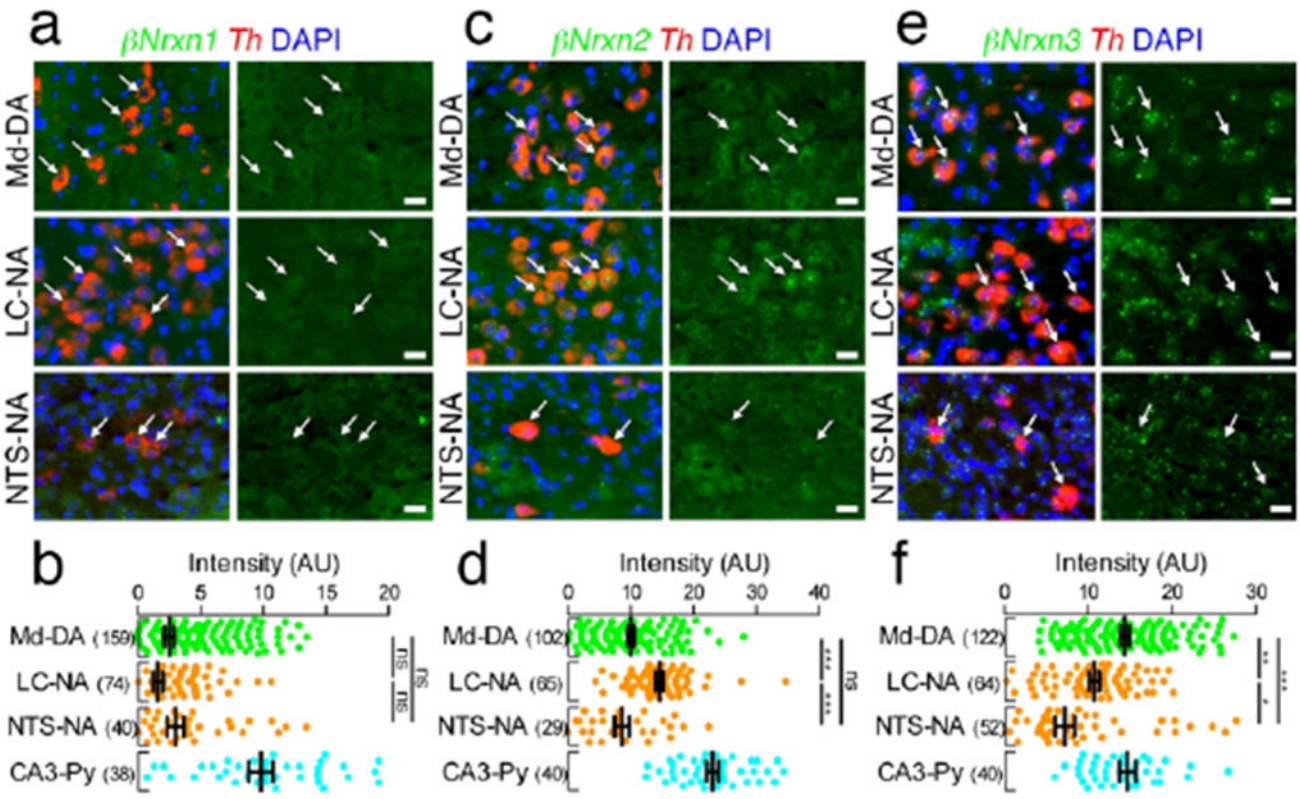


**Figure 15.**

Distinct expression of βNrxn mRNAs in catecholaminergic neurons. (a, c, e) Double FISH for βNrxn1 (a), βNrxn2 (c), or βNrxn3 (e) and Th mRNAs showing distinct expression patterns of Nrxn mRNAs (green) in Th mRNA (red)-labeled DA neurons in the midbrain (Md-DA, top) and NA neurons in the LC (LC-NA, middle) and NTS (NTS-NA, bottom). Arrows indicate catecholaminergic neurons. Nuclei are stained with DAPI (blue). (b, d, f) Summary scatter plots for βNrxn1 (b), βNrxn2 (d), or βNrxn3 (f) mRNA in Md-DA (green), LC-NA (orange), and NTS-NA (orange) neurons. Signals are compared to hippocampal CA3 pyramidal neurons (CA3-Py) obtained from the same section (agua). The number in the parentheses next to each column indicates the number of cells analyzed. Data are represented as means ± SEM. ns, not significant; * P < 0,05; ** P < 0,01; *** P < 0.001 (Kruskal-Wallis test with post hoc Dunn's test). Scale bars, 20 μm.

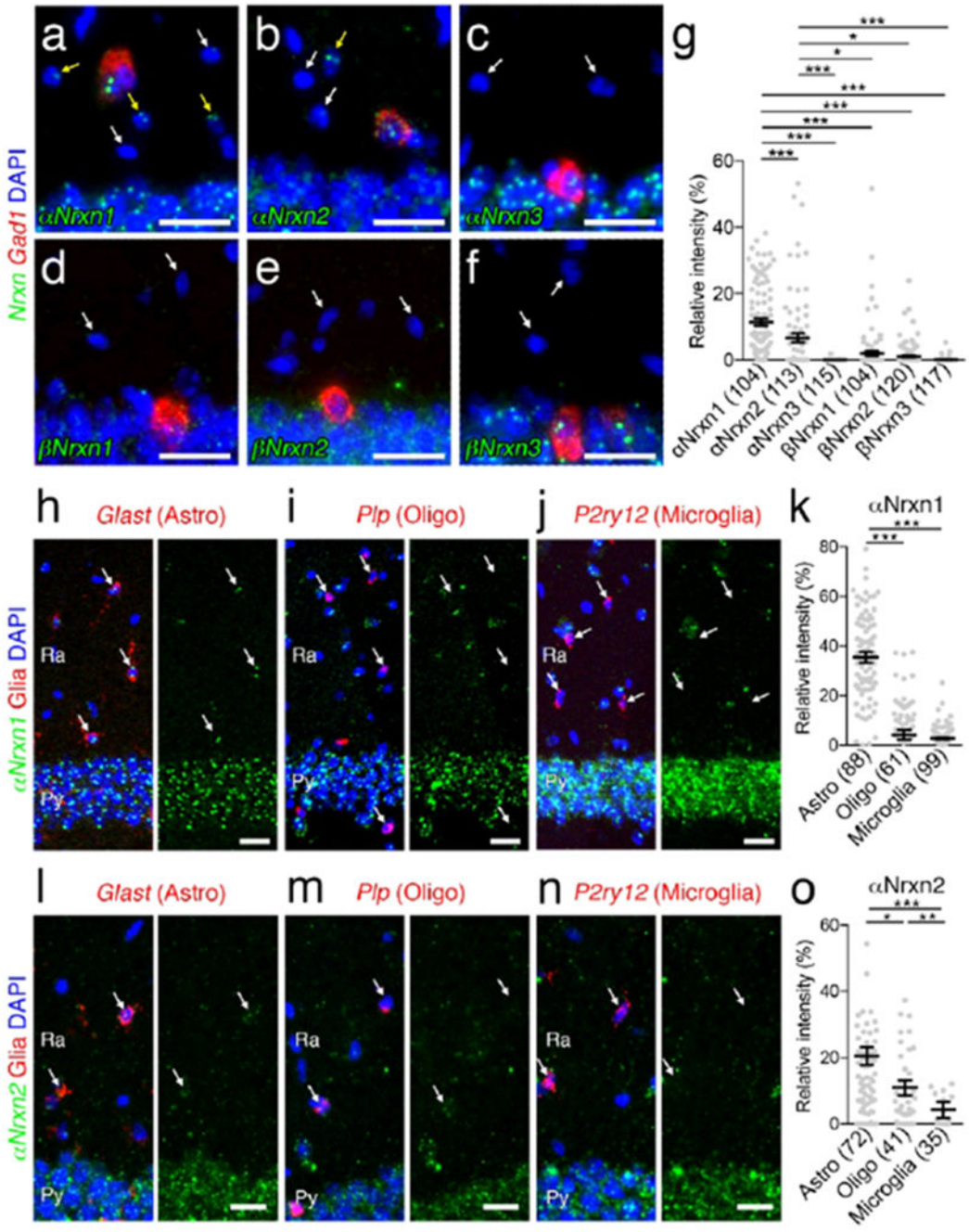


**Figure 16.**

Non-neuronal αNrxn1 and αNrxn2 expression in the hippocampal CA1 subregion. (a - f) Double FISH for αNrxn1 (a), αNrxn2 (b), αNrxn3 (c), βNrxn1 (d), βNrxn2 (e), or βNrxn3 (f) and Gad1 mRNAs in the hippocampus CA1 region showing different expression patterns of Nrxn mRNAs (green) in non-neuronal cells identified by neuropil cells negative for Gad1 mRNA (red). Yellow and white arrows indicate non-neuronal cells with or without Nrxn expression, respectively. (g) Summary scatter plot for six Nrxn mRNAs in non-neuronal cells. The signal intensity in each cell is normalized to that in CA1 pyramidal cells, (h-j, l-n)

Double FISH for αNrxn1 (h-j) or αNrxn2 (l-n) mRNA (green) and non-neuronal markers (red), including Glast (h, l), Plp (i, m), and P2ry12 (j, n) for astrocytes (Astro), oligodendrocytes (Oligo), and microglia, respectively. Arrows indicate non-neuronal cells. Nuclei were stained with DAPI (blue). Ra, stratum radiatum; Py, Pyramidal cell layer, (k, o) Summary scatter plot for αNrxn1 (k) or αNrxn2 (o) mRNA in astrocytes, oligodendrocytes, and microglia. The signal intensity in each cell is normalized to that in CA1 pyramidal cells. The number in the parentheses below the scatter plot indicates the number of cells analyzed. Data are represented as means ± SEM. * $P < 0.05$; ** $P < 0.01$; *** $P < 0.001$ (Kruskal-Wallis test with post hoc Dunn's test). Scale bars, 20 μm.

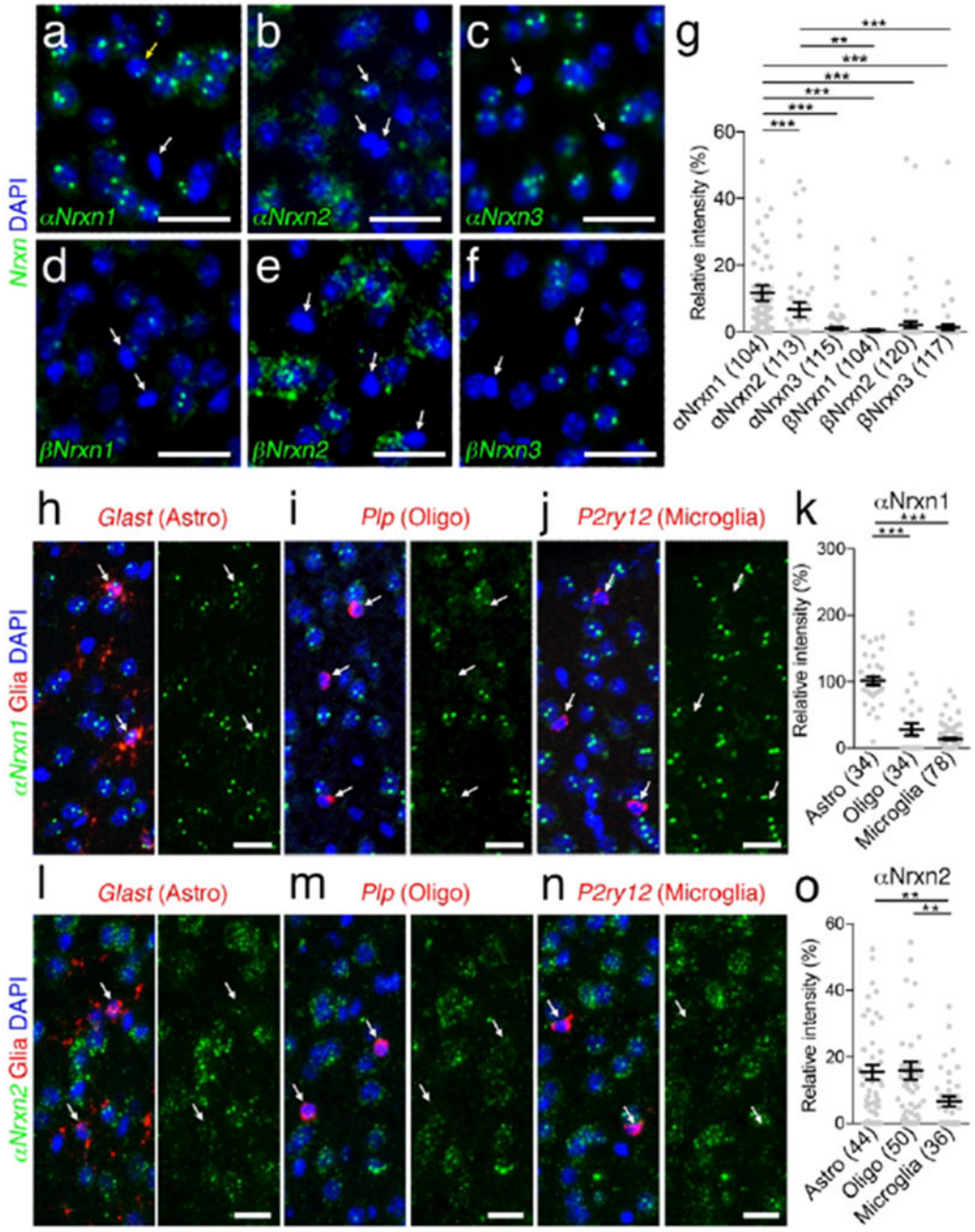


**Figure 17.**

Non-neuronal αNrxn1 and αNrxn2 expression in the somatosensory cortex. (a - f) Single FISH for αNrxn1 (a), αNrxn2 (b), αNrxn3 (c), βNrxn1 (d), βNrxn2 (e), or βNrxn3 (f) in the somatosensory cortex showing different expression patterns of Nrxn mRNAs (green) in non-neuronal cells with small and dark DAPI+ nuclei. Yellow and white arrows indicate non-neuronal cells with or without Nrxn expression, respectively, (g) Summary scatter plot for six Nrxn mRNAs in non-neuronal cells. The signal intensity in each cell is normalized to that in cortical neurons with large and pale DAPI+ nuclei. (h-i, l-n) Double FISH for

αNrxn1 (h-i) or αNrxn2 (l-n) mRNA (green) and non-neuronal markers (red), including Glast (h, l), Plp (i, m), and P2ry12 (i, n) for astrocytes (Astro), oligodendrocytes (Oligo), and microglia, respectively. Arrows indicate non-neuronal cells. Nuclei were stained with DAPI (blue). Ra, stratum radiatum; Py, Pyramidal cell layer, (k, o) Summary scatter plot for αNrxn1 (k) and αNrxn2 (o) mRNA in astrocytes, oligodendrocytes, and microglia. The signal intensity in each cell is normalized to that in cortical neurons. The number in the parentheses below the scatter plot indicates the number of cells analyzed. Data are represented as means ± SEM. * P < 0.05; ** P < 0,01; *** P < 0,001 (Kruskal-Wallis test with post hoc Dunn's test). Scale bars, 20 μm.

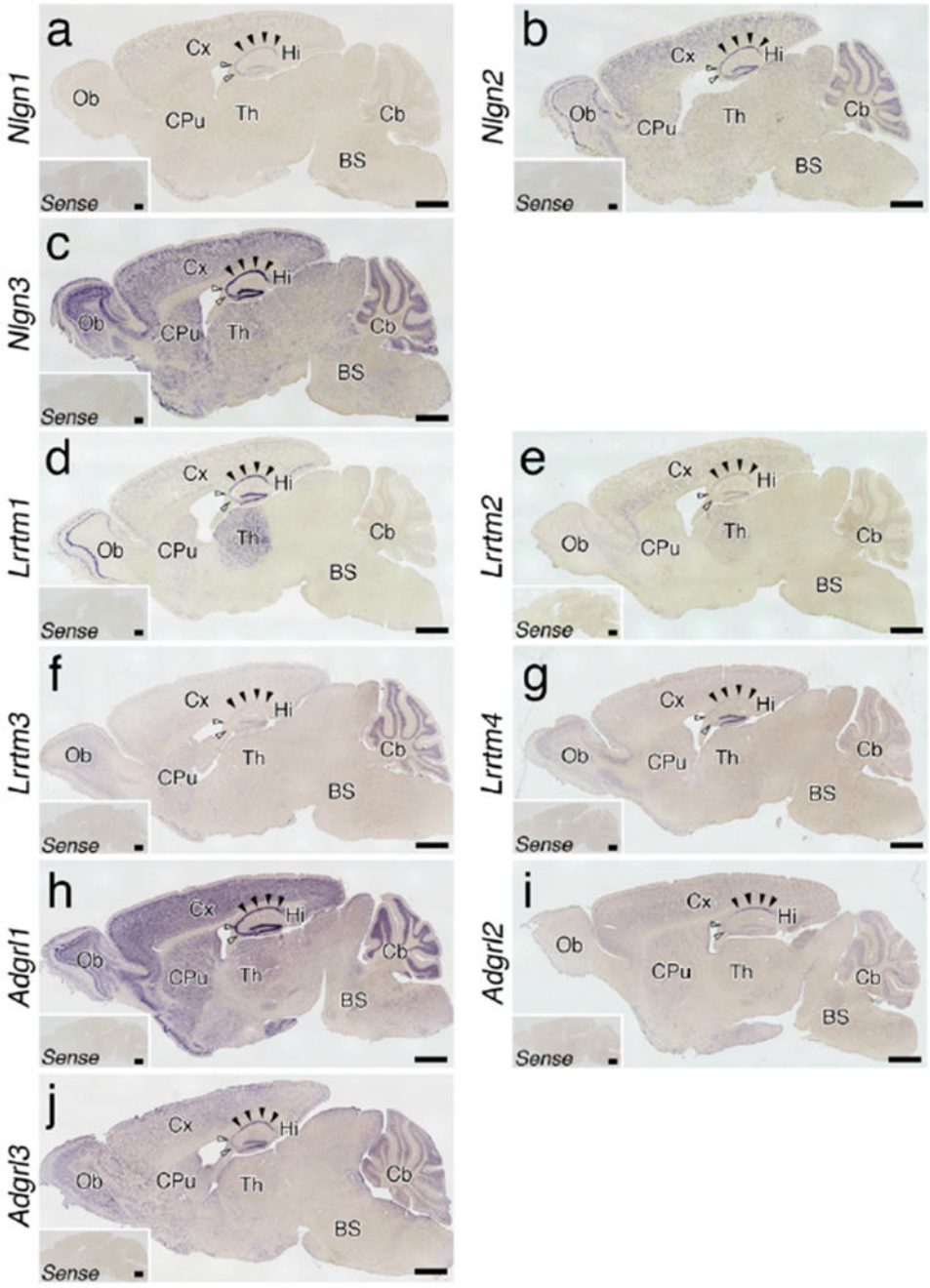


**Figure 18.**

Expression of Nrxn binding partners in the brain. (a-j) Whole brain sagittal views of chromogenic hybridization signals for Nlgn1-3 (a-c), Lrrtm1-3 (d-f) and Adgrl-4 (g-j) mRNAs. Insets showing no hybridization signals with sense cRNA probes. Filled and open arrows indicate the CA1 and CA3 pyramidal cell layers, respectively. For abbreviations, see list. Scale bars, 1 mm

**Table 1.**

List of cRNA probes used in the present study.

| Molecule | Sequence | Accession # (Genebank or NCBI) | Dilution | Hybridization Temperature (°C) | Reference |
|---|---|---|---|---|---|
| *αNrxn 1*#1 | 186–631 | NM_020252.3 | 1:1,000 | 63.5 | this study |
| | AAGGGGAATAACCAGGCAGATTTCTGAGTTCTTATAAACGTCAAAATAAAATCAAAATGCATCACCAACATACAACCAACTGACATGCTGGAGTCTTAGGGTG<br>GCCTTGCAGAGACAGAAAAAAGAAGAGTTTGAGGGATTGATTTCACCATCTAACAGCTTCTGGCTACTTCACAGCAGGGTTTGAGACCTACCTACAGGGCTC<br>CTAAACATAAAGCGAATCAGCCTGGGAGGGCATGCACAGGAAATTTGGCCTTGGCTTTAGTGGTGCTGGAAGCCCATGATATGACAGAAGTAGGCCTCTGA<br>AGCTATTCTGGTGTCTCACTCTGTCCTTTCTCCTTCTGTGCTTGGAGCCAACATCTGGAGGGGCCTCGAGGCCTGCCAAGCAGCCAAAGATCCTGGCTCAGT<br>GTTGACTTCGTGTTCCTCTCCGAGAAAAGTGTGTTTCT | | | | |
| *αNrxn1*#2 | 631–1132 | NM 020252.3 | 1:10,000 | 63.5 | this study |
| | TTCCGATTCTGCTCTCCTACTGCTGGCACCGCGCCGGTGGTACTTTGAAGGTTTTGGTCCTGGGATAGTTGAAGTACCTGTTGGTGCCACAGATGCCCTCAC<br>TTAAACATCATCGGATGCAAATGGATCAGTGATCGCTCTTGAGCCTCGGTGGCCCTCTTTTTCAGAACGTTGCCTCCAAAGTGTATCCCCCCTTTGGCCTGG<br>AAGTTCTGCAGCTATCCCATAGGACTGGGGTCTCCGCTTTCCAGTTGGAAGGAGACTACTGGGAGAGAGGAAGGGGCTGCTGGAAGAGAAGAAGAAGGAA<br>AAAAGAGCTGAAGGAGGGTGCGCCCCTCCCACTGCCGCCTCCCCCCTCCCTCCCACTCCTCTGCGGACCCCCATTTCTCTGTGAAGGTGTCCAGGACCGC<br>TTCGACCCTGTCGCCCCCGGCTCCCCCCCCGCCGCACCCCAGCCCCGAGCATGGGGACGGCGCTGGTCCAGCGCGGGGGCTGCTGTCTCCTCTGCCTGT | | | | |
| *βNrxn1*#1 | 379–824 | XM 006523818.2 | 1:10,000 | 75 | this study |
| | GCTCTTTCATCTGCCCCTGCTTTTCCTCCGCTCGCTTTCCCCAGTTCGATCCCTGCTGTCTTCACGAGGGTGCCCACTTCCCTCTGAACCCATCGTCGGGCG<br>TAGTGTCAGGAGGCGGCGGACTCGGAGATTGCCTCTGGAGCAGGCGATGCGCGCCGCTGCTCTGCGCGCTGCCCGGGTGAGGCTGGCGGGAGCTGGAG<br>AGCTGGCCAGGGCTGAATGGAGGGACAGGGTGCCTTGCGTCCATGGGGTCTGCTTCTTTCCTGAAAGGAGGCTGGACCGGCGAAGTGGTCTCCCAGTTCC<br>CCGCGCACAATGCTAAATGGATTTACCTAGTGGATTCCCGGTGGATGGCTGTCATGTAGAAGTGAAGACCCTCCGGGAGGAGCTTTAAACAATTTCCAGGCT<br>CCCCAACCCCGGCACACACTCTCGCCCGAAACTCTTGGGGAGTA | | | | |
| *βNrxn1*#2 | 882–1490 | XM 006523818.2 | 1:10,000 | 75 | this study |
| | TGTTCTTCGGGTCTGCTTTTCCGGACAAGTCCTCCGGCCAGCTACATTCACCTCGGCTATGTTTCGGATTGTTTGGGGTACTGTTGTAGGGCACTGCAGACT<br>CCAGGACCCTGAGAAGACTGTCCGAAGGAGGGAGAGGATGGCTGCCCTGGCGCGGTAAGGCGGCCAATCCAGCAGCCAACCGCGAGCCGCCCGATCCC<br>CGGCTTCCTCTTCTCTTCTTGTGCCCCAAACTTTGCCTCCCGCGGCGGCTGCCCCTTGGCGGGCGCCCCGCCATGTACCAGAGGATGCTTCGGTGCGGCG<br>CCGATCTGGGATCGCCCGGGGGCGGCAGTGGCGGCGGCGCAGGGGGGCGCCTGGCCCTGATCTGGATAGTCCCGCTCACCCTCAGCGGCCTCCTAGGA<br>GTGGCCTGGGGGGCATCCAGTTTGGGAGCGCACCACATCCACCATTTCCATGGCAGCAGCAAGCATCATTCAGTGCCTATTGCAATCTACAGGTCACCAGC<br>ATCCTTGCGAGGCGGACACGCTGGGACAACATATATCTTTAGCAAAGGTGGTGGACAGATTACATATAAGTGGCCTCCCAATGACCGCCCCAGTACACGAG<br>CAGACAGGC | | | | |
| *αNrxn2*#1 | 120–370 | NM 001205234 | 1:1,000 | 63.5 | this study |
| | GACCAGGAGGCGCGAGGCAGCCGATATCGCTGGCCCAGGATCTGTTACCTGCCGTAGACCCAGCGGTCTCTAGGCTCGGATCCCTACCCTTCAGCTCCTG<br>GCGCCCCCAAAACCAGGCGTCCCTCCCCCACCTTCCATACGAGCCCGCCGCGGGGGAGGGGCTCCACCACCGCAGCCGCCGTCGTTGCCTTCCGGGGAC<br>GTGGACACGTGAGCCCCGGCTACTGAGTCCATGGCACTGTGAATCGGCGAGG | | | | |
| *αNrxn2*#2 | 894–1209 | NM_001205234 | 1:1,000 | 63.5 | this study |
| | TCAAAGCGGCGCGAGATGCAGGTGGCCAGCGACCTGTTCGTGGGCGGCATCCCTCCCGACGTGCGCCTATCTGCACTCACGCTCAGCACCGTCAAGTACG<br>AGCCGCCTTTCCGCGGCCTTCTGGCCAACCTGAAGCTGGGCGAGCGGCCGCCGGCGCTGCTGGGTAGCCAGGGTCTGCGCGGTGCGGCCGCCGACCCT<br>CTGTGTGCGCCTGCGCGCAATCCCTGCGCCAACGGCGGTCTCTGCACCGTGCTAGCCCCCGGCGAGGTGGGCTGCGACTGCAGCCACACTGGATTTGGC<br>GGCAAGTTCTGCAGTGAAG | | | | |
| *βNrxn2*#1 | 188–375 | AK163904.1 | 1:1,000 | 63.5 | this study |
| | TGAGGGGGGACCCCTAGCCGCCCGCGATGGATCCAGGCTTCACGGACCTTGGCCTTCCCGCTGCGCGTACCCCGGATTCCCCGGCGGGATCCAGTTGAT<br>TTGCTTGGCTCCGGACTGAGGCTCGGGCTCTGGTTTTCCTTCGCTTCACCCCTACCCCCCTCTCGGAGCTCGCAACCGGAGGGGGGCTT | | | | |
| *βNrxn2*#2 | 543–714 | AK163904.1 | 1:1,000 | 63.5 | this study |

| Molecule | Sequence | Accession # (Genebank or NCBI) | Dilution | Hybridization Temperature (°C) | Reference |
|---|---|---|---|---|---|
| | TTCTGCTGGGGCTGCTGCTGCTGCTGGGGGCGGCTGAGGGGGCCCGGGTCTCGTCCAGCCTCAGCACCACCCACCACGTCCACCACTTCCACAGCAAGC<br>ACGGCACCGTGCCCATCGCCATCAACCGCATGCCCTTCCTCACCCGCAGCGGGCACGCTGGGACCACATACAT | | | | |
| *αNrxn3*#1 | 207–795 | NM 001198587 | 1:1,000 | 63.5 | this study |
| | CCTCCCGATTACTCCTCCTCCATTACAGCACCCTGAGCCCCAGCCCTGTCCTTGGTCTTCCTGGCTAGGACGCATTTGCCGGGAGGAAGACATTACGGAAG<br>GCTTATTCCCACCCTGGGCTCCTTCTCCTCCTTGAATCAAGGCCTCCGGATCCACATGGATAGCTGAGATCTTTTCTTGGAGAAAGATACTTCTTCCTCGCCT<br>CATCCCTGATTTGCCTCACCCGACAAATCCCCTGTCTGTTTCGTCTCCCTCTTTATGGGATTTCTTGCTTGTGTGCCTATCTAGGGCCGTGTTGTCCTTTTTCC<br>TCTCCTTCCCCTTTCCTCCTAACATTCCTGTGTGTGTTCTTCTTGTGTCTTCTCTTGTACCACTCTGTTTTCCCTCTTTGCCCTCACAATCACCTATCCCCTGCC<br>TCCCGCTCCCACGGCTGATACCTGGCCTACCTGCTCCTCTGTGCTCTGACCCAGCAGGCACCATGAGCTTTACCCTCCACTCAGTTTTCTTCACCTTGAAGG<br>TGAGCATCTTTCTGGGCTCCCTGGTGGGGCTTTGCCTGGGTCTGGAGTTCATGGGCCTTCCTAACCAGTGGGCC | | | | |
| *αNrxn3*#2 | 796–1782 | NM 001198587 | 1:1,000 | 63.5 | this study |
| | CGCTACCTGCGTTGGGATGCAAGCACGCGCAGTGACCTGAGCTTCCAGTTCAAGACCAATGTTTCCACTGGGCTGCTCCTGTATTTGGATGATGGTGGTGT<br>CTGTGACTTCCTCTGTCTCTCCCTGGTGGATGGCCGCGTTCAGCTCCGCTTTAGCATGGACTGTGCCGAGACCACTGTGCTATCCAACAAGCAGGTGAACG<br>ACAGCAGTTGGCACTTCCTCATGGTGAGCCGTGATCGTGTGCGCACTGGGCTGGTGATTGATGGTGAGGGCCAGTCTGGAGAGCTACGGCCCCAGCGGCC<br>TTATATGGATGTGGTCAGTGATTTGTTCCTCGGTGGCGTCCCCGCTGACATTCGACCTTCTGCCCTGACCCTCGATGGAGTACAGAGCATGCCTGGCTTTAA<br>GGGATTAATGCTGGATCTCAAGTATGGCAACTCGGAACCTCGGCTTCTGGGGAGCCAGAGCGTCCAGTTAGAAGCAGAGGGACCCTGTGGCGAGCGTCCC<br>TGTGAAAATGGTGGGATCTGCTTCCTCTTGGATGGTCATCCCACCTGTGACTGTTCTACCACTGGCTATGGTGGCACACTCTGCTCAGAAGATGTCAGTCAA<br>GGTCCAGGCCTCTCCCATCTTATGATGAGTGAACAAGCACGAGAGGAGAACGTGGCCACCTTCCGAGGCTCAGAGTATCTGTGCTATGACCTGTCCCAGAA<br>CCCCATCCAGAGCAGCAGCGACGAAATCACCCTTTCCTTTAAGACCTGGCAACGCAATGGGCTCATCCTCCACACTGGCAAGTCGGCCGACTATGTTAACCT<br>GGCTCTGAAGGATGGTGCGGTCTCCTTGGTCATTAACCTGGGGTCCGGGGCCTTTGAGGCCATTGTGGAGCCAGTGAATGGGAAATTCAACGACAACGCCT<br>GGCATGATGTCAAAGTGACACGCAATCTTCGGCAGGTGACAATCTCTGTGGATGGCATCCTAACCACAACGGGCTAC | | | | |
| *βNrxn3*#1 | 85–530 | NM 001252074 | 1:1,000 | 63.5 | this study |
| | CTGCTCCTCTCCACCTTCTGCTACGTTGGTCTGGGTGGCTAGCTCAGTGCTGTTTCTTTTCCTCTGGCCCTTCTTGATCCCTTTCTCTGGCTACTGCTGCTGG<br>CTGATTTTCAACCTATTGGGAACTCAGGACTTAAGGCGGCTGCACCGTGGCGCTCATCCAGGACACTCAGGGTTAACAGCCTCCGCGCCCATCCACAGAGA<br>CTCCCGGGAGCAGAACTCTTCCACCTGCAGCCCCCTTTTGCCTGGCAGTTCTGCATTGCATCGCTTGGAAGTCGAAACAAGAAAGAAAGAAAGAAAAAA<br>TGTCCAAACTCCTTGGATGTTGGGAAAAACTAGCGTGAATTTACTTGGTTTTTTCCTGCTCTGTCTTCTCTCTCCGTTTCCACCTTTCCCCAGTGGCTTTCCAG<br>AGTATGCAGCTAGTACATCGGACTTGAAGTACCAAG | | | | |
| *βNrxn3*#2 | 771–1235 | NM 001252074 | 1:1,000 | 63.5 | this study |
| | TTCCCCGAAAGCTTTTATTGCTTCCCTCATCCCCAAATTGAACAACTCTTCCTCCTGCTATGATGGGCCTCTGGGCATCATGAACTTCGTTATTGCTCACTGG<br>CTGGAATTTAAACTGCCCATCTGTAGTGGTCCAGTGCGTTGACCATGCACCTGAGAATCCACCCAAGACGGAGCCCTCCTCGCCGGCCGGCCTGGACGCTT<br>GGGATCTGGTCCCTCTTCTGGGGATGTATCGTCAGCTCTGTGTGGAGTTCTTCTAATGTAGCCTCCTCCTCCTCTTCCTCTCCGGGATCTCACTCTCAGCAG<br>GAACACCATTTCCACGGCAGCAAGCACCACTCTGTGCCTATTTCTATCTATCGCTCCCCTGTTTCCCTTCGAGGAGGGCACGCTGGTGCAACATACATCTTT<br>GGGAAAAGCGGTGGCCTCATCCTCTATACCTGGCCAGCAAATGACAGACCCAGCACA | | | | |
| *Vglut1* | 301–1680 | BC054462 | 1:1,000 | 63.5 | (Yamasaki et al., 2010)<br>(Mao et al., 2018) |

| Molecule | Sequence | Accession # (Genebank or NCBI) | Dilution | Hybridization Temperature (°C) | Reference |
|---|---|---|---|---|---|
| *Gad1* | ACATGGCTCCTTTTTCTGGGGCTACATTGTCACTCAGATTCCTGGAGGATTTATCTGCCAAAAATTCGCAGCCAACAGGGTCTTTGGCTTTGCCATTGTGGCT<br>ACCTCCACCCTAAACATGTTGATCCCTTCAGCAGCCCGCGTTCACTATGGCTGTGTCATCTTCGTGAGGATCCTTCAGGGATTGGTGGAGGGGGTCACATAC<br>CCTGCTTGCCATGGCATCTGGAGCAAATGGGCCCCTCCCTTAGAACGGAGTCGGCTGGCAACGACAGCCTTTTGCGGTTCCTATGCTGGGGCGGTGGTTG<br>CCATGCCCTTGGCTGGGGTCCTTGTGCAGTATTCAGGATGGAGTTCTGTCTTCTATGTCTATGGCAGCTTCGGGATCTTTTGGTACCTGTTCTGGTTGCTTGT<br>CTCCTATGAGTCACCGGCACTGCACCCCAGCATCTCTGAGGAGGAGCGCAAATACATTGAGGATGCCATCGGGGAGAGCGCCAAGCTCATGAACCCTGTTA<br>CGAAGTTTAACACACCCTGGAGGCGCTTCTTTACGTCCATGCCCGTCTATGCCATCATCGTTGCGAACTTTTGCCGCAGCTGGACCTTCTACCTGCTCCTCA<br>TCTCTCAGCCCGCCTACTTTGAAGAAGTGTTCGGCTTTGAGATCAGCAAGGTGGGGCTGGTGTCGGCGCTGCCTCACCTTGTCATGACCATCATCGTACCC<br>ATTGGAGGCCAGATCGCTGACTTTTTGCGCAGTCGTCACATAATGTCCACTACCAACGTGCGAAAGCTCATGAACTGCGGGGGTTTCGGGATGGAAGCCAC<br>GCTGCTGCTGGTGGTCGGATACTCGCACTCCAAGGGCGTGGCCATCTCCTTCCTGGTCCTGGCTGTGGGCTTCAGTGGCTTTGCCATCTCTGGGTTTAACG<br>TGAACCACTTGGACATCGCCCCTCGCTATGCCAGCATCTTGATGGGCATTTCCAATGGCGTGGGCACACTGTCTGGGATGGTGTGCCCCATCATCGTGGGT<br>GCAATGACCAAGCACAAGACGCGGGAGGAGTGGCAGTACGTGTTCCTCATAGCCTCCCTGGTGCACTACGGCGGTGTCATCTTCTATGGGGTCTTTGCTTC<br>GGGAGAGAAGCAGCCGTGGGCAGAGCCGGAGGAGATGAGCGAGGAGAAGTGTGGCTTTGTTGGCCACGACCAGCTGGCTGGCAGTGACGAAAGTGAAAT<br>GGAGGACGAGGCTGAGCCCCCAGGGGCGCCCCCCGCGCCGCCTCCGTCCTACGGGGCCACACACAGCACAGTGCAGCCTCCGAGGCCCCCGCCCCCTG<br>TCCGGGACTACTGACCACGGGCCTCCCACTGTGGGGCAGTTTCCAGGACTTCCACTCCATACACCTC | 1036–2015 | NM_008077 | 1:1,000 | 63.5 | (Yamasaki et al., 2010)<br>(Mao et al., 2018) |
| *Th* | GTACAGCATCATGGCTGCTCGTTACAAGTACTTCCCAGAAGTGAAGACAAAAGGCATGGCGGCTGTGCCCAAACTGGTCCTCTTCACCTCAGAACACAGTCA<br>CTATTCCATAAAGAAAGCCGGGGCTGCGCTTGGCTTTGGAACCGACAATGTGATTTTGATAAAGTGCAATGAAAGGGGGAAGATAATTCCGGCTGATTTAGA<br>GGCAAAAATTCTTGATGCCAAACAAAAGGGCTATGTTCCCCTTTATGTCAATGCAACCGCAGGCACGACTGTTTACGGAGCATTCGATCCAATCCAGGAAATT<br>GCGGACATATGTGAGAAATACAACCTTTGGCTGCATGTGGATGCTGCCTGGGGTGGTGGACTGCTCATGTCCCGGAAGCACCGCCACAAACTCAGCGGCAT<br>AGAAAGGGCCAATTCAGTCACCTGGAACCCTCACAAGATGATGGGCGTGCTGCTCCAGTGCTCTGCCATTCTGGTCAAGGAAAAGGGTATACTCCAAGGAT<br>GCAACCAGATGTGTGCAGGCTACCTCTTCCAGCCAGACAAGCAGTATGACGTCTCCTATGACACCGGGGACAAGGCGATTCAGTGTGGCCGCCATGTGGAC<br>ATCTTCAAGTTCTGGCTGATGTGGAAAGCAAAGGGCACCGTGGGATTTGAAAACCAGATCAACAAATGCCTGGAGCTGGCTGATTACCTCTACGCCAAGATT<br>AAAAACAGAGAAGAGTTTGAGATGGTTTTCGATGGTGAGCCTGAGCACACAAATGTCTGTTTCTGGTACATTCCACAAAGCCTTCGAGGGGTTCCAGATAGC<br>CCTGAGCGACGAGAAAAGCTACACAGGGTGGCTCCCAAGATCAAAGCTCTGATGATGGAGTCAGGAACAACCATGGTGGGCTACCAGCCTCAAGGGGACA<br>AGGCCAACTTCTTCCGGATGGTCATCTCTAACCCAGCCGCCACCCAGTCTGACATCGATTTCCTCA | 1–1025 | AY855842 | 1:1,000 | 63.5 | this study |
| *Glast* | ATGCCCACCCCCAGCGCCTCCTCGCCACAGCCCAAGGGCTTCAGAAGAGCCGTCTCAGAGCAGGATACCAAGCAGGCCGAGGCTGTCACGTCCCCAAGGT<br>TCATTGGACGGCGGCAGAGTCTCATCGAGGATGCCCGCAAGGAGCGGGAGGCAGCAGCAGCTGCAGCAGCAGCAGCGGTAGCCTCCTCGGAACCTGGGA<br>ACCCACTGGAGGTTGTGGTATTTGAGGAGAGGGATGGGAATGCTGTTCTCAACCTGCTCTTCTCCCTGAGGGGTACAAAACCCTCCTCCTTGTCTCGGGCT<br>GTAAAAGTATTTGAGACATTTGAAGCCAAAATTCACCACTTAGAGACCCGGCCTGCCCAGAGGCCACTGGCAGGAAGCCCCCACCTGGAGTATTTTGTGCG<br>CTTCGAGGTGCCCAGTGGAGACCTGGCTGCCCTCCTCAGCTCTGTGCGTCGGGTGTCTGACGACGTGCGCAGTGCCAGAGAGGACAAGGTCCCCTGGTTC<br>CCAAGAAAAGTGTCGGAATTGGACAAGTGTCACCACCTGGTCACCAAGTTTGACCCTGATCTGGACCTGGACCACCCGGGCTTCTCTGACCAGGTGTATCG<br>CCAGCGTCGGAAGCTGATTGCAGAGATTGCCTTCCAGTACAAGCACGGTGAACCAATTCCCCATGTGGACTACACAGCGGAAGAGATTGCTACCTGGAAGG<br>AGGTATATGCCACGCTGAAGGGCCTCTATGCTACCCATGCCTGCCGGGAGCACGTGGAGGGTTTCCAGCTTCTGGAACGGTACTGTGGCTACCGAGAGGA<br>CAGCATCCCACAGCTGGAGGACGTGTCCCGCTTCTTGAAGGAGCGGACTGGCTTCCAGCTGCGACCCGTGGCCGGTCTACTGTCCGCCCGTGATTTTCTG<br>GCCAGTCTGGCCTTCCGCGTGTTTCAATGCACCCAGTATATCCGCCATGCCTCCTCACCTATGCATTCACCTGAGCCGGACTGCTGCCATGAGCTGTTGGG<br>ACATGTACCCATGTTGGCTGA | 1571–2473 | AF330257 | 1:1,000 | 63.5 | (Yamasaki et al., 2010)<br>(Mao et al., 2018) |
| | TGAAGAACCGAGATGTTGAAATGGGGAACTCGGTGATTGAGGAGAACGAAATGAAGAAGCCGTATCAGCTGATTGCCCAGGACAATGAACCGGAGAAACCC<br>GTGGCAGACAGCGAAACCAAGATGTAGACGGACAGAGAAGTGCTTTCTTAAGCACCAAGTGTTGGAAACTGTTCTACAATGTATCCATCTCCCTGGGCTCAC<br>TTTCCCAGTGAGCTCCTCTTTCCTCCCTACTCTGATAGGATTGGAAAACGGCCAAACACAAAGGAGGGCTCTGCAGCAGCCCAAACCTATCGGTTTTAGCCT<br>ACATTTGAAAATTTTAAGTCATTTCATATTATTCTTACCAAGTAAGCTACTACAATCAAACACAGTTTCGATATTACCAATTTAGGTGGCAAACGATCCTGTGCC<br>ATTGCTCTGTAAGTAAAAGAATTAAGCAAATGATAGGCTACCGAAAAAAAAAAGTTTTAAAATCAACTTTCAAGATGTAAAAATCCTTCAGAATGCAACTGAGTTT<br>TAATCTTAAAACATTACAACTTGATGAGCAATTATCAGTTACCCATTGAGTAGCTGAGAGGTTCCCATTTCTTCTGACTCCTGCCCTGACTTTGTCAGCATCAG<br>GGCAATCCCCACATGCACACAGCACAGCTGTGAGGAGGAGCGGAGAGTGAGGCTCCCAAATGGTCTAGAGTGAGCCTTGTCTCATCCATTGGCCTCAGTGT<br>TCTCATCCGGAAAATGAGTGACTCCTAGACAGGCCTCTCTAGCCCAAACTTCTGGAACATCAGGAAGGACCCTGCCCCTGTACACCATGAGGATCTCAGACA<br>GGACACTTATTGGGAATGGACATTTCTCTCTAGGGGCAGGCTGTGTGTGGCTCACTAGATCCTGGGTTCAAAATGTTCGTT | | | | | |

| Molecule | Sequence | Accession # (Genebank or NCBI) | Dilution | Hybridization Temperature (°C) | Reference |
|---|---|---|---|---|---|
| *Plp* | 1–1359 | NM_011123 | 1:1,000 | 63.5 | (Yamasaki et al., 2001) |
| | CTTTTCATTGCAGGAGAAGAGGACAAAGATACTCAGAGAGAAAAAGTAAAGGACAGAAGAAGGAGACTGGAGAGACCAGGATCCTTCCAGCTGAGCAAAGT<br>CAGCCGCAAAACAGACTAGCCAACAGGCTACAATTGGAGTCAGAGTGCCAAAGACATGGGCTTGTTAGAGTGTTGTGCTAGATGTCTGGTAGGGGCCCCCT<br>TTGCTTCCCTGGTGGCCACTGGATTGTGTTTCTTTGGAGTGGCACTGTTCTGTGGATGTGGACATGAAGCTCTCACTGGTACAGAAAAGCTAATTGAGACCT<br>ATTTCTCCAAAAACTACCAGGACTATGAGTATCTCATTAATGTGATTCATGCTTTCCAGTATGTCATCTATGGAACTGCCTCTTTCTTCTTCCTTTATGGGGCCC<br>TCCTGCTGGCTGAGGGCTTCTACACCACCGGCGCTGTCAGGCAGATCTTTGGCGACTACAAGACCACCATCTGCGGCAAGGGCCTGAGCGCAACGGTAAC<br>AGGGGGCCAGAAGGGGAGGGGTTCCAGAGGCCAACATCAAGCTCATTCTTTGGAGCGGGTGTGTCATTGTTTGGGAAAATGGCTAGGACATCCCGACAAG<br>TTTGTGGGCATCACCTATGCCCTGACTGTTGTATGGCTCCTGGTGTTTGCCTGCTCGGCTGTACCTGTGTACATTTACTTCAATACCTGGACCACCTGTCAGT<br>CTATTGCCTTCCCTAGCAAGACCTCTGCCAGTATAGGCAGTCTCTGCGCTGATGCCAGAATGTATGGTGTTCTCCCATGGAATGCTTTCCCTGGCAAGGTTT<br>GTGGCTCCAACCTTCTGTCCATCTGCAAAACAGCTGAGTTCCAAATGACCTTCCACCTGTTTATTGCTGCGTTTGTGGGTGCTGCGGCCACACTAGTTTCCCT<br>GCTCACCTTCATGATTGCTGCCACTTACAACTTCGCCGTCCTTAAACTCATGGGCCGAGGCACCAAGTTCTGAGCTCCCATAGAAACTCCCCTTTGTCTAATA<br>GCAAGGCTCTAACCACACAGCCTACAGTGTTGTGTTTTAACTCTGCCTTTGCCACTGATTGGCCCTCTTCTTACTTGATGAGTATAACAAGAAAGGAGAGTCT<br>TGCAGTGATTAATCTCTCTCTGTGGACTCTCCCTCTTAGTACCTCTTTTAGTCATTTTGCTCCACAGCAGGCTCCTGCTAGAAATGGGGGATGCCTGAGAAGG<br>TGACTCCCCAGCTGCAAGTCGCAGAGGAGTGAAAGCTCTAATTGATTTTGCAAGCATCTCCTGAAGACCAGGATGTGCTTCCTTCTCAAAGGGCACTTCCAA<br>CTGAGGAGAGCAGAACGGAAAGGTTCTCAGG | | | | |
| *P2ry12* | 347–846 | NM_027571 | 1:1,000 | 63.5 | this study |
| | ACTCAAGGCTGCCTTGCTGAAGTCTCTGCAGAGTCTCTATCACAGAGGGCTTTGGGAACTTATGCAAGTCACTGAGAAGAAAGCAACAGATGCCAGTCTGCA<br>AGTTCCACTAACTAGTATTCCCGGAGACACTCATATCCTTCAGATTCAGCAGAACCAGGACCATGGATGTGCCTGGTGTCAACACCACCTCAGCCAATACCA<br>CCTTCTCCCCTGGGACCAGCACCCTGTGCGTCAGAGACTACAAGATCACCCAGGTTCTCTTCCCATTGCTGTACACCGTCCTGTTCTTTGCTGGGCTCATCA<br>CGAACAGCTTGGCAATGAGGATTTTCTTTCAGATCCGCAGTAAATCCAACTTCATCATTTTTCTTAAGAACACGGTCATCTCTGATCTACTAATGATTCTAACTT<br>TTCCATTTAAAATTCTTAGTGATGCTAAACTGGGAGCCGGGCCTCTGAGAACCTTGGTGTGCCAAGTTACTTCAGTCACATTTTATTTT | | | | |
| *Nlgn1* | 3098-3790 | NM_138666 | 1:1,000 | 63.5 | this study |
| | CCAGAAAGACCAGCTTTATCTCCATATTGGATTAAAACCGAGAGTTAAAGAGCATTACAGAGCCAATAAGGTAAATCTCTGGCTGGAGCTGGTACCTCATCTG<br>CATAATCTCAATGACATTTCTCAGTATACCTCGACAACAACTAAAGTGCCATCCACGGACATCACTCTCAGACCTACAAGGAAGAATTCCACACCAGTCACAT<br>CAGCCTTTCCCACTGCCAAACAGGATGATCCCAAGCAACAACCAAGCCCCTTCTCGGTGGATCAGAGGGACTACTCCACAGAGCTAAGTGTCACTATCGCA<br>GTGGGGGCCTCTCTGCTGTTTCTCAACATCTTGGCTTTTGCAGCCCTGTACTACAAGAAGGATAAGAGGAGACATGATGTCCACCGGAGGTGCAGCCCTCA<br>GCGCACGACCACCAACGACCTAACCCATGCTCCAGAAGAGGAAATTATGTCTCTCCAAATGAAGCACACTGACTTGGATCACGAGTGTGAGTCCATCCATCC<br>ACATGAGGTGGTTCTTCGGACCGCCTGTCCCCCAGATTATACTCTAGCTATGAGGAGGTCACCTGATGATATTCCACTAATGACACCTAACACCATCACAATG<br>ATTCCCAACACTATACCAGGGATTCAGCCCTTACATACATTCAACACATTTACTGGAGGACAGAATAATACACTGCCCCA | | | | |
| *Nlgn2* | 2041-2895 | NM_198862 | 1:1,000 | 75 | this study |
| | ACTGGTGACCCCAACCAGCCTGTGCCACAGGACACCAAGTTCATCCACACCAAGCCCAACCGCTTTGAAGAGGTAGTGTGGAGCAAGTTCAACAGCAAGGA<br>AAAGCAGTATCTGCACATAGGCTTGAAACCACGCGTGCGCGACAACTACCGTGCCAACAAGGTGGCCTTCTGGCTGGAGCTCGTGCCCCACCTGCACAACC<br>TGCACACAGAGCTCTTCACCACCACCACTCGCCTGCCTCCCTATGCCACACGCTGGCCACCTCGCACACCTGGTCCTGGCACTTCCGGCACACGCCGTCCT<br>CCCCCACCTGCCACTCTGCCACCTGAGTCTGATATTGACCTAGGCCCAAGGGCCTATGACCGCTTCCCCGGTGACTCGAGGGACTACTCCACGGAGCTAAG<br>CGTGACTGTGGCAGTGGGTGCCTCCCTCCTCTTCCTCAACATCCTTGCCTTTGCCGCCCTCTATTACAAGCGGGACCGGCGCCAGGAGCTGCGGTGCCGG<br>AGGCTTAGCCCACCAGGAGGCTCAGGCTCAGGTGTGCCTGGTGGGGGCCCCCTGCTTCCCACTGCTGGCCGTGAGCTACCCCCGGAGGAGGAGCTAGTA<br>TCGCTGCAGCTGAAGCGGGGTGGTGGTGTTGGGGCGGACCCTGCTGAGGCCCTGCGCCCTGCCTGTCCACCCGACTATACCCTGGCCTTGCGCCGGGCA<br>CCGGACGATGTGCCTCTCTTGGCCCCCGGGGCCCTAACCCTGCTGCCTAGTGGCCTGGGGCCCCCGCCCCCGCCCCCACCCCCTTCTCTCCATCCCTTTG<br>GGCCCTTCCCACCCCCACCCCCTACTGCTACCAGCCACAACAACACGCTACCC | | | | |
| *Nlan3* | 2939-3782 | NM_172932 | 1:1,000 | 63.5 | (Tanaka et al., 2010) |

| Molecule | Sequence | Accession # (Genebank or NCBI) | Dilution | Hybridization Temperature (°C) | Reference |
|---|---|---|---|---|---|
| | ATGCACCCGCATGTACAAAAACACAAATCCAGACGTGAACCTGAATAGGCCCTTCAAATGGGGACACATACGAGTCCTTGGTACCAAGGGCCCATGGAACA<br>GCAGCTGGAACCAGCTCCTTGAGCCCGACCACAGACACTCCTGGGGCCCTGGAAGCCACAGCCGGACACCCCCTTGGTGCTTGCCTTCTCGGAACTGCAC<br>CTCTACCAACTGCAGACTCGGGAGCTTTAAAGAGCAGGATAGCTCTTCCTCCCCCAGACTTGGTCTTTTCTCTGGGTCTTGTTTTTGTTGATTTTTTTCATTTT<br>TAAATTGGAACCAATGCTTTTCCAACCCATTGAGTGCTAAGCAGCTCTGGAAGGGAGGGCTCCAAGATCAGGACGCTCTGGCTCTGGGACTCCCAATGTTCA<br>TACAATCAGACCAAGGAGAAGGACCTTCCAAGACAGTGACAGATGGGCACAAGACTATGGGGTAAGAGGAGGAAGAGGCTAGCAATGGATGGGGCTTGAG<br>GGCCAGCAAGGACAGAGCACCAACTGGCTCTGGGCCTCCCAGAGAGGACTACAGAGCCTACAGGGTGACCTGCTTCTGCAAAGGCCAGCAGCAGCAGCCT<br>GCCTGGAGAAGCCTAGGTTTGATGAACTAAGTACTGTGGAGGCCCTGACCTTATTGGGCCCCTGGGTATATAATCTGGGTTCTGCCTCTGCCCTTGGGGAC<br>ATGATATCAGAAATTTGCCCCATTTTCTTTACAGTCTCTTTGTGTCTGTCATTTCTCTTTCAAAACAACAGTGTTTTGGTTTTTTTTTTTTTTTCGGTTGTTGTTGG<br>CTTTTTTTTTTTTTTTTTTTTTAAGAAAA | | | | |
| *Lrrtm1* | 1286-2134 | NM_028880.3 | 1:1,000 | 75 | this study |
| | AGGCGGAATAAGGTTGCCATTGTGGTCAGCTCTCTCGACTGGGTTTGGAATTTGGAGAAAATGGACTTGTCTGGGAACGAGATCGAATACATGGAGCCCCAT<br>GTGTTCGAGACCGTTCCCTACCTGCAGACCCTGCAGCTGGACTCCAACCGCCTCACCTACATTGAGCCCCGTATTCTCAACTCCTGGAAGTCCCTTACGAGC<br>ATCACTCTGGCCGGGAACCTGTGGGACTGCGGGCGCAACGTGTGTGCTCTAGCTTCCTGGCTCAGCAACTTCCAGGGACGTTACGATGCTAACTTGCAGTG<br>CGCCAGCCCAGAGTACGCACAGGGCGAGGACGTCTTGGATGCAGTGTATGCTTTCCACCTGTGTGAGGATGGGGCCGAGCCCACCAGCGGCCACCTCCT<br>GTCGGTGGCCGTCACTAACCGCAGTGACCTAACGCCCCCAGAGAGCTCAGCCACGACTCTGGTGGACGGTGGGGAGGGGCACGATGGCACGTTTGAGCC<br>CATCACTGTGGCTCTTCCAGGCGGCGAGCACGCAGAGAACGCTGTGCAAATCCACAAAGTGGTCACTGGCACCATGGCCCTCATCTTCTCCTTCCTCATCG<br>TGGTCCTCGTACTCTACGTATCCTGGAAGTGTTTCCCAGCCAGCCTCAGGCAGCTCAGACAGTGCTTTGTCACGCAGCGCAGGAAGCAGAAGCAGAAACAG<br>ACCATGCATCAGATGGCTGCTATGTCTGCCCAGGAATACTATGTTGATTACAAACCTAACCACATCGAGGGGGCCCTGGTTATCATCAACGAGTACGGTTCG<br>TGTACCTGTCACCAGCAGCCTGCGAGGGAATGCGAGGTGTGA | | | | |
| *Lrrtm2* | 183-682 | NM_178005.4 | 1:1,000 | 63.5 | this study |
| | TATTAACTTATAATCAAAGCCGGTTTAGGGGATCAGAGCACAGGGAAAATGACACCAGTGCTTTCCAGAGGAATATCCTAAGGGAAAAAACAATTCACCCTGA<br>TAGACTTGAATTTTACTTGAAAAGCCTGGGGCACAGAAAACAGGAAACTGGTCAAAGGCTCCTGCATGTTAGAGCCTTTTACAGACTCACTGCGTTGAGTCTG<br>ACAACCTCGACTGAATGCAGCCTCCAATGTGCTCAGAAGAATGGGCTTACATTTCAAGTGGCCATTAGGGGCCCCTATGCTGGCAGCAATATATGCAATGAG<br>TGTGGTATTAAAAATGCTGCCTGCCCTGGGTATGGCGTGTCCACCTAAATGCCGCTGTGAGAAGCTGCTATTCTACTGCGACTCTCAGGGCTTCCACTCAGT<br>GCCAAACGCCACAGACAAGGGTTCTTTGGGTCTGTCCCTGAGGCACAATCACATCACAGCGCTTGAAAGAGATCAATTTGCCAGCTTCAG | | | | |
| *Lrrtm3* | 1882-2281 | NM_178678 | 1:1,000 | 63.5 | this study |
| | CCGCGAGCATGAAGCAGCTGCAGCAGCGCTCCCTCATGCGAAGGCACCGGAAGAAGAAACGGCAATCGCTCAAGCAGATGACTCCAGGCACCCAGGAATT<br>TTATGTAGATTATAAACCCACCAACACGGAGACCAGCGAGATGCTGCTGAACGGAACGGGACCCTGCACCTATAGCAAATCAGGCTCCAGGGAATGTGAGA<br>TACCTTTATCAATGAATGTGTCAACCTTTCTGGCATATGACCAGCCCACAATAAGTTACTGTGGGGTCCATCATGAACTCCTCTCCCATAAGTCCTTTGAAACG<br>AATGCACAGGAAGACACGATGGAAAGCCACCTAGAGACTGAGCTGGACTTGAGCACAATCACGTCAGCTGGCCGCATCAGTGACCATAAACCACA | | | | |
| *Lrrtm4* | 1608-2107 | NM_001134743 | 1:1,000 | 63.5 | this study |
| | CTCCGTGGCCATGATTCTCCTGGTGATCTATGTGTCTTGGAAACGGTACCCAGCCAGCATGAAACAACTCCAACAGCACTCACTTATGAAGAGGAGACGGAA<br>AAAGGCGAGGGAGTCGGAGAGACAGATGAATTCCCCTTTACAGGAATACTACGTGGACTACAAACCGACGAACTCTGAGACCATGGATATATCGGTTAATGG<br>ATCTGGTCCCTGCACATATACCATCTCTGGCTCCAGGGAGTGTGAGATACCCCACCATGTGAAGCCCCTGCCGTATTACAGCTATGACCAACCAGTGATTGG<br>GTACTGCCAGGCCCACCAGCCTCTCCACATCAACAAGGCTTATGAAGCTGTGTCTATAGAACAGGATGACAGCCCCAGTTTGGAGCTTGGGAGAGACCACA<br>GCTTCATTGCCACCATAGCCAGGTCGGCTGCACCTGCCATTTATCTGGAGAGAATAACAAACTAACAGCGAAACTAACTTCTAGATGAAGAGC | | | | |
| *Adgrl1* | 2943-3392 | NM_181039 | 1:1,000 | 63.5 | this study |
| | TCCTGGAGGTAACTGTGCTGAACACGGAGGGCCAAGTGCAGGAGTTGGTGTTCCCCCAAGAGTATCCCAGTGAGAACTCCATTCAGCTCTCCGCCAACACC<br>ATCAAGCAGAACAGCCGCAACGGTGTGGTGAAAGTTGTCTTCATTCTCTACAACAACCTGGGCCTCTTCTTGTCCACGGAGAATGCCACAGTGAAGCTGGCA<br>GGTGAGGCAGGGACAGGTGGCCCTGGAGGTGCCTCCCTGGTGGTCAACTCACAGGTCATCGCAGCATCTATCAATAAGGAGTCTAGCCGCGTCTTCCTCAT<br>GGACCCTGTCATCTTTACTGTAGCCCACTTGGAGGCCAAGAACCACTTCAATGCAAACTGCTCCTTCTGGAACTACTCAGAGCGCTCCATGCTGGGCTACTG<br>GTCAACCCAGGGCTGCCGATTGGTGGAGTCCAATAAGACCCATA | | | | |
| *Adgrl2* | 1834-2233 | NM_001081298 | 1:1,000 | 63.5 | this study |

*J Comp Neurol*. Author manuscript; available in PMC 2020 August 15.

| Molecule | Sequence | Accession # (Genebank or NCBI) | Dilution | Hybridization Temperature (°C) | Reference |
|---|---|---|---|---|---|
| | | | | | GCAATTGTGGACACGGTAGACAACCTTCTGAGAGCTGAGGCTTTGGAATCCTGGAAACACATGAATTCTTCAGAGCAGGCGCACACAGCCACAATGTTGTTG |
| | | | | | GATACCTTGGAAGAAGGAGCATTCGTCCTAGCAGACAACCTTTTGGAACCAACCAGGGTCTCCATGCCAACAGAAAATATTGTTTTAGAAGTTGCTGTCCTCA |
| | | | | | GCACGGAAGGGCAGGTCCAAGACTTTAAATTCCCTCTGGGCTTAAAGGGGTTGGGCAGCTCCATCCAGCTCTCTGCCAAACACGGTCAAACACAGAACAGCAGG |
| | | | | | AATGGGCTGGCCAAGCTGGTATTCATCATTTACCGGAGCCTGGGACAATTCCTAAGCACTGAGAACGCAACCATAAAGCTGGGTGCAGACCTCA |
| | Adgrl3 | 2410-2809 | NM_001347367 | 1:1,000 | 63.5 | this study |
| | | | | | CTGGATAGTAGATCAGGGCCGGTACATCATGGACAAGTCTCCTACATCTCTCCACCAATTCACCTCGACTCTGAACTAGAAAGGCCCCCTGTCAGAGGGATT |
| | | | | | TCTACCACAGGATCCCTGGGTATGGGAAGCACGACCACCAGCACCACCCTCCGGACCACAACCTGGAACATAGGCAGGAGTACCACCGCATCCTTGCCGG |
| | | | | | GCAGAAGAAACCGCAGTACCAGCACGCCATCCCCCCGCGGTAGAGGTGCTGATGACGTCACCACACACCTGCCCTCGGCAGCCTCCCAAATCCCAGCTAT |
| | | | | | GGAAGAGAGCTGCGAGGCTGTGGAAGCCCGAGAAATCATGTGGTTTAAGACCAGACAGGGGCAGGTAGCAAAGCAGCCATGCCCAGCAGGAACCATAG |

**Table 2**

Expression levels of 6 isoforms of *Nrxn* mRNAs in individual regions

| | ***Nrxn* mRNA expression** | | | | | | |
|---|---|---|---|---|---|---|---|
| **Region** | **αNrxn1** | **αNrxn2** | **αNrxn3** | **βNrxn1** | **βNrxn2** | **βNrxn3** | **Figures** |
| Telencephalon | | | | | | | |
| Olfactory bulb (Ob) | | | | | | | |
| Glomerular layer (Gl) | +++ | + | +++ | + | ++ | + | 2 |
| Mitral cell layer (Mi) | +++ | ++ | +++ | ++ | +++ | +++ | 2 |
| Granule cell layer (GrO) | +++ | ++ | +++ | + | ++ | ++ | 2 |
| Neocortex (Primary somatosensory cortex: S1) | | | | | | | |
| Layer 1 | + | + | + | - | - | +/− | 3, 8, 9 |
| Layers 2/3 | ++ | ++ | ++ | ++ | ++ | + | 3, 8, 9 |
| Layer 4 | ++ | + | + | ++ | + | ++ | 3, 8, 9 |
| Layer 5 | ++ | ++ | ++ | ++ | + | + | 3, 8, 9 |
| Layer 6 | ++ | + | ++ | + | + | + | 3, 8, 9 |
| Neocortex (Primary motor cortex: M1) | | | | | | | |
| Layer 1 | + | + | + | − | − | − | 2 |
| Layers 2/3 | ++ | ++ | ++ | ++ | ++ | +§ | 2 |
| Layer 5 | ++ | ++ | ++ | + | + | + | 2 |
| Layer 6 | ++ | + | ++ | + | + | + | 2 |
| Neocortex (Primary auditory cortex: A1) | | | | | | | |
| Layer 1 | + | + | + | + | − | − | 3, 4 |
| Layers 2/3 | ++ | ++ | ++ | ++ | ++ | ++ | 3, 4 |
| Layer 4 | ++ | + | ++ | ++ | + | ++ | 3, 4 |
| Layer 5 | ++ | ++ | ++ | + | + | + | 3, 4 |
| Layer 6 | ++ | + | ++ | + | + | + | 3, 4 |
| Retroslpenial granular cortex (RSG) | ++ | ++ | ++ | ++ | + | + | 3, 4 |
| Piriform cortex (Pir) | +++ | +++ | +++ | +++ | +++ | +++ | 2, 3 |
| Lateral entorhinal cortex (LEnt) | ++ | ++ | ++ | ++ | ++ | 4,5 | |
| Medial entorhinal cortex (MEnt) | ++ | ++ | + | ++ | ++ | + | 5 |
| Olfactory tubercule (OT) | + | + | +++ | + | + | ++ | 2 |

| | *Nrxn* mRNA expression | | | | | | |
|---|---|---|---|---|---|---|---|
| **Region** | **αNrxn1** | **αNrxn2** | **αNrxn3** | **βNrxn1** | **βNrxn2** | **βNrxn3** | **Figures** |
| Hippocampus | | | | | | | |
| CA1 | +++ | ++ | +++ | + | +++ | ++ | 3, 4, 10, 11 |
| CA2 | +++ | +++ | +++ | +++ | +++ | ++ | 3, 4, 10, 11 |
| CA3 | +++ | ++ | +++ | +++ | +++ | ++ | 3, 4, 10, 11 |
| Subiculum (Su) | ++ | ++ | ++ | + | + | ± | 4 |
| Dentate gyrus (DG) | +++ | ++ | ++ | +++ | +++ | ± | 3, 4, 10, 11 |
| Caudate-putamen (CPu) | + | + | +++ | + | + | ++ | 2 |
| Nucleus accumbens (NAc) | + | + | +++ | + | + | ++ | 2 |
| Island of Calleja (ICj) | ++ | +++ | +++ | +++ | + | +++ | 2 |
| Lateral septal nucleus (LS) | + | ++ | ++ | + | + | + | 2 |
| Nucleus of the diagonal band (NBD) | ++ | ++ | ++ | ± | + | + | 2 |
| Amygdala | | | | | | | |
| Lateral nucleus (LA) | ++ | ++ | ++ | ++ | ++ | + | 3 |
| Basal nucleus (BA) | ++ | ++ | ++ | + | ++ | + | 3 |
| Central nucleus (CA) | ++ | ++ | ++ | + | ++ | ++ | 3 |
| Claustrum (Cl) | ++ | + | +++ | ++ | ++ | ± | 3 |
| Diencephalon | | | | | | | |
| Epithalamus | | | | | | | |
| Lateral habenular nucleus (LHb) | ++ | + | ± | − | + | ± | 3 |
| Medial habenular nucleus (MHb) | +++ | +++ | ±§ | - | ++ | - | 3 |
| Thalamus | | | | | | | |
| Ventral posteromedial nucleus (VPM) | ++ | + | + | + | + | ++ | 3 |
| Ventral posterolateral nucleus (VPL) | ++ | + | + | + | + | ++ | 3 |
| Lateral dorsal nucleus (LD) | ++ | + | + | ++ | + | ++ | 3 |
| Lateral posterior nucleus (LP) | ++ | + | + | ++ | + | ++ | 3 |
| Mediodorsal nucleus (MD) | ++ | + | ± | ++ | + | ++ | 3 |
| Centromedian nucleus (CM) | ++ | + | ± | ++ | + | ++ | 3 |
| Paraventricular nucleus (PVT) | ++ | ++ | ± | + | ++ | ± | 3 |
| Medial geniculate nucleus (MGN) | ++ | + | + | ++ | + | ++ | 4 |
| Reticular thalamic nucleus (Rt) | + | + | ++ | − | + | ± | 3 |

| | *Nrxn* mRNA expression | | | | | | |
|---|---|---|---|---|---|---|---|
| **Region** | **αNrxn1** | **αNrxn2** | **αNrxn3** | **βNrxn1** | **βNrxn2** | **βNrxn3** | **Figures** |
| Subthalamic nucleus (STN) | ++ | + | + | − | ± | ± | 3 |
| Hypothalamus | | | | | | | |
| Lateral area (LH) | ++ | ++ | ± | − | + | ± | 3 |
| Dorsomedial nucleus (DMH) | +++ | +++ | ++ | − | ++ | ++ | 3 |
| Ventromedial nucleus (VMH) | ++ | +++ | + | − | + | + | 3 |
| Arcuate nucleus (Arc) | +++ | ++ | +++ | + | ++ | + | 3 |
| Midbrain | | | | | | | |
| Superior colliculus(SC) | ++ | ++ | ±§ | − | + | ±§ | 4,5 |
| Inferior colliculus (IC) | ++ | ± | ±§ | + | ++ | ±§ | 5,6 |
| Parabigeminal nucleus (PBG) | ++ | ++ | + | ± | ± | ± | 5 |
| Periaqueductal gray (PAG) | ++ | + | + | ± | + | − | 4,5 |
| Nucleus of Darkschewitsch (ND) | + | ++ | +++ | − | + | ± | 4 |
| Edinger-Westphal nucleus (EW) | + | ++ | ± | − | + | ± | 4 |
| Dorsal raphe nucleus | | | | | | | |
| Dorsal part (DRD) | ++ | ++ | + | − | ++ | ± | 5 |
| Ventral part (DRV) | ++ | ++ | + | − | ++ | ± | 5 |
| Lateral part (DRL) | ++ | ++ | ++ | − | + | ± | 5 |
| Substantia nigra pars reticulate (SNr) | + | + | ± | − | ± | ± | 4 |
| Substantia nigra pars compacta (SNc) | + | ++ | ++ | − | + | + | 4, 14, 15 |
| Ventral tegmental area (VTA) | ++ | ++ | ++ | − | + | + | 4 |
| Interpeduncular nucleus (IPN) | ++ | ++ | ++ | + | + | + | 4 |
| Pons | | | | | | | |
| Dorsal nucleus of lateral lemniscus (DLL) | + | + | ++§ | − | − | ± | 5 |
| Nucleus of trapezoid body (NTB) | + | − | ++§ | − | − | − | 5 |
| Paraolivary region of superior olivary complex (SOP) | + | − | ±§ | − | − | + | 5 |
| Pontine reticular nucleus (PRN) | + | − | ±§ | − | − | +§ | 5 |
| Laterodorsal tegmental nucleus (LDTg) | ++ | ++ | ++ | − | + | ± | 6 |
| Locus coeruleus (LC) | + | ++ | + | − | ++ | + | 6, 14, 15 |

| | *Nrxn* mRNA expression | | | | | | |
|---|---|---|---|---|---|---|---|
| **Region** | **αNrxn1** | **αNrxn2** | **αNrxn3** | **βNrxn1** | **βNrxn2** | **βNrxn3** | **Figures** |
| Lateral parabrachial nucleus (LPB) | ++ | + | + | – | + | ±§ | 6 |
| Medial parabrachial nucleus (MPB) | + | ± | + | – | ± | + | 6 |
| Ventral cochlear nucleus (VC) | ± | – | ±§ | – | ± | ±§ | 6 |
| Facial nucleus (VII) | + | ++ | – | – | + | – | 6 |
| Principal sensory nucleus of trigeminal nerve (PrV) | ± | – | ±§ | – | ± | ±§ | 6 |
| Medulla | | | | | | | |
| Gigantocellular reticular nucleus (GRN) | + | + | ++§ | – | – | ±§ | 6 |
| Spinal nucleus of trigeminal nerve (SpV) | + | + | ± | + | + | + | 7 |
| Nucleus of the tractus solitarius (NTS) | ++ | ++ | ++ | + | ++ | ++ | 7, 14, 15 |
| Dorsal motor nucleus of vagus nerve (DMX) | ++ | ++ | ++ | ± | ++ | ± | 7 |
| Hypoglossal nucleus (XII) | + | ++ | + | – | ++ | + | 7 |
| Inferior olivary complex (IO) | + | ± | – | + | ++ | – | 7 |
| Medullary reticular nucleus (MRN) | + | + | ±§ | – | ± | + | 7 |
| Lateral reticular nucleus (LRN) | + | + | ± | – | + | ± | 7 |
| Cerebellum | | | | | | | |
| Purkinje cell layer (PCL) | ± | ++ | +++ | ± | ++ | ± | 6, 7, 12, 13 |
| Granule cell layer (GrC) | +++ | ++ | ±§ | +++ | +++ | +++ | 6, 7, 12, 13 |
| Molecular layer (ML) | + | + | +§ | - | - | - | 6, 7, 12, 13 |

+++, strong; ++, moderate; +, weak; –, very weak or not detected. See Materials and Methods for the criteria to determine the expression levels of *Nrxn* isoforms in individual regions.

§Regions including sparse cells highly expressing *Nrxn* isoforms.

*J Comp Neurol*. Author manuscript; available in PMC 2020 August 15.